31. SYNTHESIS OF DRILLING RESULTS FROM THE MID-PACIFIC MOUNTAINS: REGIONAL CONTEXT AND IMPLICATIONS[1]

E. L. Winterer[2] and W. W. Sager[3]

ABSTRACT

The results of drilling on Resolution and Allison guyots, in the Mid-Pacific Mountains (MPM), document a long history of volcanism, subsidence, and accumulation of Hauterivian–Albian shallow-water carbonate sediments. Mid-Cretaceous emersion was followed by subsidence and accumulation of pelagic sediments.

Basement beneath Resolution Guyot is subaerial flows of alkalic basalt, with radiometric dates averaging 127.6 ± 2.1 Ma, emplaced at about 14°S. Overlying shallow-water carbonates are 1620 m thick. Sediments at Site 866, 2 km inward from the platform edge, were deposited in shallow subtidal to intertidal depths, with intermittent subaerial exposure. At Site 867, 0.5 km from the platform edge, beach and storm deposits are common, and at Site 868, 0.1 km from the edge, sponges and rudists in life positions indicate a platform-margin environment.

At Allison Guyot, alkalic basalt sills were cored at the bottom of Hole 865A. Seismic profiles suggest as much as 600 m of sediments underlie the sills, which have $^{40}Ar/^{39}Ar$ radiometric dates averaging 110.7 ± 1.2 Ma. The drilled strata, 730 m thick, extend from near the base to nearly the top of the Albian. The section begins with about 200 m of clayey limestone deposited in quiet, swampy waters. Upward, clays gradually disappear, reflecting the burial of volcanic hills as the seamount subsided. The rest of the series is wackestone deposited in subtidal to intertidal environments.

Core and logging data at both guyots show shallowing-upward cycles of 3 to 10 m thick. Fourier analysis yields estimates of about 100 ka as the most common frequency. Longer-term fluctuations in sea level are suggested by facies successions at a decameter scale. Diagenesis was dominated by dissolution of aragonite, and cements are now marine, low-magnesium calcite. Pore-water data show the entire succession to be open to modern seawater. Dolomite dominates in the lower 400 m of carbonate strata at Resolution Guyot, and Sr-isotope data suggest much of it formed 15 to 20 m.y. after deposition. Compaction of limestone over buried basement topography proceeded apace with deposition and continued after drowning of the guyots.

During the latest Albian, a fall in relative sea level of nearly 200 m exposed limestone strata on both guyots to subaerial and wave erosion, but whether the cause was tectonic or eustatic is not yet known. By mid-Turonian time, the guyots had re-submerged, but only pelagic sediments accumulated. Why no further shallow-water sediments accumulated on the guyots is a mystery. They were at about 8°S (Resolution) to 11°S (Allison) at the time of emergence. Upper Cretaceous pelagic sediments are preserved only in cavities within Albian limestone. Eocene and Paleocene sediments on Allison Guyot, about 120 m thick, were deposited at near-equatorial latitudes. The Lower Cretaceous platform is variably encrusted with phosphorite and ferromanganese oxides, even where buried beneath pelagic sediments.

Primary control on acoustic-wave velocity is from diagenetic changes in density. Chaotic reflections around the guyot edges may be caused by the thick ferromanganese pavements, rather than by massive reefs. Drilling showed that the perimeter rims are not framework reefs, but erosional features carved from sand shoals and lagoonal sediments.

A significant residual remains in the free-air gravity anomalies over Resolution Guyot after subtracting topographic effects. Drilling results imply that most of this excess mass can be explained by the density contrast between dolomitized limestone and low-density sediments surrounding the edifice.

Inversion of magnetic anomalies over MPM seamounts gives a wide geographic scatter in paleomagnetic pole location. Poles near the geomagnetic pole can be attributed to induced magnetization. Some seamounts have complex anomalies perhaps explained by a complex magnetization structure containing magnetic reversals.

INTRODUCTION

Ocean Drilling Program (ODP) Leg 143 was part of a larger effort, including Leg 144, designed to explore deeply into a number of sunken, flat-topped seamounts—guyots—in the northwest Pacific. Each of these legs had multiple objectives of general, topical interest, in addition to objectives of more regional character. A brief review of the evolution of ideas about guyots will place the main objectives in historical perspective.

At the time of the original discovery of guyots, by Hess (1946) during wartime echo-sounding in the Pacific, they were thought to be a part of the ancient "permanent" ocean. This hypothesis, which was embedded in the theory of the permanence of continents and ocean basins, was tested in 1950, when the Scripps Institution of Oceanog-

raphy launched the MidPac expedition, to survey bathymetry and to take dredge and core samples in the Mid-Pacific Mountains (MPM; Fig. 1). The findings of that expedition, mainly reported in Hamilton (1956), showed that rather than being Precambrian, the guyots in the MPM were capped by shallow-water limestone of mid-Cretaceous age, now at depths of about 1500 m. This, of course, did not disprove that the seafloor itself might be Precambrian, but only that there were Mesozoic seamounts and, perhaps even more importantly, that the whole region had subsided since the drowning of the carbonate platforms, as originally hypothesized by Darwin (1842).

Menard (1964) went on to elaborate the consequences of the subsidence by asking whether if all guyots owed their flat summits to processes at sea level, such as reef-building and wave-planation, could the present-day height of guyots above the surrounding ocean floor be used to establish paleobathymetry? He applied this method to the central and northwest Pacific, in the region of the MPM, the Marcus-Wake seamounts, the Line Islands seamount chain, and the Marshall Islands seamount chain, assuming all the seamounts were of about the same age (roughly mid-Cretaceous to early Cenozoic). He thereby derived a regional paleobathymetric map that showed a large
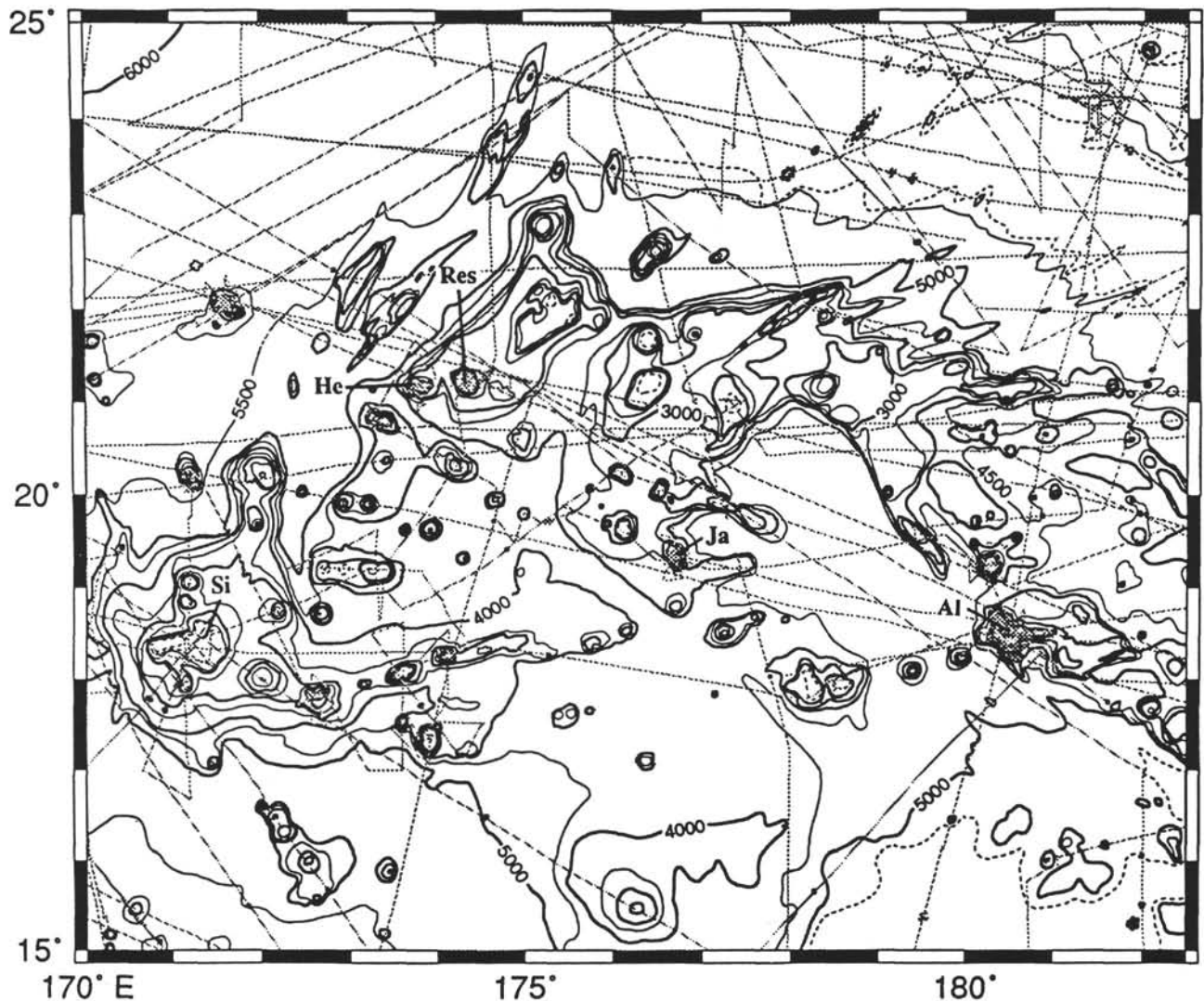
A

Figure 1. Bathymetry of Mid-Pacific Mountains. **A.** Western part. **B.** Eastern part. Contour interval = 1000 m, with additional 500- and 100-m contours shown where appropriate. Tracks of precision echo-sounding lines shown. Guyots labeled, from west to east, are Si, Sio; He, "Heezen"; Res, Resolution; Ja, Jacqueline; Al, Allison; CJ, Cape Johnson; Re, Renard; Ho, Horizon (with DSDP Site 171). No contours are shown in the northeastern corner of **B**, near the Hawaiian seamounts (from Winterer et al., this volume).

bulge centered over the central Pacific between the Line and Marshall islands. He termed this feature the "Darwin Rise," comparing it to the modern East Pacific Rise (this was before the advent of the seafloor-spreading hypothesis).

When Menard first postulated the Darwin Rise, age data from Pacific seamounts were few. Besides the Cretaceous fossils dredged from the MPM, ages were gradually established for the limestone caps and basaltic foundations of seamounts and guyots in the MPM and other western Pacific seamount chains. This was accomplished by radiometric and paleontological dating of dredge and drill samples, both from the seamounts themselves and from redeposited sediments on their flanks (Fischer, Heezen, et al., 1971; Heezen et al., 1973; Winterer, Ewing, et al., 1973; Ladd et al., 1974; Matthews et al., 1974; Larson, Moberly, et al., 1975; Schlanger, Jackson, et al., 1976; Jarrard and Clague, 1977; Jackson, Koisumi, et al., 1980; Larson and Schlanger, 1981; Shipboard Scientific Party, 1981; Thiede et al., 1981; Ozima et al., 1983; Schlanger et al., 1984; Duncan and Clague, 1985; Moberly, Schlanger, et al., 1986; Smith et al., 1989; Lancelot, Larson, et al., 1990; Lincoln et al., 1993; Pringle, 1993;

Pringle and Dalrymple, 1993; Winterer et al., 1993b). A gross pattern of trends in seamount age emerged, from youngest—including active volcanoes—in the southeast Pacific, in the region of the Society, Austral, Cook, and Samoan islands, to progressively older groups of seamounts toward the northwest Pacific. As these dates accumulated, it gradually became clear that Menard's simultaneity assumption could not hold.

Wilson (1963) and Morgan (1972a, 1972b) proposed that seamount chains are progressively formed as lithospheric plates move over deep melting anomalies, called "hotspots." Indeed, this explanation was successful for explaining most of the age pattern within individual seamount chains back to about 85 Ma. Since about 85 Ma, the motion of the Pacific Plate over the seamount-generating hotspots has been northwestward, as described most graphically by the trends of the two longest chains, the Hawaiian-Emperor chain (Clague and Dalrymple, 1987) and the Louisville Ridge (Lonsdale, 1988). On the other hand, it has not yet been possible to derive a plate-motion model that cleanly fits seamounts older than about 85 Ma. There is a question of whether the plate might have had a southern component in its
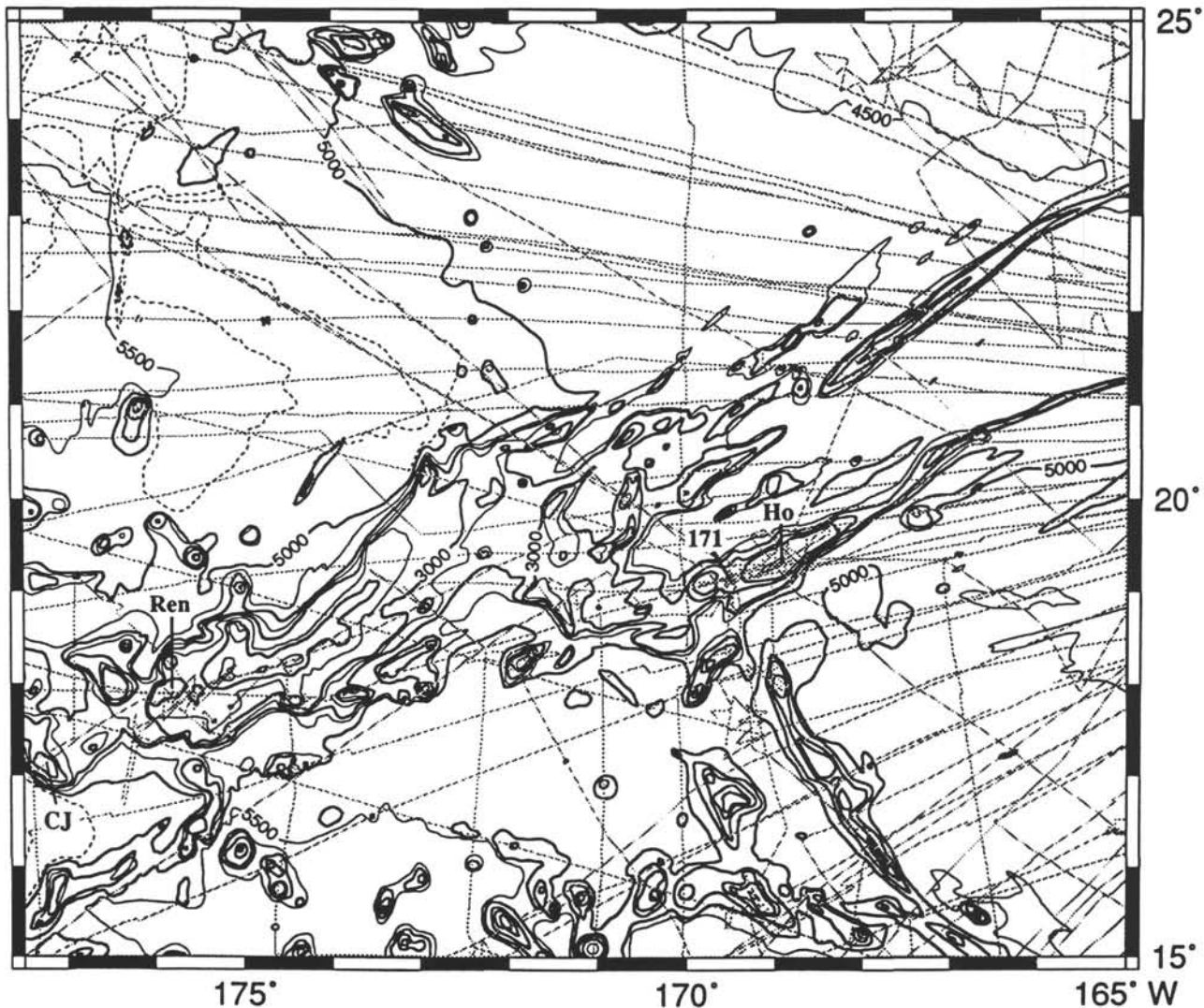
B

25°

20°

15°

175° 170° 165° W

Figure 1 (continued).

motions at times before 85 Ma, as suggested by magnetic-inclination data from Jurassic and Lower Cretaceous drill cores (Larson and Lowrie, 1975; Sayre, 1981; Cox and Gordon, 1984; Larson et al., 1992; Steiner and Wallick, 1992). One of the objectives of Leg 143 was to obtain reliable paleomagnetic data from both the volcanic basement rocks and the sedimentary cover to define a paleolatitude history for the MPM.

Dating the basaltic basement was one of the primary objectives of Leg 143. Whether any age progression occurs among the seamounts in the MPM is a matter of speculation. As pointed out by Winterer and Metzler (1984), the gradual increase from west to east in the depth to guyot summits in the MPM, taken together with the greater age of crust beneath the western MPM, suggests that western edifices are older: they have subsided less since the time of general drowning in the MPM. Before Leg 143, few dates and age estimates existed for the chain, but these data generally supported this hypothesis (Fig. 2).

The southeast Pacific region of young seamount chains and active mid-plate volcanoes is also characterized by having a seafloor somewhat shallower than seafloor of the same age elsewhere, by rates of seamount subsidence that are slower than elsewhere, and by basaltic rocks of distinctive isotopic composition. The region has been termed the Superswell (McNutt and Fischer, 1987), or the South Pacific Iso-

topic and Thermal Anomaly (SOPITA) (Staudigel et al., 1991). The inferred subsidence history of northwest Pacific guyots led McNutt et al. (1990) to conclude that these guyots, early in their histories, had thermal characteristics similar to those of the Superswell, and that the Superswell might thus be long-lived and include the ancestral Darwin Rise. One of the objectives of Leg 143 was to see if the petrologic and isotopic compositions of the lavas and the subsidence history of the MPM guyots reflected an origin in the Superswell, SOPITA region.

A major motivation for coring and logging through the sedimentary cover on the guyots was to establish a history of relative sea level in a region far removed from the "type" areas on the continental margins of the North and Central Atlantic and the circum-Mediterranean Tethys, and also in a completely different tectonic environment. Wheeler and Aaron (1991) suggested that atolls can act as "dipsticks," recording fluctuations in sea level within their limestone caps. Because we knew from previous dredging and drilling that the sedimentary rocks on MPM guyots are mainly shallow-water carbonates, deposited on a carbonate bank (Hamilton, 1956; Heezen et al., 1973; Shipboard Scientific Party, 1973, 1981; Kroenke et al., 1985; van Waasbergen and Winterer, 1993; Winterer et al., 1993b), we hypothesized that they might record changes in Cretaceous sea level. Likewise, from seismic-reflection profiler records, the thickness of lime-
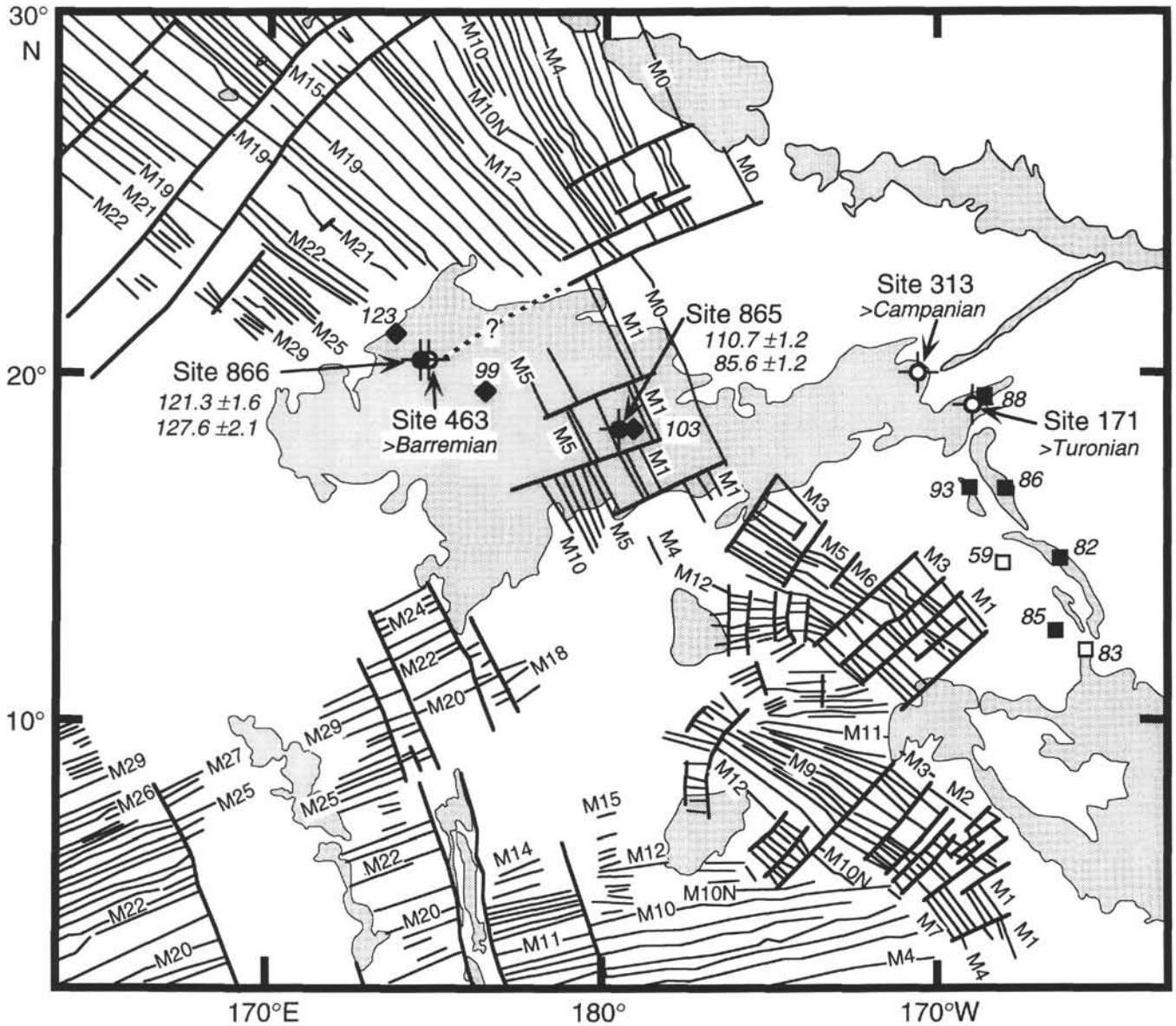
Figure 2. Magnetic lineations and radiometric and paleontologic dates from the Mid-Pacific Mountains region. Heavy dark lines represent fracture zones; lighter dark lines are magnetic isochrons, identified by M-series polarity chron numbers (from Nakanishi et al., 1992). Stippled areas are bathymetric highs. Circles with crosses denote DSDP (open symbols) and ODP (filled symbols) sites in the Mid-Pacific Mountains. Radiometric dates (Pringle and Duncan, this volume) for drilled basalts are given in italics next to site number. Fossil ages of oldest cored sediments are given in italics next to the numbers of sites in which basement was not reached or dated (Shipboard Scientific Party, 1973, 1975, 1981). Squares and diamonds show the locations of dredges from which $^{40}Ar/^{39}Ar$ dates were determined from basalts; numbers in italics adjacent to the symbols give the age to the nearest Ma. Open and filled squares in the Line Islands denote dates from Saito and Ozima (1976) and Schlanger et al. (1984), respectively. Filled diamonds in the Mid-Pacific Mountains indicate dates from Winterer et al. (1993a).

stone strata could be estimated (Heezen et al., 1973; Thiede, Vallier, et al., 1981; Kroenke et al., 1985; van Waasbergen and Winterer, 1993; Winterer et al., 1993b; Winterer et al., this volume), albeit with great uncertainty both about the velocity structure of the carbonate rocks and the identification of volcanic basement. Estimates for the carbonate thicknesses of Allison and Resolution guyots, where Leg 143 drilling occurred, ranged from 500 to 900 m, an amount considered adequate to cover at least several million years, and thus to provide a basis for correlating sea-level-related events in the MPM to events elsewhere in the world.

Furthermore, single-channel reflection seismic records also showed a series of relatively continuous reflectors within the limestones in the central parts of the MPM guyots. We thought these might have the same origin as seismic reflectors observed at Anewetak Atoll (Grow et al., 1986), where drilling showed these to be the result of impedance changes induced by diagenesis of limestone while exposed during late Cenozoic lowstands of sea level (Wardlaw and Quinn, 1991). We therefore aimed to core continuously through the sequence of reflectors, so as to detect changes in sonic impedance through measurements of sonic velocity and bulk density of core samples and by downhole logging, and to relate the seismic reflectors to lithofacies in the limestone succession.

Perhaps the most puzzling question about guyots is why they drowned. From previous dredging and coring in the MPM and in other western Pacific seamount groups, the time of drowning over most of this vast region appeared to be sometime between Aptian and

Turonian, but the paleontological data about timing were scant (Winterer et al., 1993b). One of the main objectives of Leg 143 was to fix as narrowly as possible the time of drowning of two widely separated guyots in the MPM, and then to compare these dates with those from other guyots farther northwest in the Pacific, to be drilled during Leg 144. Knowing the times of drowning can narrow the choices among competing hypotheses about the cause of drowning (e.g., local or regional tectonism, a eustatic shift of sea level, or a paleoceanographic "killer" event).

The geomorphology of the summit regions of guyots all across the Northwest Pacific Ocean poses a potentially related problem: are the atoll- and barrier-reef-like forms constructional or erosional (van Waasbergen and Winterer, 1993)? Some features seen in multibeam bathymetric profiles strongly suggest karstic landscapes and wave-cut benches sculpted during subaerial exposure. One objective of Leg 143 was to sample the uppermost limestones to test whether they contain evidence of substantial and prolonged subaerial exposure.

Other topical questions about the limestone succession included their inorganic and organic geochemistry and their clay-mineral contents. One problem of general interest was to try to determine the degree to which the limestone successions have remained open to the circulation of water from the adjacent open sea, and to what extent circulation within the limestones has been influenced by heat flow from the underlying volcanic basement.

Finally, many of the MPM guyots are partly covered with pelagic sediments. On Allison Guyot, these were estimated to be about 160 m thick, but with signs that erosion had removed some of the younger layers. Because the Pacific Plate in the region of the MPM has been moving northward at rates between about 0.25° and 0.5°/m.y. over the past 85 m.y. (Sager and Pringle, 1988), Allison Guyot was very close to the equator at the beginning of the Cenozoic, and pelagic-sediment accumulation rates should have been at a maximum. These circumstances suggested that an expanded and well-preserved record of equatorial calcareous plankton for the early Cenozoic was present at Allison Guyot, and plans were made to sample this completely with the advanced hydraulic piston-coring (APC) system.

In this chapter, we attempt to bring together most of the varied research results from the Leg 143 cruise itself and the initial phase of post-cruise science. We focus on the MPM because most of the time and effort of the cruise was concentrated there. Because the subjects addressed are varied, we have broken the text into several broad topics to which groups of studies relate. We have attempted to make each section as independent as possible, so background and implications are discussed in each.

DRILLING OVERVIEW

After the *JOIDES Resolution* transited from Honolulu to Allison Guyot in the central MPM (Fig. 1), Hole 865A was drilled approximately halfway between the summit of the pelagic mound and the south edge of the guyot (Fig. 3). The purpose of drilling at this location was to sample and log the supposed lagoonal sediments in the interior of the Cretaceous carbonate platform as well as a section of Tertiary pelagic sediments. The hole penetrated 871 mbsf, through 140 m of pelagic sediment and 698 m of shallow-water limestone, before bottoming in 33 m of intercalated basaltic sills and limestone (Fig. 4; Shipboard Scientific Party, 1993b). Hole 865A was terminated owing to lack of time, even though seismic reflection profiles suggested that as much as 600 m of sediments, perhaps with interspersed basaltic sills, lay beneath. Two additional holes (865B and 865C) were drilled at the site. These were cored with the APC to obtain relatively undisturbed high-recovery cores through the Tertiary section for biostratigraphic and paleoceanographic study. In Hole 865B, the drilling apparatus was changed over to the extended core barrel (XCB) to drill the shallow-water/pelagic sediment contact, from which recovery was poor in the first hole.

Much of the time allotted for Leg 143 was spent drilling on Resolution Guyot (informally termed "Huevo" Guyot before Leg 143), located approximately 716 km northwest of Allison Guyot (Fig. 2). Before Leg 143, a hole was drilled in the basin about 25 km to the northeast of the guyot, at Site 463. This hole penetrated to a depth of 823 mbsf, near the estimated depth of igneous basement, and recovered a mid- to Late Cretaceous succession of pelagic chalk overlying shallow-water carbonate debris and volcaniclastics shed from the guyot (Shipboard Scientific Party, 1981). Leg 143 targeted a transect across the summit rim of the guyot (Fig. 5), to provide data complementary to those from Site 463. Hole 866A was a deep hole, sited approximately 2 km inward from the perimeter mound at a location where it was thought that both lagoonal and reefal facies sediments would be cored. The hole penetrated 1744 mbsf, through a thin cover of pelagic sediments, 1619 m of shallow-water limestone and dolomite of Hauterivian to late Albian age, and 124 m of subaerial basalt (Fig. 6; Shipboard Scientific Party, 1993c).

Holes 867A and 867B were drilled at the crest of the perimeter mound north of Site 866 for sampling the framework reef-facies rocks expected at that location. After only 10 m of penetration, Hole 867A was abandoned because the stresses of the unsupported hard-rock spud-in caused the drill bit and bottom hole assembly (BHA) to fail. A second try was successful, and Hole 867B was drilled to a depth of 77 m through late Albian shallow-water limestones (Fig. 7; Shipboard Scientific Party, 1993d). In an effort to improve recovery, Hole 867B was drilled with an experimental, polycrystalline diamond bit. It did enhance recovery, to an average of 30%, but penetration was slow. After it became apparent that the mound was not a framework reef and the recovered facies were mainly lagoonal wackestones (Shipboard Scientific Party, 1993d), the site was abandoned so that we could use our remaining time to drill on the bench, approximately 400 m seaward of the mound and 33 m deeper.

Because the next drill site was so close, the ship was moved with the drill string and an attached video camera lowered to just above the seafloor. In this manner, we examined the seafloor, where we found a pavement of ferromanganese slabs with a dusting of pelagic sediments. In many places, cracks several centimeters to several tens of centimeters wide penetrated the slabs; it appeared that the ferromanganese coating was about 10 to 20 cm thick. As the camera passed over the edge of the mound, a steep slope declined to the bench below, leading us to interpret this bench as a wave-cut terrace backed by erstwhile sea cliffs.

Hole 868A was drilled on the terrace with the same polycrystalline bit used to drill the previous hole. It produced good recovery, averaging 46%, but the penetration rate was slow and the hole was only 20 m deep when time ran out and it had to be abandoned. As at the previous site, a succession of Albian shallow-water limestones was recovered, albeit of a slightly different facies (Fig. 7; Shipboard Scientific Party, 1993d).

After Hole 868A, the *JOIDES Resolution* steamed out of the MPM toward the Marshall Islands, where three additional holes were drilled at two sites. Two holes at Site 869 penetrated distal archipelagic-apron sediments near the atoll-guyot pair, Pikinni-Wodejebato. The final Leg 143 drilling was done as a test for shallow-water drilling at Site 870 in the lagoon of Anewetak Atoll.

IGNEOUS FOUNDATIONS

Although the MPM are one of the most prominent Pacific seamount chains, information about the origin and evolution of their volcanic foundations is poor owing to a paucity of igneous rock samples. Before Leg 143, basaltic rocks had been dredged (Hamilton, 1956; Heezen et al., 1973; Nemoto and Kroenke, 1985; Winterer et al., 1993b) and drilled (Shipboard Scientific Party, 1973, 1975) at several locations along the chain; thus, it was clear that a large volcanic pile underlies the MPM. Nevertheless, drilling during Leg
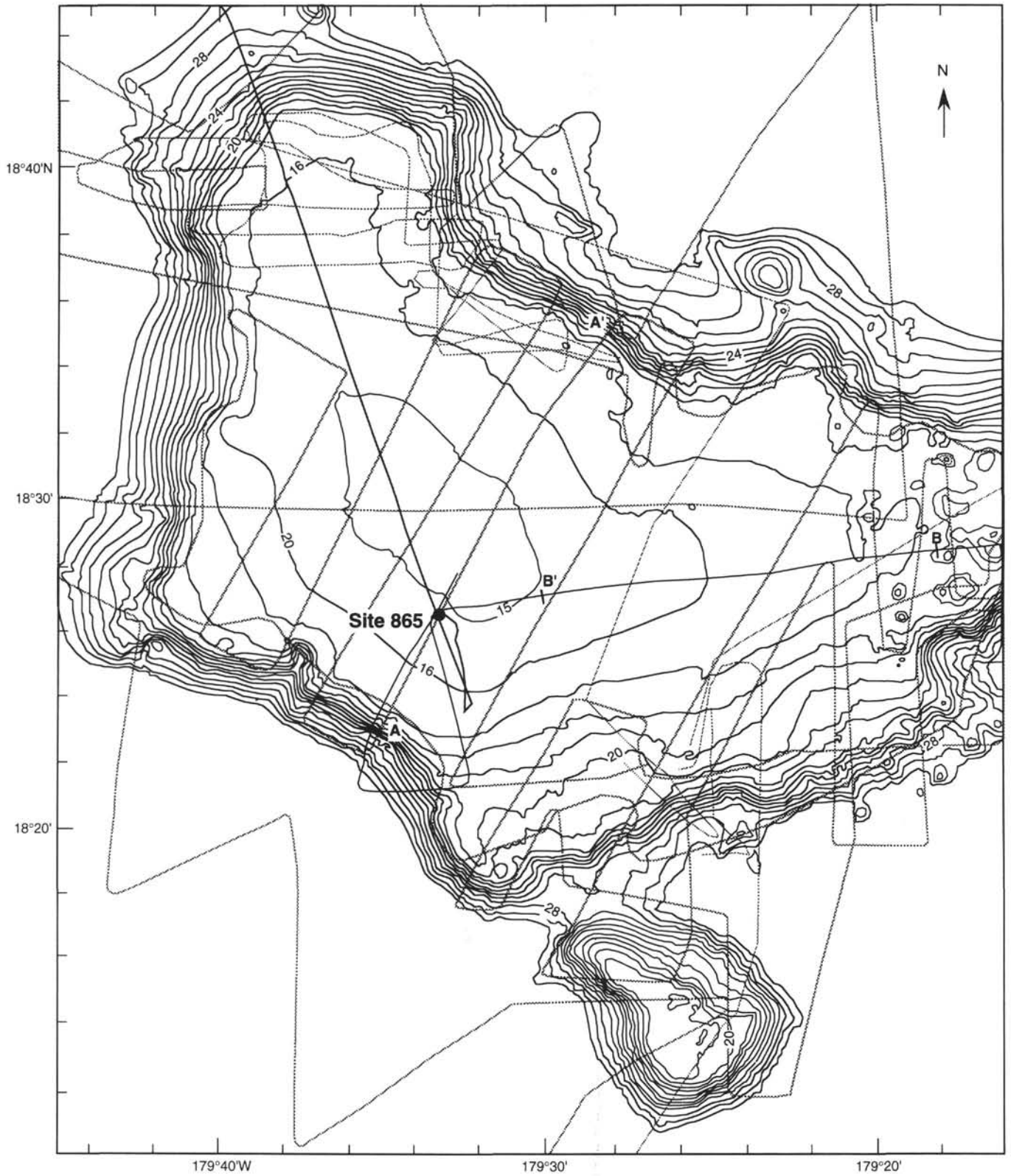
Figure 3. Bathymetry of Allison Guyot summit and geophysical ships' tracks. Bathymetric contours at 100-m intervals above 3000 m are shown; heavy contours at 400-m intervals. Numbers on contours are in hundreds of meters. Bathymetric data were obtained with the SeaBeam multibeam echo-sounder during the 1988 Roundabout Expedition Leg 10 site survey, on board the research vessel *Thomas Washington* (ship's tracks as lighter lines). The darker line is the ship's track of the *JOIDES Resolution* on approach and exit from Site 865. Line A-A' marks the ends of the seismic profile shown in Figure 17, and Line B-B' marks the ends of the seismic profile shown in Figure 18 (modified from Shipboard Scientific Party, 1993b).
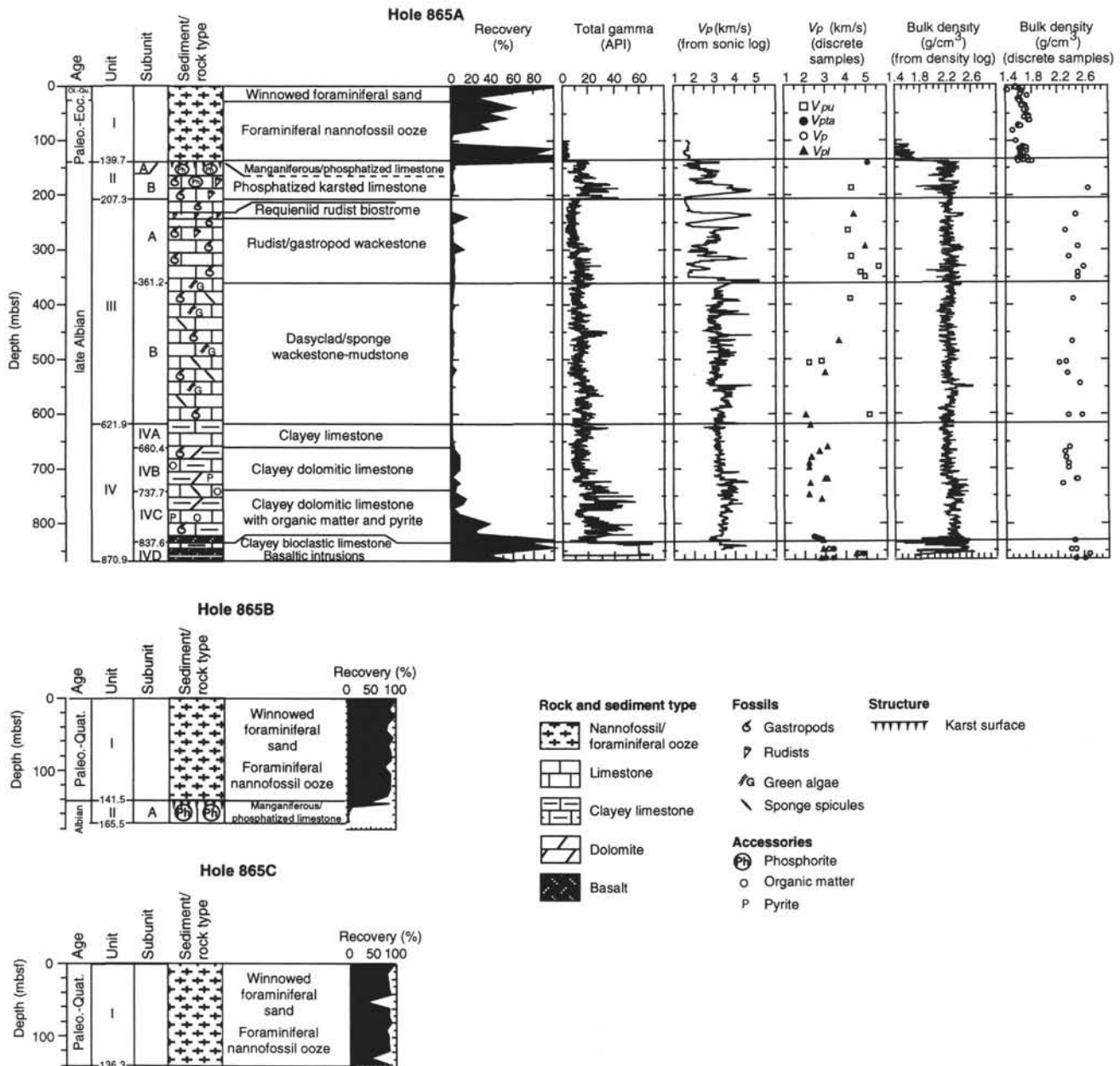
Figure 4. Summary of lithologic units, biostratigraphic dates, physical properties, and logging data from Site 865. Measurements of discrete sample *P*-wave velocities are labeled by orientation: V_{pu} is unoriented; V_{pta} and V_{ptb} are transverse (horizontal); and V_{plv} is longitudinal (parallel to core axis) (from Shipboard Scientific Party, 1993a).

143 obtained the first basalt cores from the central and western parts of the province and represented the first deep penetration of a basaltic edifice in the region.

Basalt Geochemistry and Emplacement

Baker et al. (this volume) discuss the origin, petrology, and geochemistry of basalts cored at Sites 865 and 866. At Site 865, atop Allison Guyot, three highly altered, alkalic basalt sills, with a cumulative thickness of about 25 m, were cored in the bottom 35 m of Hole 865A (Shipboard Scientific Party, 1993b). The structure of the sill contacts implies that the igneous units were intruded while the surrounding clayey limestones were unconsolidated. This observation indicates that sedimentation and igneous activity were simultaneous. On the other hand, seismic-reflection profiles show layering below

the level of the cored sills and onlapping of these layers against a buried hill (Shipboard Scientific Party, 1993b), suggesting that sills were emplaced after significant erosion had begun on the volcano summit. Thus, the relation of the sills to the volcanic edifice is unclear; at the very least, they are probably post-erosional, but they may also be a separate episode of volcanism unrelated to the main phase.

Hole 866A, atop Resolution Guyot, yielded a 124-m section consisting of moderately to highly altered alkalic basalts intercalated with breccia and clay layers (Shipboard Scientific Party, 1993c). The clay layers and oxidized zones indicate that the basalt layers were weathered subaerially and exposed for an extended period of years before being covered by subsequent eruptions. Although we initially thought that the section consisted exclusively of subaerial lava flows, subsequent analysis revealed geochemical variations that, when taken along with the bimodal distribution of radiometric dates (see "Radio-
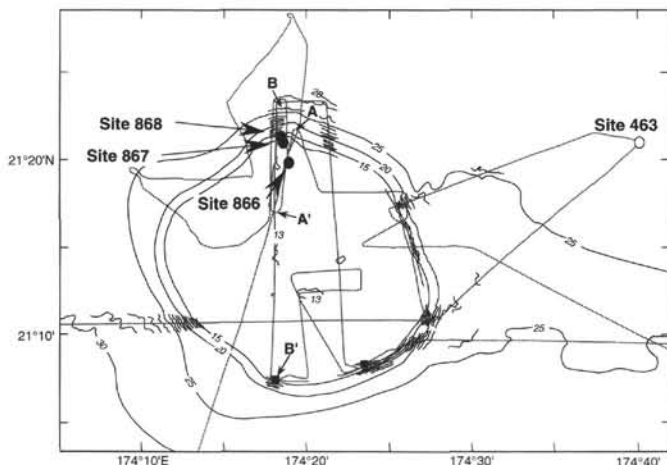
Figure 5. Bathymetry of Resolution Guyot and geophysical ships' tracks. Thin contours shown at 100-m intervals where multibeam data are available; heavy contours show 500-m intervals. Contours labeled in hundreds of meters. Thin gray lines show ships' tracks: site-survey cruise, Roundabout Leg 10 of the Scripps Institution of Oceanography research vessel *Thomas Washington*, and path of *JOIDES Resolution*. Roundabout cruise dredges shown by filled squares. Lines A-A′ and B-B′ denote ends of seismic reflection lines shown in Figures 11 and 12 (from Shipboard Scientific Party, 1993b).

metric Dates" section, this chapter), imply some of the sequence may contain intrusive bodies (Baker et al., this volume). The Hole 866A basalts also display geochemical trends, from mildly alkalic at the bottom to more alkalic in the middle to more tholeiitic at the top, that indicate differentiation of the magma source.

Baker et al. (this volume) conclude that isotopic data show Allison and Resolution guyots probably originated within the region of intense hotspot volcanism known as the South Pacific Isotopic and Thermal Anomaly (SOPITA; Staudigel et al., 1991). Indeed, backtracking the sites (using the plate-motion model of Duncan and Clague, 1985) places them in the SOPITA region (Fig. 8). Both volcanoes probably followed a similar tectonic path and may have passed over more than one hotspot within the region. Indeed, Baker et al. (this volume) consider that the compositional differences between the two sites may be the expression of influxes from two mantle components having different relative contributions at two different hotspots. Geochemical evidence shows the two sites to have distinct, but similar, compositions that are closest to those of the Marshall, Samoan, and Austral islands (Fig. 9); however, available plate-motion models do not backtrack the two sites to a currently active hotspot (Henderson, 1985; Duncan and Clague, 1985).

Radiometric Dates

Constraints on the age of the volcanic underpinnings of the MPM have been and remain few in number. Before Leg 143, age data from the chain consisted of radiometric dates of dredged basalts at a few locations as well as minimum ages determined from DSDP cores in which fossiliferous sediments either contain volcanic detritus or overlie basalt. During Leg 143, basalt was cored at two locations in the MPM, Sites 865 and 866. Pringle and Duncan (this volume) report $^{40}Ar/^{39}Ar$ radiometric dates for these basalts.

Two samples from the basalt sills cored on Allison Guyot (Site 865) gave indistinguishable, concordant, incremental-heating dates with a mean of 110.7 ± 1.2 Ma (Pringle and Duncan, this volume). A third sample gave a slightly younger age, 104.9 ± 2.0 Ma, similar to the 102.7 ± 2.7 Ma age reported for a sample dredged off the guyot flank (Winterer et al., 1993b). Although these dates might show an 8-m.y. history of volcanism on the guyot, Pringle and Duncan argue (this volume) that both of the younger dates may be biased by experi-

mental error or alteration. Thus, they prefer the 110.7-Ma date as the best estimate of the age of the sill complex.

Nevertheless, other evidence suggests that at least two, and as many as three, separate episodes of volcanism occurred on Allison Guyot. Seismic reflection records clearly show layering below the reflector that correlated to the sills at the bottom of Hole 865A (Shipboard Scientific Party, 1993b). These layers onlap the basement; consequently, these sills are probably not the igneous "basement" of the volcanic pedestal. Whether the sills represent a period of post-erosional volcanism or a rejuvenation of the volcano is unclear. Thus, a separate episode of volcanism may have occurred before the emplacement of the sills. On the other hand, a later episode is suggested by the 85.6 ± 1.3 Ma date for another dredge sample from the eastern guyot flanks (Pringle and Duncan, this volume). This later episode may be the source of the volcanic cones on the eastern side of the guyot summit (Winterer et al., this volume). Furthermore, the complex magnetic anomaly suggests post-Cretaceous Quiet Period volcanism (see "Geophysical Signatures" section, this chapter).

Pringle and Duncan (this volume) report incremental-heating results from six samples of the basalts cored in Hole 866A on Resolution Guyot. The dates range from 119.7 to 128.5 Ma, but the authors argue that the data fall into two significantly different groups, with mean ages of 127.6 ± 2.1 Ma and 121.3 ± 1.6 Ma. Because the dates display no simple progression from old to young upsection, Pringle and Duncan contend that the younger units may have been intrusives emplaced approximately 6 m.y. after the extrusive basalts.

Unlike the Site 865 basalts, those cored at Site 866 probably represent the age of the igneous pedestal of Resolution Guyot. This is in part because the cored section is 124 m long and post-erosional eruptions are thought typically to have only small volumes (e.g., Batiza, 1977), and also because the basalt/sediment contact in Hole 866A is thought to be only about 500 m above the top of the igneous plateau that underlies the MPM (Shipboard Scientific Party, 1993c). Furthermore, the younger dates from Hole 866A basalts are in excellent agreement with a $^{40}Ar/^{39}Ar$ radiometric date of 123.1 ± 0.6 Ma from basalt dredged on nearby "Heezen" Guyot (Winterer et al., 1993b). Whether these dates are indicative of the age of the underlying igneous plateau is unclear.

Age data of the Mid-Pacific Mountains generally support the hypothesis that the chain contains an age progression, from Late Jurassic to Early Cretaceous on the western end, to Late Cretaceous on the eastern end (Winterer and Metzler, 1984; Duncan and Clague, 1985). In the western part of the chain, Heezen and Resolution guyots gave ages of 121 to 128 Ma and nearby Site 463 yielded Barremian sediments near basement (Fig. 2). Allison Guyot, in the center of the province, is at least 111 m.y. old. In addition, at the eastern terminus of the chain, Horizon Guyot yielded an age of 88 Ma and nearby Sites 171 and 313 have oldest sediments of Turonian and Campanian age.

Some dates do not fit this progression. Besides the younger, 85.6-Ma date for Allison Guyot, a dredge sample from "Jacqueline" Guyot gave a $^{40}Ar/^{39}Ar$ total-fusion date of 98.5 ± 1.4 Ma (Winterer et al., 1993b). Furthermore, the gap in ages at Allison suggests that younger volcanism may have overprinted the older trend, perhaps as a result of the passage of the province over another hotspot (Henderson, 1985).

Latitudinal Drift

Tracking the Mesozoic tectonic drift of the Pacific Plate has been difficult because of problems in obtaining geophysical data that measure this drift. The plate is covered by water, virtually in its entirety, so paleomagnetic data for the Mesozoic cannot be obtained by traditional means. Furthermore, because Mesozoic hotspot volcanic chains crisscross the western Pacific, often overprinting one another (Henderson, 1985; Duncan and Clague, 1985), the record of the drift of the plate relative to the hotspots has not yet been deciphered for this period. Leg 143 research produced apparently reliable paleolatitude data from three sites (865, 866, and 869). Comparing these data with existing
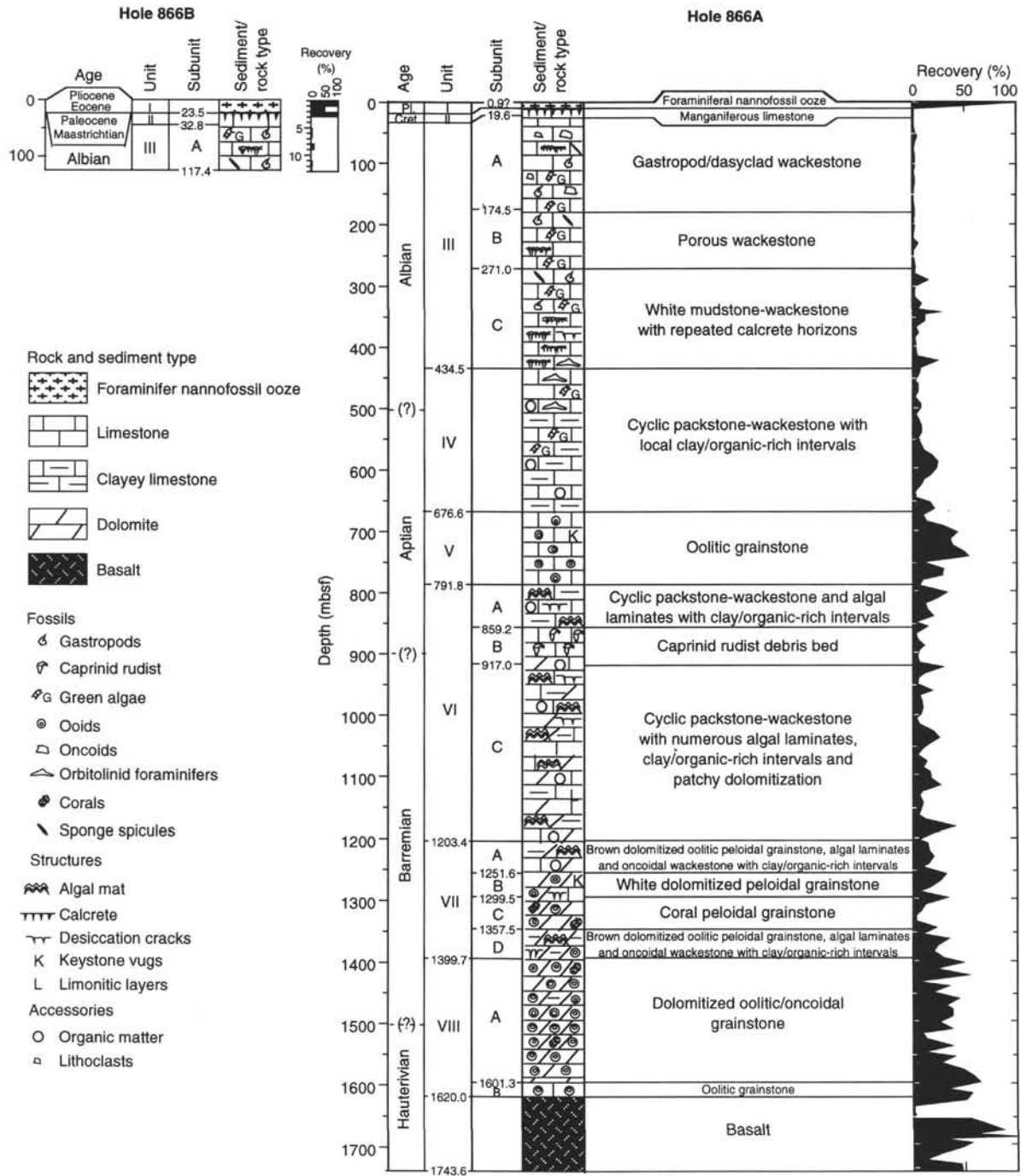
Figure 6. Summary of lithologic units, biostratigraphic dates, physical properties, and logging data from Site 866. Measurements of velocity on discrete samples are labeled according to orientation: V_{pu} is unoriented; V_{pt} (**A**) is transverse (horizontal) for Hole 866A; V_{pl} (**A**) is longitudinal (parallel to core axis) for Hole 866A; V_{pt} (**B**) and V_{pl} (**B**) are transverse and longitudinal for Hole 866B (from Shipboard Scientific Party, 1993c).

Pacific paleomagnetic data, we have been able to determine the latitudinal drift of the MPM with a remarkable degree of precision.

Paleolatitudes were determined from measurements on shallow-water platform limestones at Sites 865 (Sager and Tarduno, this volume) and 866 (Tarduno et al., this volume), and on volcaniclastics from Site 869 (Sager et al., this volume). Paleomagnetic measurements from basalt cores are usually preferable over those from sediment cores because commonly the latter seem to give paleoinclinations that are too shallow, probably owing to the effects of compaction (Gordon, 1990; Tarduno, 1990; Steiner and Wallick, 1992). Unfortunately, insufficient basalt units were cored during Leg 143 to average secular variations

and thereby give accurate paleolatitudes. Nevertheless, Holes 865A, 866A, and 869B all yielded sediments recording paleomagnetic data that compared favorably with existing Pacific paleomagnetic data, including data not derived from sediments.

A paleolatitude for Site 865 was determined using the clayey limestones from the bottom 130 m of Hole 865A (Sager and Tarduno, this volume). Measurements were restricted to this portion of the hole because only the clayey limestones, which contain detritus probably eroded from a nearby volcanic island, were sufficiently magnetic to give reliable paleomagnetic data. These samples indicated a paleolatitude of 14.3° ± 1.1°S (95% confidence limits), and the time to which
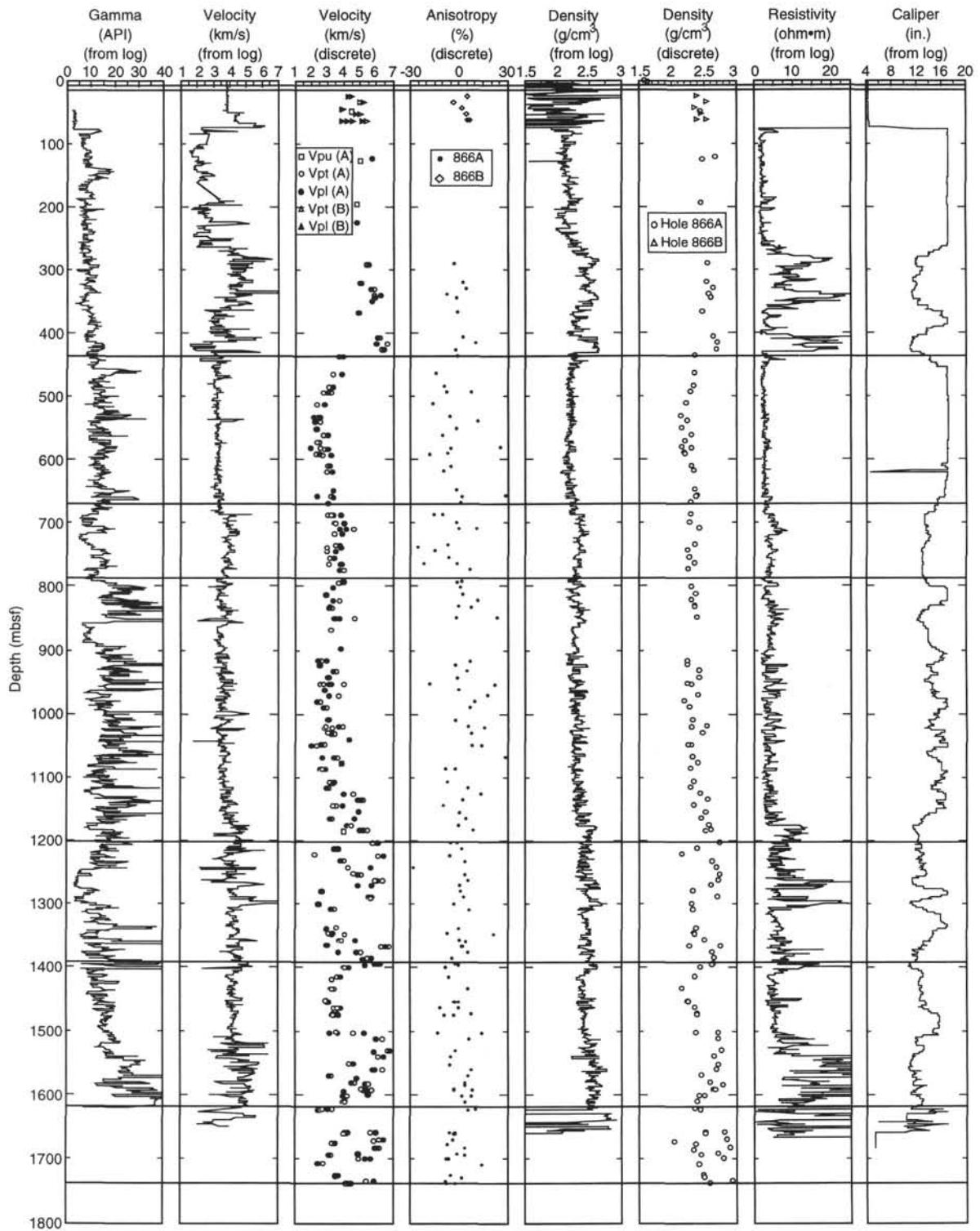
Figure 6 (continued).

it corresponds is probably best estimated by the mean $^{40}Ar/^{39}Ar$ radiometric date for the sills that intruded these sediments, 110.7 ± 1.2 Ma (Pringle and Duncan, this volume).

As at Allison Guyot, paleomagnetic data were obtained only from the bottom part of the Hole 866A section because the upper part was also too weakly magnetic (Tarduno et al., this volume). The Resolution Guyot limestones gave a mean paleolatitude of $14.6° \pm 2.3°S$. Adopt-

ing a date for this datum is complicated by inconsistencies in the M-sequence polarity-reversal time scale. The limestone section records reversals that are probably Chrons M1 through M7 (Tarduno et al., this volume). By the Harland et al. (1990) time scale, these chrons span 124.8 to 132.8 Ma, but the mean of the oldest set of $^{40}Ar/^{39}Ar$ radiometric dates for the basalts beneath the limestones is 127.6 ± 2.1 Ma (Pringle and Duncan, this volume), apparently younger than some
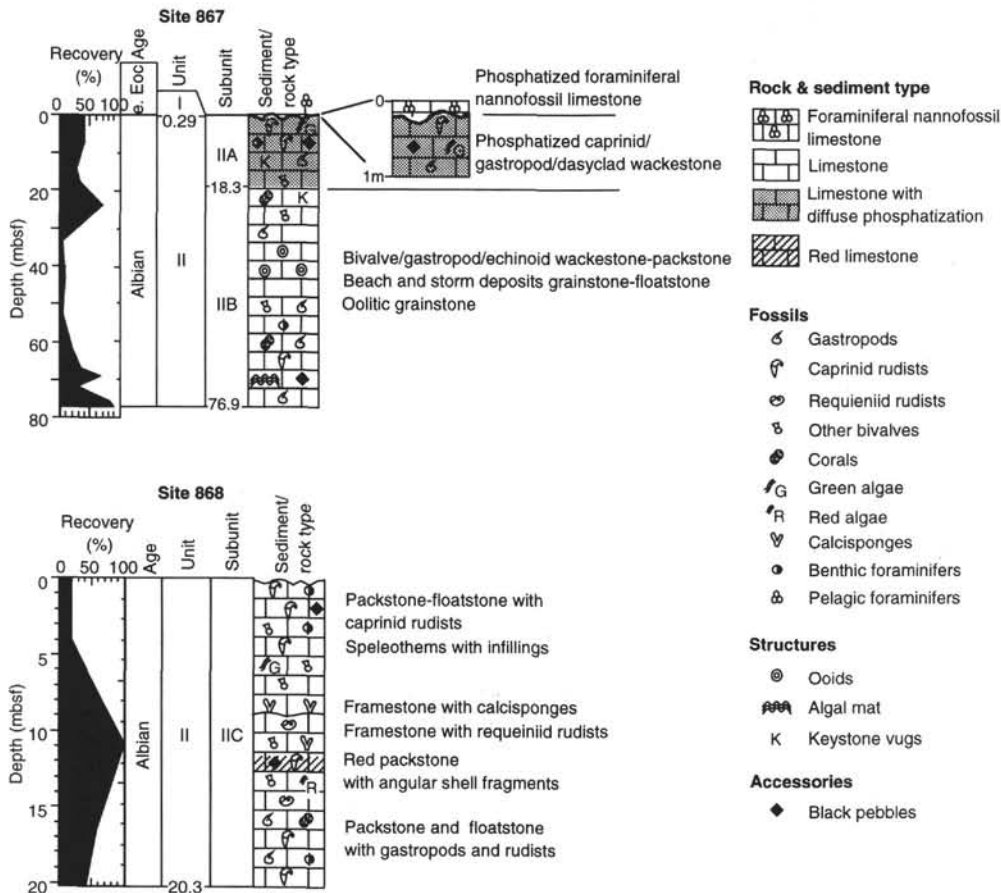
Figure 7. Lithologic summary for Sites 867 and 868 (from Shipboard Scientific Party, 1993a).

of the magnetic reversals. This discrepancy is probably a result of slight errors in the calibration of the time scale and possibly imprecision in the radiometric dates for the basalts.

At Site 869, a thick section was sampled of rapidly deposited Cenomanian volcaniclastics in the Marshall Islands near the atoll-guyot pair, Pikinni and Wodejebato (Shipboard Scientific Party, 1993e). These sediments indicated a paleolatitude of $18.2° \pm 1.2°$S (Sager et al., this volume), whereas a basalt clast recovered from this section yielded a ^{40}Ar/^{39}Ar radiometric date of 96.6 ± 0.8 Ma (Pringle and Duncan, this volume).

To compare paleolatitude data and to derive a paleolatitude curve for the MPM, we "shifted" the above paleolatitudes to Site 866 by subtracting the present-day latitude difference between sites. Although this makes the implicit assumption that the Pacific Plate has not rotated significantly, the assumption should be adequate because Pacific paleomagnetic data indicate that the plate has not rotated by more than 15° to 20° since mid-Cretaceous time (Sager and Pringle, 1988). For more constraints on paleolatitude, we also used mean paleomagnetic poles determined by combining several different types of paleomagnetic data: paleopoles determined from seamount magnetic anomaly inversions, paleopoles calculated from the skewness of seafloor magnetic lineations, as well as DSDP and ODP basalt- and sediment-core paleomagnetic data (Cox and Gordon, 1984; Sager and Pringle, 1988). Revising published poles (Cox and Gordon, 1984; Sager and Pringle, 1988), we derived three poles with mean ages of 126, 104, and 92 Ma. To help in bracketing the age range of the MPM, we also used a paleopole for 85 Ma that was constrained mainly by seamount-anomaly inversions (Sager and Pringle, 1988) and two anomaly-skewness-based poles for the end of the M-series reversals, M0 to M5 and M6 to M10N (Larson and Sager, 1992).
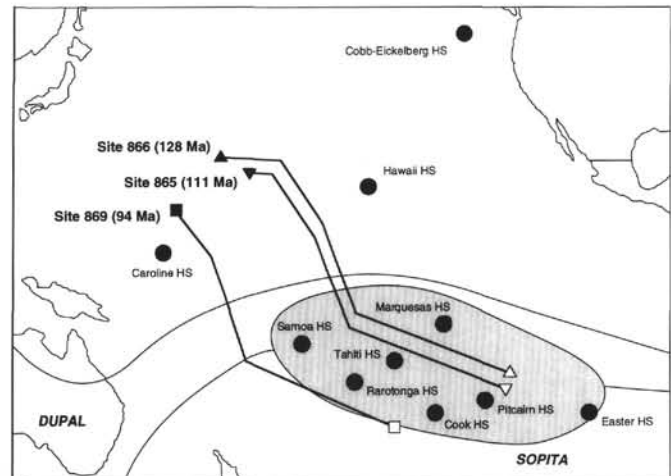
Figure 8. Present-day (filled square and triangles) and original (open square and triangles) locations of Sites 865, 866, and 869, calculated by backtracking using the model of Duncan and Clague (1985) of Pacific Plate motion relative to the hotspots. Ages of volcanism for each site are from Pringle and Duncan (this volume). Geochemical anomaly zones corresponding to the modern SOPITA (Staudigel et al., 1991) and DUPAL (Hart, 1984) are shown for reference. Filled circles show modern active hotspots (from Pringle and Duncan, this volume).

Figure 9. Plot of Nb vs. Zr for basaltic rocks from Leg 143 sites, compared with lavas from other South Pacific seamounts and archipelagos. Note that Sites 865 and 866 points show a simil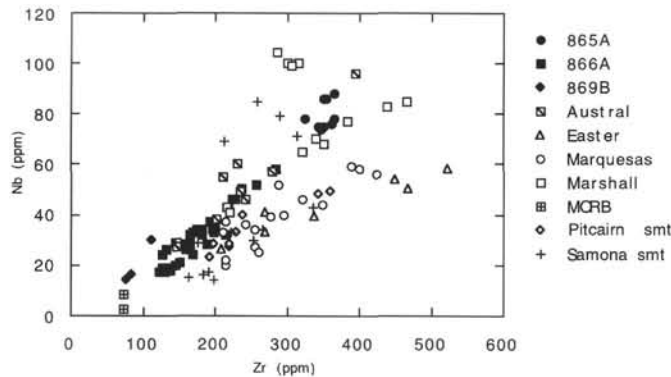ar trend but distinct groupings; also note the similarity to results from the Austral and Marshall islands. Data sources and discussion are given in Baker et al. (this volume).

The resulting paleolatitude curve for Site 866 shows a gradual northward drift, from paleolatitudes of about 14°S, at about 130 Ma, to about 8°S at 98 Ma (Fig. 10). This was followed by a stillstand at a nearly constant latitude, or possibly a turnaround and a slight shift southward, to a paleolatitude of about 10°S at 85 Ma. The turnaround is uncertain because total southward drift between 98 to 85 Ma is within the 95% confidence limits of the paleolatitudes; nevertheless, the alignment of the paleolatitudes in Figure 10 is suggestive. If confirmed, this southward trend is one previously unrecognized in Pacific tectonics because it is currently thought that the plate was moving northward at this time (e.g., Duncan and Clague, 1985). Indeed, a southward drift is in conflict with the apparent northwestward motion shown by seamounts in the Musicians province from 96 to 85 Ma (Pringle, 1993).

According to Larson et al. (1992), the ancestral Pacific Plate drifted southward by approximately 12°, before turning to a northward drift during Barremian to Aptian time. Our results from Hole 866A imply that the turnaround for Resolution Guyot was at about 14°S and that neither this guyot nor others in the MPM ever traveled far enough south to cross the present-day Darwin point. Thus, the hypothesis that southward drift killed the carbonate platforms atop these guyots, by carrying them out of the tropical zone suitable for reef growth (Winterer and Metzler, 1984), is unfounded unless it can be shown that the zone conducive to carbonate growth was significantly narrower during the Cretaceous. Moreover, some investigators have suggested that the carbonate platforms may have been killed by drifting to the dry zone at the equator (Erba et al., 1993), but in Figure 10, we show that Resolution Guyot was at 8°S at the end of the Albian when its carbonate factory shut down. Allison Guyot, which died simultaneously, must have been 3° farther south.

Origin and Formation of Igneous Basement

The MPM have an unusual morphology in comparison with other western Pacific seamount chains. Rather than consisting of a linear grouping of relatively discrete seamounts, the MPM appears as more of a plateau, with large areas above the regional seafloor depths (Fig. 1). On the other hand, unlike most Pacific plateaus (except for the Tuamotu Plateau), which consist of large, amorphous volcanic piles, the MPM is surmounted by numerous guyots. It appears that beneath the MPM exists a plateau 1 to 2 km in height (Winterer and Metzler, 1984; Kroenke et al., 1985). This is topped by guyots surrounded by as much as 1 km of sediment.

The age and composition of the MPM plateau is still uncertain because it has never been sampled, although Hole 866A may have come close. Magnetic lineations surround the plateau, becoming younger
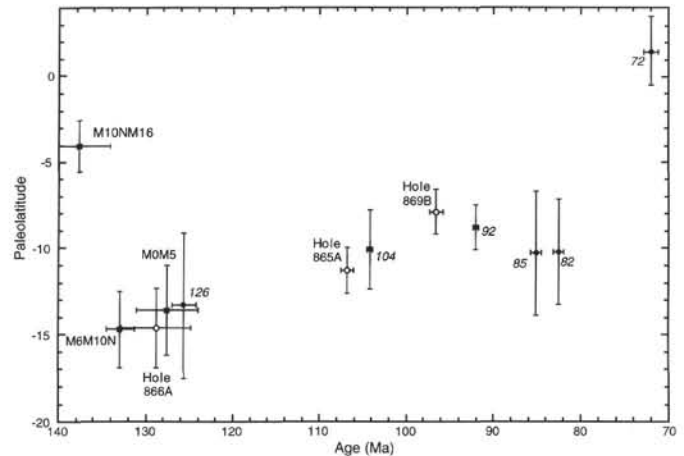

Figure 10. Paleolatitude vs. age curve for Site 866. Open squares represent paleolatitudes determined from sediment cores for Sites 865 (Sager and Tarduno, this volume), 866 (Tarduno et al., this volume), and 869 (Sager et al., this volume). The paleolatitudes from Sites 865 and 869 were corrected to the latitude of Site 866. Filled circles denote paleolatitudes inferred from mean paleomagnetic poles from the Pacific apparent polar wander path (Sager and Pringle, 1988; Sager et al., unpubl. data, 1994). These poles were calculated by combining paleomagnetic data from seamount anomaly inversions as well as paleolatitudes determined from DSDP and ODP basalt and sediment cores. They are labeled, in italics, by age in millions of years. Filled squares show paleolatitudes determined from the skewness of seafloor magnetic lineations M0 to M5, M6 to M10N, and M10N to M16 (Larson and Sager, 1992). Vertical bars show 95% confidence limits of paleolatitude; horizontal bars show either one standard deviation of error on mean age or on basalt radiometric dates, or age ranges for points having ages constrained by biostratigraphy or magnetostratigraphy. The stippled band shows paleolatitude trend, fit by eye.

eastward, and range from M0 to M29 (Fig. 2; Nakanishi et al., 1992). The closeness of geologic dates from the guyots and the extrapolated age of the underlying lithosphere indicates that the plateau cannot be much younger than the lithosphere. For example, at Resolution Guyot, where the oldest radiometric dates average 128 Ma, the underlying lithosphere is estimated to be either M23 age (152 Ma) or M11 (136 Ma) age, depending on whether it is on the north or south side of the major offset fracture zone that runs through the western MPM (Fig. 2). Likewise, Allison Guyot, which is at least 111 Ma in age, sits near M2 (128 Ma). Thus, it may be that some of the guyot pedestals formed at the same time as the plateau. Indeed, this may be the case for Resolution Guyot, whose basalt pedestal cannot rise much above the plateau, given the depth to basalt in Hole 866A.

Some investigators have suggested that the MPM formed as the Pacific Plate drifted over a relatively stationary hotspot (Henderson, 1985; Duncan and Clague, 1985). In general, these models have the MPM formed during the period from about 150 to 100 Ma, but have poor age constraints, owing to a paucity of age data. These models also imply that the MPM and Line Islands crossed more than one hotspot, potentially giving rise to a mixture of age trends. Age data from the MPM are broadly consistent with the hotspot hypothesis: ages seem to become younger eastward and are in the expected age range. Some ages and other evidence (see "Magnetic Anomalies" section, this chapter) imply overprinting, perhaps caused by a second hotspot. Although the hotspot models indicate the MPM originated over the South Pacific Superswell (Fig. 8), the chain cannot yet be traced to a present-day hotspot. In part, the problem may be the complexities of intersecting hotspot traces, but the hotspot-based plate-motion models also require updating.

A comparison of the MPM bathymetry with the paleolatitude curve (Fig. 10) gives some interesting insight to the plate-motion question. Indeed, if we assume that the bathymetric trends show the

plate motion relative to a hotspot, a remarkable similarity to the paleolatitude trend exists. The MPM can be divided into three segments, the western and eastern parts, both of which trend northeast, and the central segment, which trends southeast (Fig. 1). If this shape were formed by the drift of the plate over a nearly fixed hotspot, the northeast trends indicate a southward latitudinal drift, whereas the southeast trend denotes a northerly drift. Thus, the western end of the MPM may represent the continued southward drift of the ancestral Pacific Plate, noted by Larson et al. (1992). The turnaround near Resolution Guyot corresponds to the southernmost paleolatitudes, shown in Figure 10, at about 130 Ma. The plate then proceeded north until another turnaround, to the east of Allison Guyot. This could be the paleolatitude turnaround seen at about 98 Ma (Fig. 10). We note that the distance between the northern and southern turns in the MPM bathymetry is approximately 4° to 5° and that this is reasonably close to the 6° paleolatitude difference indicated in Figure 10.

After 98 Ma, the paleolatitudes suggest that the plate stayed at the same latitude or drifted slightly southward, which corresponds to the easternmost segment of the MPM (Fig. 1). As noted above, this conflicts with age/trend data from the Musicians Seamounts. On the other hand, both the Musicians and northern Line Islands seamounts are copolar and are thought to have formed contemporaneously (Pringle, 1993), but the northern Line Islands seem to be younger where they intersect the MPM. Consequently, either a problem exists with the assumption that they formed simultaneously by drift over two hotspots or the age data are misleading.

After 85 to 82 Ma, the Pacific apparent polar wander path contains a bend at nearly right angles and shows subsequent rapid apparent polar wander northward toward the pole (Sager and Pringle, 1988). The later polar-wander trend is widely accepted as an indication of relatively rapid northward motion of the Pacific Plate during the Late Cretaceous, which continued into the Cenozoic. Radiometric dates from the northern Line Islands, near the intersection with the easternmost MPM, are virtually contemporaneous with this abrupt shift (Fig. 2; Schlanger et al., 1984), which suggests that both resulted from the same reorganization in plate motions. The trend of the Line Islands is consistent with post-82-Ma northward drift, and several authors have modeled the formation of the bulk of the Line Islands by the northwestward drift of the plate over a hotspot from about 85 to 43 Ma (Epp, 1984; Duncan and Clague, 1985; Henderson, 1985).

LOWER CRETACEOUS LIMESTONE SUCCESSION

One of the main objectives of Leg 143 was to piece together the stratigraphy of the Lower Cretaceous limestone successions, known previously only from dredging and from reflection seismic profiling. Before drilling, we knew that the uppermost parts of the limestone were Albian in age (Winterer et al., 1993b), but we had few clues for estimating the basal ages of the limestone caps on any of the many Cretaceous guyots in the northwest Pacific. At DSDP Site 171 on Horizon Guyot (Fig. 2), the drill penetrated about 135 m of pre-late Cenomanian shallow-water limestone to basaltic basement (Shipboard Scientific Party, 1973). At DSDP Site 463, in the basin only 25 km northeast of Resolution Guyot, the drill bottomed in beds of upper Barremian deep-water limestone with interbeds of redeposited shallow-water limestone debris, indicating that the base of the platform limestone succession of the adjacent bank was at least that old.

Many of our hypotheses of the evolution of the limestone caps atop MPM and other Pacific guyots were derived from seismic reflection lines across these features, typically acquired using a single-channel hydrophone array and an air gun or water gun of modest size. At both guyots, the reflections are reasonably coherent and traceable over the central parts of the guyot, which is blanketed with a variable thickness of pelagic sediments. Our interpretation was that these horizontal reflectors below the pelagic cap represent well-stratified lagoonal sediments (van Waasbergen and Winterer, 1993). The reflections become incoherent where the pelagic sediments are thin or

absent, which is the general case around the outer parts of the platform. Before drilling, we had interpreted these seismically incoherent zones as massive, framework reefs (van Waasbergen and Winterer, 1993). However, in light of our inability to find such reefs, we now think that this effect is probably the result of the presence of a rough pavement of phosphorite and ferromanganese oxides where pelagic carbonate sediments are not present (see Winterer et al., this volume).

This picture of guyot architecture was further reinforced by the morphology of the guyots, both in the MPM and elsewhere in the northwest Pacific, as revealed in multibeam swath maps. Many guyots have a reeflike perimeter rim standing from about 20 to almost 200 m above a deeper, interior, lagoonlike region. It was only with multibeam swath-mapping surveys (van Waasbergen and Winterer, 1993) that the rims were recognized to be primarily of erosional origin, probably produced during a regional episode of emergence and subaerial erosion in post-latest-Albian, pre-Turonian time.

From the seismic profiles, estimates could in principle be made of the thickness of limestone strata above basaltic basement. This procedure requires (1) that the velocity structure of the limestone be known and (2) that there be a clear indication of a deepest reflector to mark the top of basaltic basement, rather than some high-impedance layer above basement that masks deeper layers. Neither of these conditions was satisfactorily met with the data at hand before drilling during Leg 143. The top of basement was impossible to fix at Resolution Guyot because of the lack of a strong reflector marking the base of the succession of reflectors; instead, the reflections gradually attenuated the deeper we looked. Velocity estimates were based on reflection times through limestone to good reflectors in the guyot interior compared with reflection times through water to the projected outcrop of the same reflector traced as closely as possible to the edge of the guyot. Because of the omnipresent zone of incoherent reflectors around the perimeter of the platforms, reflectors could not be traced satisfactorily to the outer slope, except on the southeastern side of Allison Guyot, where a slump has carried away a big slice of the perimeter region, exposing beds in the guyot interior. As shown by drilling results, most of our velocity estimates were too low, and we thus underestimated the total thickness of the limestone at both guyots.

Resolution Guyot: Sites 866, 867, and 868

To characterize the major platform-carbonate facies at Resolution Guyot, a transect of three sites was drilled along a line perpendicular to the north margin (Figs. 5, 11, and 12). The three sites constitute a radial transect from very close to the platform edge to a point about 1.8 km inward from the edge. Only the upper 80 m of strata, all in the upper Albian and truncated at the top by an irregular erosional surface, was sampled at all three sites. For deeper levels, we must rely only on data from Hole 866A, keeping in mind that it is located in the platform's interior, in late Albian coordinates. At the time of accumulation of the carbonates succession, Resolution Bank—it was a bank at sea level before it became a guyot—was located in the Southern Hemisphere, between about 8° and 14°S. The bank thus was located in the belt of the southeast trade winds, and the northern side of the bank would have been sheltered from the main force of the waves generated by these winds. Typhoon winds, on the other hand, can come from any direction. We summarize below the main features of the stratigraphy of the Lower Cretaceous limestone successions at the three sites.

Age Control

Several independent methods were used to date rock samples recovered at Site 866. For the basaltic basement, we have $^{40}Ar/^{39}Ar$ dates and extrapolation from ages of overlying sediments. For the shallow-water limestone succession, we have strontium- and carbon-isotopic data, which can be compared to strontium- and carbon-isotopic data from well-dated Lower Cretaceous successions in
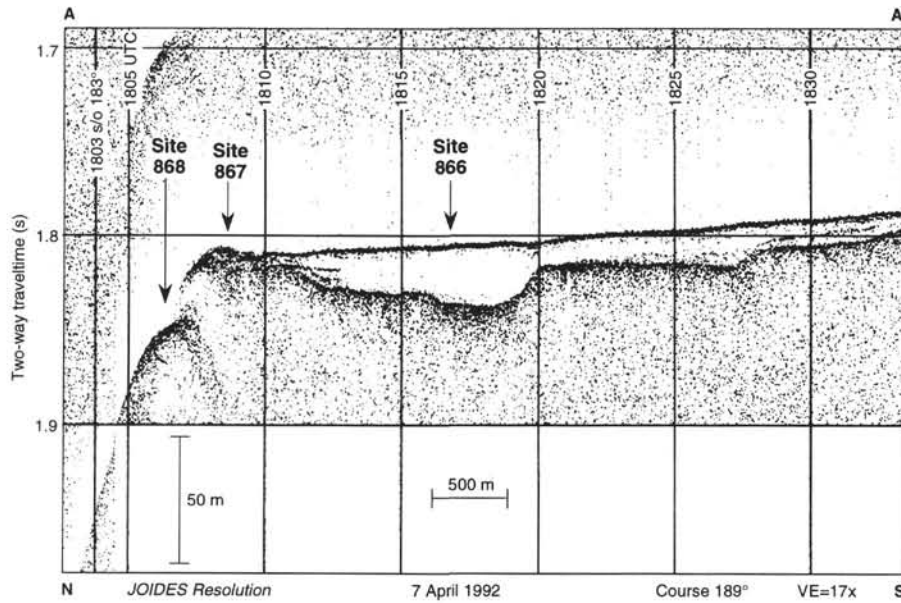
Figure 11. 3.5-kHz echo-sounder profile over Sites 866, 867, and 868 taken on board the *JOIDES Resolution* during pre-drilling site survey on 7 April 1992. Time plotted along horizontal axis; two-way traveltime plotted vertically. Location shown by Line A-A′ in Figure 5 (from Shipboard Scientific Party, 1993c). VE = vertical exaggeration at the seafloor.
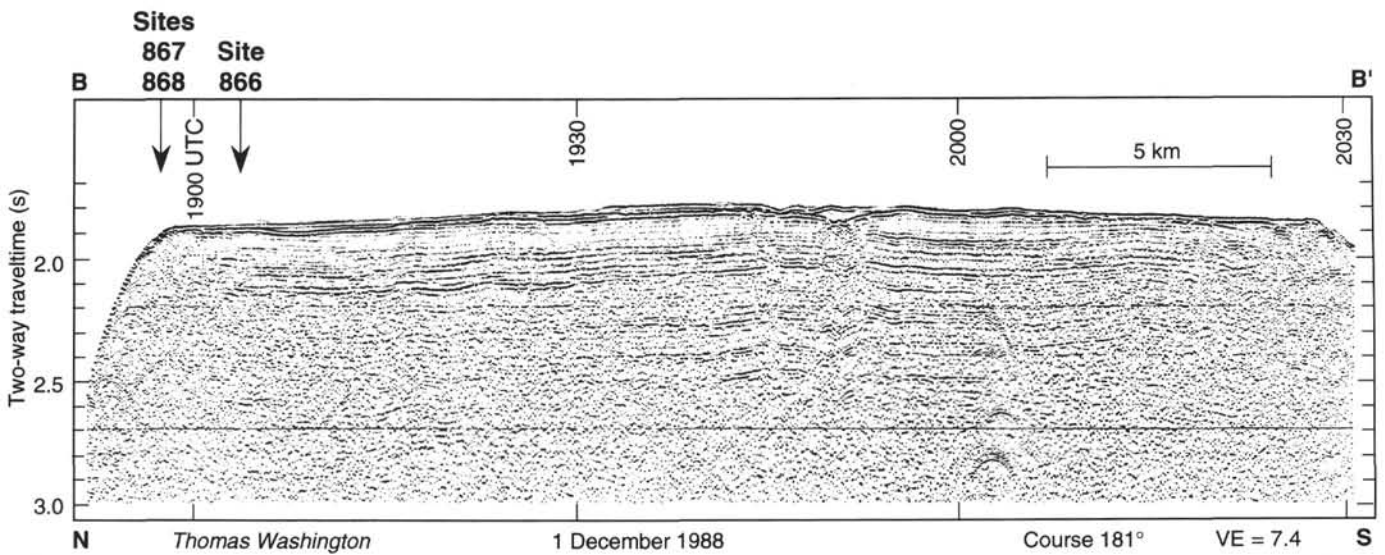

Figure 12. Seismic reflection profile across Resolution Guyot, taken by the research vessel *Thomas Washington* during the Roundabout Leg 10 site-survey cruise on 1 December 1988. Time plotted along horizontal axis; two-way traveltime plotted vertically. Location shown by Line B-B′ in Figure 5. Locations of Sites 866, 867, and 868 were projected into the line from their actual locations about 0.9 to 1.9 km to the east (from Shipboard Scientific Party, 1993c). VE = vertical exaggeration at the seafloor.

Europe, and we have age estimates from benthic foraminifers, whose age ranges are known with varying degrees of certainty from other parts of the world. In addition, magnetic reversals observed in the lower limestone section can be correlated with polarity-reversal time scales. Results for these dating schemes are summarized in Figure 13.

Age Estimates from $^{87}Sr/^{86}Sr$

Jenkyns et al. (this volume) determined the $^{87}Sr/^{86}Sr$ ratio for 97 samples from the 1620-m succession of shallow-water carbonates drilled at Hole 866A, averaging about one sample per 16 m. Owing to pervasive diagenesis, sampling had to be limited in the dolomitic part of the succession, below about 1200 m depth. Because curves of

$^{87}Sr/^{86}Sr$ values vs. time show distinctively shaped maxima and minima within the paleontologically well-dated Cretaceous successions in England (Jones, 1992; Jones et al., 1994), Jenkyns et al. (this volume) were able to compare this reference curve with an analogous curve derived for the Hole 866A section and thereby to estimate ages. Column 1 in Figure 13 shows the placement of stage boundaries in the succession at Hole 866A, as estimated by this procedure (Jenkyns et al., this volume).

Jenkyns et al. conclude that the succession ranges in age from Hauterivian to latest Albian (Fig. 13). The estimate of Hauterivian age for the basal 100 m or so is not as well constrained as are the Barremian/Aptian and Aptian/Albian boundaries. The top of the succession is judged to be near the Albian/Cenomanian boundary, keep-

ing in mind that the Sr-isotope curve for England is nearly flat for the upper third of the Albian.

Age Estimates from δ¹³C

Jenkyns (this volume) has determined $\delta^{13}C$ values for about 150 samples from Hole 866A, with an average spacing of about 10 m. Sample spacing was roughly equal over all parts of the succession. Comparisons with values from well-dated Cretaceous pelagic-limestone successions from Italy (Weissert and Lini, 1991) provided the basis for estimating stage boundaries in Hole 866A, as shown in Column 2 of Figure 13. Agreement with the Aptian/Albian and Barremian/Aptian boundaries, estimated from strontium data, is good and the placement of the Hauterivian/Barremian boundary at about 1400 m is not much different from the more loosely constrained estimate of about 1500 m from the strontium data.

A notable feature of the carbon-isotopic data from Hole 866A is the strong negative spike in carbon-rich claystone layers between about 831 and 859 mbsf. Jenkyns (this volume) correlates this spike with the similar spike seen in carbon-isotope records, and in organic-carbon contents, from the so-called Selli Level in lower Aptian strata (*Globigerinelloides blowi* Zone) at many places around the world (e.g., Sliter, 1989; Weissert, 1989; Weissert and Lini, 1991). Using this spike as a starting point, Jenkyns correlates the carbon-isotope curve between 600 and 800 mbsf from Site 866 with the succeeding planktonic foraminifer zones of the lower and middle Aptian, namely the *Leupoldina cabri, G. ferreolensis, G. algerianus*, and *Hedbergella trochoidea* zones.

Age Estimates from Benthic Foraminifers

The virtual absence of planktonic foraminifers, calcareous nanno-fossils, and palynomorphs and the patchy occurrence and incomplete preservation of rudists and other stratigraphically significant mollusks in the shallow-water limestone strata of Resolution Guyot means that the biostratigraphy of these rocks is based almost entirely on benthic foraminifers (Fig. 13, Col. 4; Arnaud-Vanneau and Sliter, this volume). Although the stratigraphic distribution of the more important Lower Cretaceous benthic foraminifers is well known in the Tethyan realm from Mexico to the Crimea, knowledge of the distributions in the Pacific Ocean was poor before the work of Legs 143 and 144 (Arnaud-Vanneau and Sliter, this volume).

For the lowermost part of the succession at Hole 866A (about 1223–1620 mbsf), correlations to Romania suggest that the entire Hauterivian sequence may be present. In addition, the interval from 763 to 1223 mbsf has been assigned an age of Barremian–early Aptian. The sequence from 522 to 763 mbsf is regarded as late Aptian(?) to early Albian(?) in age. At MIT Guyot, drilled during Leg 144, the late Aptian–early Albian(?) benthic foraminifer fauna is well documented (Shipboard Scientific Party, 1993f), but at Resolution Guyot, the record seems less complete and continuous and may include hiatuses (Arnaud-Vanneau and Sliter, this volume). At Hole 866A, the orbitolinid species *Paracoskinolina* cf. *sunnilandensis* suggests that middle Albian strata occur as low as 434 mbsf, suggesting the possibility of an unconformity between middle Albian beds above and either lower Albian or upper Aptian strata below. Notably, this is also the contact between lithologic Units III and IV, where an abrupt change in physical properties and a significant seismic reflector occur. Arnaud-Vanneau and Sliter (this volume) assign the strata between 522 and 135 mbsf to the middle(?)–upper Albian, and the beds between 135 and 20 mbsf to the upper Albian.

At Sites 867 and 868, benthic foraminifers of Albian age were identified (Shipboard Scientific Party, 1993d), and in Hole 866A, the upper 115 m of limestone has been dated as late Albian by Arnaud-Vanneau and Sliter (this volume). Judging from the nearly horizontal reflectors on the seismic profile between Sites 866, 867, and 868
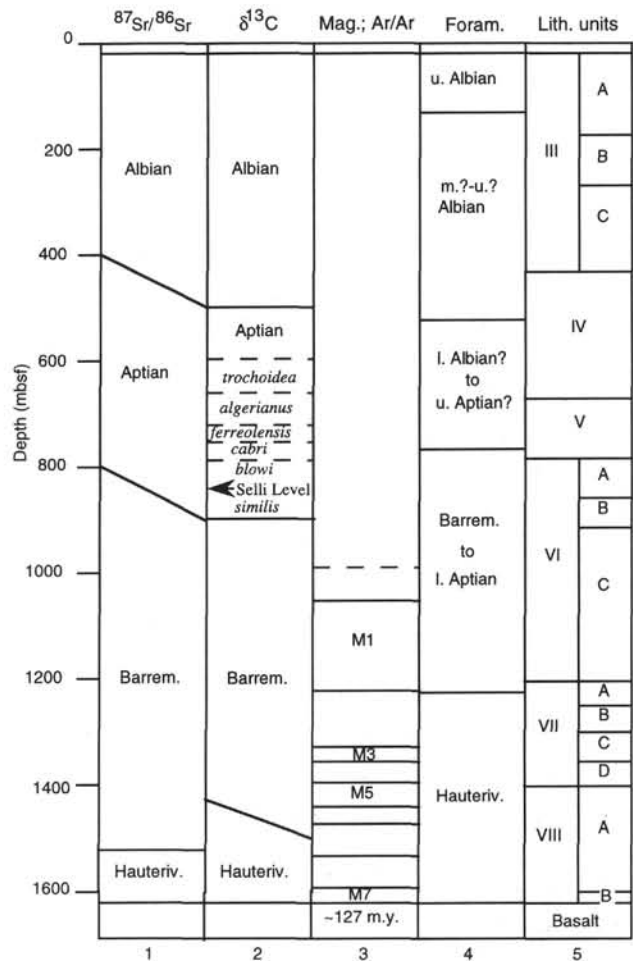

Figure 13. Lower Cretaceous stratigraphy in Hole 866A. Age constraints are Sr-isotope ratios for Column 1 (Jenkyns et al., this volume), $\delta^{13}C$ values for Column 2 (Jenkyns, this volume), magnetic stratigraphy and radiometric dates for Column 3 (Tarduno et al., this volume; Pringle and Duncan, this volume), and benthic foraminifers for Column 4 (Arnaud-Vanneau and Sliter, this volume). Lithologic units are shown for comparison in Column 5 (Shipboard Scientific Party, 1993c).

(Figs. 11 and 12), the lower 44 m of strata penetrated at Site 867 correlates with the uppermost 44 m of limestone at Site 866, whereas the upper 33 m of limestone at Site 867 is missing at Site 866 by reason of erosion. At Site 868, the entire 20 m of drilled limestone correlates with the uppermost 20 m of limestone at Site 866.

Isotopic vs. Foraminifer Age Estimates

The only significant discrepancy between the foraminifer and isotopic age estimates is the placement of the Hauterivian/Barremian boundary, which is estimated at about 1400 to 1500 mbsf isotopically, but at about 1223 mbsf using foraminifers (Fig. 13). Examination of the chart showing distribution of key species at Hole 866A (Arnaud-Vanneau and Sliter, this volume) indicates that the main marker fossil for the upper Hauterivian, *Campanellula capuensis*, has its highest occurrence at 1387 mbsf, whereas the possible Barremian species do not appear until 1223 mbsf. If the boundary were placed at the base, rather than at the top, of this gap, the discrepancy with the isotopic estimates narrows to no more than about 100 m. Given the sparse isotopic data in the lower part of the succession, the two methods result in about the same placement of the boundary: at about 1400 mbsf.

Age Constraint from Rudists

Although rudists have been dredged from many guyots in the northwest Pacific, their stratigraphic distribution is as yet poorly known, and it is necessary to use the better known ranges in other parts of the Tethys to estimate ages. Rudists occur only sporadically in Hole 866A, but their occurrences add useful information about the ages of the strata. From a depth of 1233 mbsf, Swinburne and Masse (this volume) identified a rudist belonging to *Petalodontia*, a genus elsewhere not known in strata older than Barremian (although rudist data from the Hauterivian are sparse). Caprinid rudists occur commonly between 859 and 917 mbsf, and the forms in this interval, according to Swinburne and Masse (this volume), most closely resemble those described from the lower Aptian of the Tethys. In addition, Swinburne and Masse (this volume) report *Caprina(?)* cf. *mulleri* in strata dated as Albian with benthic foraminifers at Site 867.

Age Estimates from Magnetic Polarity

Magnetic polarity measurements from limestone samples from Hole 866A, reported by Tarduno et al. (this volume), indicate a sequence of reversals in the lower 600 m of the section (Fig. 13, Col. 3). Preliminary identification of these reversals with the standard polarity-reversal sequence and the correlation with biostratigraphic ages suggest that the uppermost reversed interval in Hole 866A (1054–1219 mbsf) plausibly correlates with polarity Chron CM1. This correlation depends in part on the carbon-isotopic identification of the Selli Level in the *G. blowi* Zone of the lower Aptian, above the highest polarity reversal detected at Hole 866A (at about 840 mbsf). Assuming no polarity chrons are missing, the successively deeper reversals may be assignable to CM2–CM7.

As pointed out by Tarduno et al. (this volume), such a correlation scheme implies considerable variations in rates of sedimentation. Notably, the relative thickness of postulated polarity Chron CM3 is much less than expected from the polarity-reversal time scale. Thus, an unconformity may exist within this interval. If the chrons are correctly identified, sedimentation rates for CM7 through CM4 would have been only about half those for CM2 through CM1, implying a significant departure from the expected exponentially decreasing subsidence rate for a seamount.

The combination of radiometric dates, biostratigraphy, and magnetic stratigraphy from Resolution Guyot may have an important role in refining the geologic and magnetic polarity-reversal time scales. The radiometric dates place the formation of Resolution Guyot near the Hauterivian/Barremian stage boundary. In the widely cited time scale of Harland et al. (1990), this boundary is dated at 131.8 Ma and is just beneath polarity Chron M7. Isotopic stratigraphy from Hole 866A implies that the base of the limestone section is Hauterivian in age (Jenkyns et al., this volume). Furthermore, results from magnetic stratigraphy suggest that the lower limestone section records Chrons CM1 through CM7 (Tarduno et al., this volume). Thus, Leg 143 results suggest that the Hauterivian/Barremian boundary may be slightly younger and occur above M7. Indeed, a more recent time scale has the boundary at 127.0 Ma, correlated with M5 (Gradstein et al., in press).

Lithofacies

Facies Succession at Site 866

At Hole 866A, a column of Lower Cretaceous limestone about 1620 m thick was drilled and continuously cored (Fig. 6), with an average core-recovery rate of about 14%. Owing to the strength of the cemented rocks, the hole was remarkably stable, and even though washouts increased the hole diameter in some intervals, we were able to obtain a nearly complete set of downhole logs. These logs compensate in the upper parts of the hole for poor core recovery; and, by comparing log responses to cores in parts of the hole where recovery was good, a nearly complete reconstruction of the lithologic succession could be made (Cooper et al., this volume).

As shown in the cores, this succession is composed almost entirely of shallow-water facies, with water depths that range mainly from intertidal to only shallow subtidal (Strasser et al., this volume). Given the potential short-term rates of sedimentation for modern low-latitude, shallow-water carbonates of between about 0.2 and 1.2 cm/k.y. (200–1200 m/m.y.) (Schlager, 1981), it is clear that the long-term rates of sedimentation on the Resolution platform were limited by subsidence rates, which ranged from about 30 to 70 m/m.y. (Fig. 14) (Jenkyns, this volume). This in turn implies that much (perhaps as much as 90%) of the 30 m.y. may not be represented by sediments, but rather is lost in diastems between strata. As shown by Strasser et al. (this volume), the stratal succession within the cores is dominated by meter-scale, shallowing-upward sequences that commonly show exposure features, such as calcrete, bird's-eye vugs, desiccation fissures, calcified algal-microbial mats, and karstified surfaces at their tops. Because carbonate sedimentation ceases above sea level on the platforms, time spent in the supratidal environment is not registered by the accumulation of strata. A similarly punctuated succession of lagoonal carbonates is documented from drill-hole data for the Neogene at Anewetak lagoon by Quinn and Matthews (1990).

Although the limestone succession seems to be more or less complete, from Hauterivian to Albian, the sparse age control may hide one or more significant unconformities. As indicated above, there is a suggestion in the foraminifer data that the upper Aptian–lower Albian succession at MIT Guyot, drilled during Leg 144, is more complete than the same interval at Hole 866A. This issue reappears when subsidence rates are considered (see "Subsidence Rates" section, this chapter). Furthermore, the thickness of magnetic-polarity units, observed in the lower limestone section, does not match well with the polarity-reversal time scale, suggesting punctuation by hiatuses.

In detail, the succession in Hole 866A divides itself into six major and two minor lithologic units (Fig. 6). The lowest 220 m (Unit VIII), of Hauterivian age, consists of oolitic and oolitic-oncoidal grainstone, strongly dolomitized, except for the lowest 20 m directly above volcanic basement. This unit is interpreted as having been deposited on a shallow ramp facing the open sea. The occurrence of oolites is consistent with a relatively rapid rate of subsidence of the platform early in its history (Fig. 14). These beds pass upward into about 200 m of more restricted facies (Unit VII), with dolomitized peloidal grainstone, oolitic grainstone, oncoidal wackestone, and algal laminites. Peritidal environments are inferred, with meter-scale, shallowing-upward sequences that begin at the base in shallow, subtidal facies and change upward to intertidal facies having desiccation cracks, keystone vugs, and blackened grains indicating exposure. Dolomitization decreases progressively toward the top of this interval. Above 1200 mbsf, dolomite is present only intermittently, and it disappears entirely above about 900 mbsf.

From about 1200 to 435 mbsf (Units VII, V, and IV), with the exception of two intervals described below, the succession consists of repetitive, meter-scale, shallowing-upward, peritidal successions of packstone and wackestone and intervals of algal mats. In the subtidal facies, benthic foraminifers, ostracodes, mollusks, and dasycladacean algae are abundant, but echinoderms and corals, which indicate normal salinities, occur only sporadically. The intertidal parts of the successions are marked by desiccation features. Oolites are virtually absent.

The normal succession is interrupted by an interval of beds of rudists and rudist debris, between 917 and 859 mbsf (Subunit VIB). The rudists are partly in place as they lived and partly in beds of broken shells, probably representing storm washovers, formed perhaps during a shift of facies from quiet waters behind a protecting barrier to more turbulent conditions close to the barrier.

Between 792 and 677 mbsf (Unit V), the normal succession is again interrupted by an interval of oolitic grainstone. Where core recovery was more complete, small-scale, shallowing-upward se-
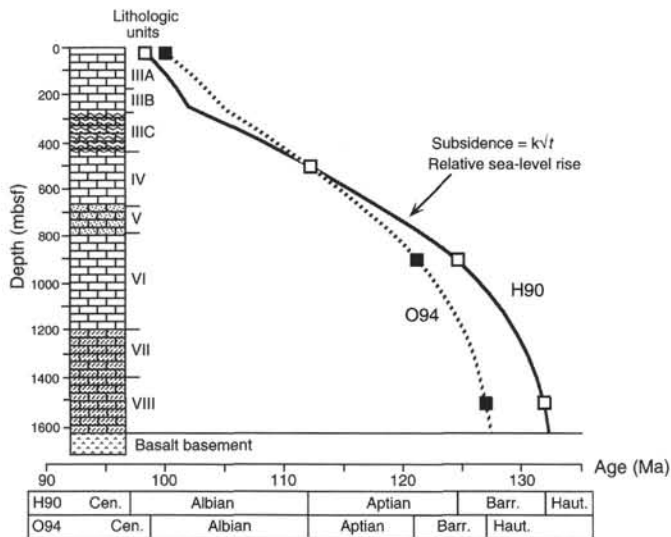
Figure 14. Inferred Early Cretaceous subsidence curves for Hole 866A. Two curves are shown that correspond to the time scales of Harland et al. (1990, "H90") and Obradovich (1994, "O94"). Age control points are from the Sr-isotopic data of Jenkyns et al. (this volume). The equation, depth = $k\sqrt{T}$ is shown for each curve. Roman numerals at the left denote lithologic units used in the site report (Shipboard Scientific Party, 1993c).

quences could be discerned, marked at the top by keystone vugs (Strasser et al., this volume). Planar, oblique laminations suggest formation of beaches and sand bars. Possible fresh-water cementation is suggested by blocky cements that succeeded early, fringing, marine cement. This interval resembles parts of the succession at Hole 867B (see below), which are interpreted as beach deposits. The occurrence of this facies about 1.4 km inward from Site 867 suggests a backstepping of facies, associated with a relative rise in sea level (Arnaud et al., this volume; Jenkyns and Strasser, this volume).

Above the oolite beds, between 677 and 435 mbsf (Unit IV), the strata are again organized in meter-scale, shallowing-upward successions, which commonly begin at the base with algal-microbial laminites that pass upward to burrowed peloidal packstone. In some successions, the base is marked by a layer of pebbles of reworked limestone. This interval is interpreted as deposited in peritidal depths, in a protected, "lagoonal" setting.

From 435 mbsf to the top of the Lower Cretaceous limestone (Units III and II), recovery was generally poor, and the downhole logs are of poor quality, owing to the large diameter of the drill hole. The samples available are mainly wackestone and micrite, commonly with molds of gastropods and with dasycladacean algae. Bands of calcrete are also common. The entire succession, from 677 mbsf to the top of the limestone, is interpreted as having been deposited in peritidal depths in a setting where circulation to the sea was restricted.

Facies Succession at Site 867

Site 867 is located near the crest of the perimeter rim that encircles Resolution Guyot; it was situated to test the possibility that a shallow-water constructional reef framework ringed the carbonate platform, with a deeper lagoon behind. The alternative possibility was that the rim was erosional in origin, carved during the time of emergence of the guyot, following the cessation of shallow-water platform-carbonate accumulation near the end of the Albian.

In general, the sediments at Site 867 are different from those at Site 866. Below a thin crust of phosphatized nannofossil limestone, the column consists of interbedded coarse- and fine-grained layers, com-

monly in fining-upward sequences. The coarser-grained layers of floatstone and rudstone contain abundant fragments of caprinid rudists and nerineid gastropods, as well as intraclasts and fragments of corals, bryozoans, echinoids, and red and green algae. Some of the mollusks are in life position. The finer-grained layers are mainly wackestone, packstone, and oolitic and peloidal grainstone. Microfossils include benthic foraminifers and ostracodes. Blackened pebbles and keystone vugs give evidence of exposure, and the grainstone layers commonly show low-angle cross-stratification. Large burrow traces are common. We interpret these strata as mostly shallow, subtidal, and beach and storm deposits, some of which were exposed during low tides.

In the lowest 10 m of the drilled section, the strata are mainly wackestone and mudstone with gastropods and abundant moldic porosity, strongly resembling the facies cored in the upper 271 m at Site 866. As at Site 866, we interpret these sediments as mainly subtidal, relatively low-energy, protected, "lagoonal" environments.

A striking feature of the upper 17 m of the limestone beds at Site 867 is the presence of centimeter-scale cavities within the host limestone. These generally have smooth walls, but some cavities are decorated with pendant, stalactite-type calcite on cavity roofs and button-like mounds of calcite on the cavity floors, as stalagmites. At a depth of about 25 mbsf, the drill pipe appeared to drop freely for a distance of 9 m, as if it had entered a high cavern or series of thinly separated caverns. Some of the cavities are partly to wholly filled with younger pelagic sediments. Both these internal sediments and the adjacent host limestones are variably phosphatized. We interpret these cavities as having formed during subaerial emergence, from leaching by meteoric waters (see "Mid-Cretaceous Emergence" section, this chapter).

Facies Succession at Site 868

Having discovered that the perimeter rim at Site 867 was underlain, not by reef-framework strata, but by storm and beach deposits above typical platform-interior facies, we drilled Site 868 on a bench close to the break in slope at the summit edge (Fig. 11). Part of the objective of Site 868 was to learn if this terrace is an erosional feature or a perimeter reef, constructed during a post-Albian, lowstand in sea level. In fact, the traverse from Sites 867 to 868, which was done with the pipe hanging below the ship and a TV camera aimed at the seafloor, showed that the terrace is separated from the rim by a steep step about 25 m high, which suggests that the terrace may be a wave-cut bench.

The facies cored at Site 868 include several intervals of boundstone, consisting of calcareous sponges in upright growth positions, and floatstone and minor grainstone rich in requieniid and caprinid rudists, gastropods, and sponge fragments. Solution porosity is abundant, and one section contains reddish grainstone, suggesting exposure. We interpret these rocks as representing mainly an open-marine environment near a fairweather wave base, where erosion surfaces developed across sponge colonies.

A reconstruction of facies relationships in the upper part of the Albian, cored at all three sites, is shown in Figure 15, in which the full thickness of Albian limestone formerly present on this part of the guyot has been restored. The limestone shown above the post-Albian unconformity is still present in the central parts of the guyot, as shown on seismic profiles (Fig. 12). In the interpretation shown in Figure 15, the facies are pictured as retreating toward the center of the guyot, with no outbuilding on the outer slope, in keeping with the form of the post-Albian subaerial erosion surface. As set out in detail below (see "Mid-Cretaceous Emergence" section, this chapter), we interpret the terrace between Sites 868 and 867 as a wave-cut bench that eroded during the post-Albian, pre-Turonian lowstand in sea level and thus the 25° slopes below Site 868 have been essentially unaffected by subaerial erosion and can be projected upward to the uppermost level of the guyot, before emergence.
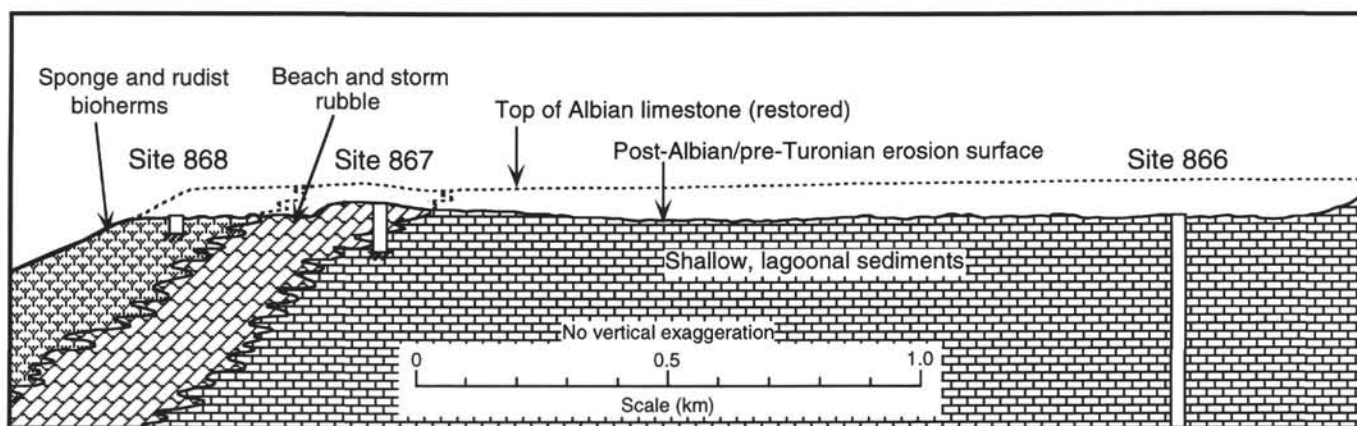
Figure 15. Restored cross section through Sites 866, 867, and 868, showing inferred facies relationships and with the inferred original top surface of the Albian limestone. Dotted lines show the inferred original top of the platform, above the erosional unconformity. The thickness of eroded limestone is estimated from Figures 12 and 13. These layers are present near the center of the guyot, where they are indented by sinkholes about 75 m deep (Winterer et al., this volume), whose floors are assumed to be at the same level as the lowstand terrace at Site 868.

Facies Recovered in Dredges

Rocks were dredged from Resolution Guyot during the Scripps Institution of Oceanography Cruise, Roundabout Leg 10, aboard the *Thomas Washington*. The dredge site was along the southeastern margin of the summit platform, at a depth of 1337 to 1346 m, in a position corresponding to the terrace between Sites 867 and 868 (Fig. 5). The dredge recovered about 200 kg of manganese-encrusted rudist limestone and fragments of coralline limestone, along with slabs of phosphorite. Compositionally, the rocks are similar to the rudist-bearing strata from Hole 868A and confirm that the extreme perimeter of the platform was an environment in which caprinids thrived. Some of the samples show imbrication of rudist fragments, which indicates deposition in strong currents (van Waasbergen, this volume).

Clays and Organic Matter

Besides the main carbonate components of the platform sediments in Hole 866A, clay minerals and organic matter are minor, though important constituents (Baudin et al., this volume). Baudin et al. show that the organic content of the typical gray limestone strata is mainly less than 0.5%, but values greater than about 3% are found in laminated limestones, algal mats, and claystone layers. The highest concentration of organic matter analyzed was 34.5%, in a laminated algal mat within the lower Aptian section, correlated by Jenkyns (this volume) with the organic-rich Selli beds of the Tethys on the basis of carbon isotopes. Based on pyrolysis analyses, Baudin et al. (this volume) conclude that some of the organic matter is assignable to Types III and IV, representative of transported and degraded terrestrial plant debris. Most of the organic matter, however, is in laminated limestones and algal mats and is of Types I and II, of lacustrine and marine origin, from algae and bacteria. Pyrolysis analyses and vitrinite-reflectance data indicate that the organic matter at all levels in Hole 866A is immature, and only the algal mats and laminated limestones have good petroleum potential. Petrographic studies by Baudin et al. (this volume) indicate that most of the organic matter in the lower Aptian carbon-rich interval is lamalginite and bituminite of marine origin, and that most of the organic matter in Units IV, VI, and VII is derived from cyanobacterial mats, along with some terrestrial higher plant debris.

Carbonate contents of limestones from Hole 866A are mainly greater than 98%, and the principal contaminating component is clay. Clay minerals occur throughout virtually the entire 1620-m-thick limestone succession at Hole 866A, but these tend to be concentrated in marly or claystone laminae within the nearly clay-free limestone strata (Shipboard Scientific Party, 1993c). Illite and illite/smectite mixed-layer clays dominate the clay assemblages, and kaoloinite and chlorite are minor components.

As suggested by the gamma-ray log from Hole 866A (Shipboard Scientific Party, 1993c), clay minerals decline steadily in abundance from the base of the sedimentary section upward to about 1250 mbsf. This is in accord with the available seismic profiles, which suggest that any original volcanic relief on Resolution Guyot was buried after accumulation of not more than the first few hundred meters of sediments. In agreement with observations of clay in the cores, the gamma-ray log shows moderately high values at many levels between about 1100 and 800 mbsf (upper Barremian and lower Aptian), low values in the highly winnowed, oolitic interval of Unit V, and then an irregular upward decline above Unit V to very low values at the top of the section. Although gamma-ray logs do not discriminate between potassium in clay and uranium and thorium in organic matter (the clay and organic matter commonly are closely associated in the same layers), the main trend is toward declining values from the middle of the Barremian upward, implying the progressive disappearance of clays.

For the origin of the clays, Baudin et al. (this volume) suggest transformation of smectite to illite at surface temperatures in potassium-rich, supratidal environments subject to repeated wetting and drying cycles. The origin of the original smectite is unknown, but we postulate that the Valanginian and lower Barremian clay is mainly of local origin, from the erosion of remnant volcanic relief on Resolution Guyot. For the younger clay, we suggest that progressive formation and subaerial erosion of new volcanoes in the MPM east of Resolution Guyot supplied smectite to westward-flowing ocean currents driven by the southeast trade winds and that these clays reached Resolution Guyot, where they were altered on tidal flats to mixed-layer smectite-illite and illite. The relatively high concentration of clayey layers in the upper Barremian and lower Aptian at Resolution Guyot may reflect nearby emplacement of slightly younger volcanoes as the MPM volcanic source moved relatively eastward. Indeed, the upward decline of clays in the limestone succession may also reflect this eastward migration and the increasing distance between active volcanism and the site.

Subsidence Rates

Based on the age estimates for stage boundaries from strontium-isotopic data from Hole 866A (Jenkyns et al., this volume), and taking into account the radiometric data of Pringle and Duncan (this volume), we derive subsidence curves for Resolution Guyot for both the Harland et al. (1990) and Obradovich (1994) time scales (Fig. 15). These curves depend on the fact that sedimentation on the carbonate platform was

nearly always within about 10 m of sea level. The assumed form of the curves is exponential, using the widely accepted expression, depth (m) $= k \sqrt{T}$, where T is the elapsed time (in m.y.) since thermal subsidence began and k is a constant. The total amount of subsidence is taken as 1620 m, the thickness of the shallow-water carbonate strata. This is a simplifying assumption that ignores pre-sediment subsidence of the basaltic foundation. The curves represent the total subsidence, from both tectonic (thermal) and isostatic causes. The two curves, from the base through the Albian/Aptian boundary, are each fitted to strontium-isotopic age estimates for the Valanginian/Barremian, Barremian/Aptian, and Aptian/Albian boundaries, yielding a different value of k for each time scale. Owing to the assumption about their exponential form, the curves depict a gradual slowing of subsidence through the Aptian. Average subsidence (equals sedimentation) rates for the lithologic units shown in Figure 14, using the two different time scales, are as follows: Unit VIII = 175–200 m/m.y.; Unit VII = 122–145 m/m.y.; Unit VI = 50–80 m/m.y.; Unit V = 40–50 m/m.y.; Unit IV = 30–40 m/m.y.; Subunit IIIC = 25–30 m/m.y.; and Subunits IIIA and IIIB = 60–70 m/m.y. These estimated rates are consistent with the data of Cooper (this volume) on cyclicity for predicting sediment cycle lengths close to Milankovitch frequencies of about 40 and 100 k.y. per cycle.

The curves in Figure 14, because of their simple form, do not show any of the deviations from the idealized curve that can result from eustatic fluctuations in sea level. The most frequent of these (20–400 k.y.) probably had amplitudes of about 1 to 10 m (see "Cycles and Sea Level" section, this chapter) and would not show at the scale in the figure. We have no data for estimating the magnitudes and durations of longer-term (>400 ka) eustatic swings.

The curves, if extrapolated upward from the Albian/Aptian boundary into the Albian, would not pass near the end point required by the strontium-isotope and foraminifer data from the uppermost limestone strata cored on Resolution Guyot, judged to be close to the Albian/Cenomanian boundary (Jenkyns et al., this volume; Arnaud-Vanneau and Sliter, this volume). For the subsidence curves to be close to the top of the Albian at the top of the limestone section, a change in rate is required. Based on lithology, two different stratigraphic levels are plausible places for such a change. The interval between 435 and 271 mbsf (Subunit IIIC) is distinctive in being much better cemented and thus has greater log-resistivity, sonic velocity, and density than strata of adjacent lithologic units above and below. The unit also includes many layers of calcrete, an indicator of subaerial exposure. The abrupt change in lithology at the base of Subunit IIIC might result from an unconformity at this level, but a hiatus only makes the problem worse by requiring an even faster rate of subsidence for strata above.

Early diagenetic cementation and the formation of calcretes and better-than-average cementation in Subunit IIIC is consistent with a slowing of subsidence rates. If extrapolated from below into this interval, the subsidence rate slows to about 25 to 35 m/m.y. and under these conditions, the proportion of time during successive rises and falls of sea level, when the sediment surface is within intertidal depths, is longer than for faster subsidence rates inferred for older strata at this hole. These slower rates should favor the formation of calcretes.

The return to more porous wackestone sedimentation above 271 m can be interpreted as a return to dominantly subtidal environments, which are most simply explained by an increase in the rate of relative rise in sea level, either from tectonic or from eustatic causes. As for the eustatic possibility, the coastal-onlap chart of Haq et al. (1987) shows three downward shifts at about 5, 7, and 9 m.y. after the beginning of the Albian, and the 271-m level in Hole 866A has an estimated age of about 7 m.y., using the Obradovich (1994) scale, and of 10 m.y., using the Harland et al. (1990) time scale, younger than the base of the Albian. We regard the dating of the events in the model of Haq et al. (1987) to be too uncertain to attempt any correlation of these coastal onlapping effects, which are documented mainly from the circum-North Atlantic region, with the strata at Site 866.

Because all the upper 271 m of sediments was deposited within about 10 m of sea level, their accumulation—the creation of the required accommodation space—must be accounted for by some combination of tectonic subsidence and eustatic rise in sea level. If the tectonic (thermal) subsidence rates of about 25 to 35 m/m.y., which prevailed for the previous part of the subsidence history before deposition of Subunit IIIC, continued until the end of the Albian, this would account for about 100 to 140 m of sediment thickness, and the remaining 130 to 170 m would have to be from a eustatic rise over the last 4 m.y. of the Albian. We consider this unlikely. Even the eustatic curve of Haq et al. (1987) shows only about 50 m of rise at any time during that interval. We therefore favor tectonics as the main cause.

The 225-m-thick oolitic limestone (677–792 mbsf) is an indication of a moderately rapid relative rise in sea level (Jenkyns and Strasser, this volume). The main cause can be either tectonism or eustatism; however, we have no reliable way of choosing. Although an unconformity at about 500 m is suggested by Arnaud-Vanneau and Sliter (this volume), an unconformity anywhere in the Albian at this site only worsens the subsidence problem by reducing the time available for sedimentation of the upper 500 m of strata even further from the foregoing estimates.

Returning to the possible role of tectonics, an increase in subsidence rate (from about 25 to 35 m/m.y. to the 70 m./m.y. rate indicated for the sediments above 271 mbsf) implies rejuvenation beginning about 4 m.y. before the end of the Albian. This is too late to be connected to the construction and early subsidence of Allison Guyot (which is about 700 km east of Resolution Guyot). Furthermore, no evidence is present in the sediments at Resolution Guyot or at Site 463 in the adjacent basin (Shipboard Scientific Party, 1981) for local volcanism in the later part of the Albian, keeping in mind that core recovery rates for both the guyot and the basinal site were only a few percent for the upper Albian. We must hypothesize some unidentified locale of middle-late Albian volcanism or tectonism in the region of Resolution Guyot to account for at least part of the increased rate of subsidence estimated from isotopic and faunal data.

Allison Guyot: Site 865

At Allison Guyot (Fig. 3), three holes were drilled at the single site. Our main objective was to sample the top of the shallow-water limestone sequence and a section of lagoonal-facies limestones for correlating with data from Resolution Guyot. This was achieved with the 872-m-deep Hole 865A. A second objective was to use the APC and two offset holes (865B and 865C) for achieving complete recovery of the pelagic sediments section, shown in Hole 865A to be of Eocene/Paleocene age.

Age Control

Age control within the Cretaceous shallow-water limestones in Hole 865A, as at sites on Resolution Guyot, is loosely controlled by microfossils and by Sr-isotopic data. When combined with radiometric ages on sills at the bottom of Hole 865A, we infer that the age of the drilled section extends from near the Albian/Aptian boundary to nearly the top of the Albian. Seismic data suggest that as much as 600 m of sediments probably lies below the bottom of Hole 865A.

Age Estimates from Foraminifers

Rare specimens of planktonic foraminifers occur in the shallow-water limestone beds in Hole 865A (Sliter, this volume). The oldest of these is observed at about 588 m below the top of the limestone succession and was assigned to an age near the Aptian/Albian boundary. Rare specimens in the upper 106 m of platform limestone were assigned to the upper Albian.

Underscoring the synchroneity of strata on the two guyot summits, Arnaud-Vanneau and Sliter (this volume) recognize in cores from Hole 865A the upper three benthic foraminifer assemblages found in the top parts of Hole 866A, at Resolution Guyot. From the
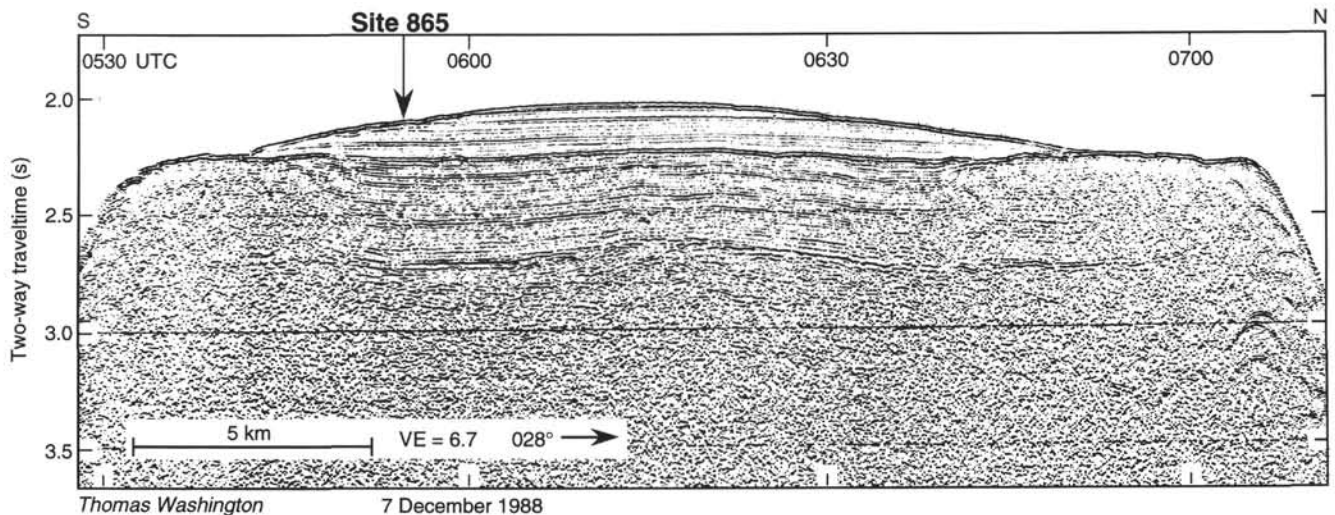
Figure 16. Single-channel seismic profile over the summit of Allison Guyot. This line was obtained from the Scripps Institution of Oceanography research vessel *Thomas Washington* during the Roundabout Leg 10 site-survey cruise on 7 December 1988. See Line A-A' - in Figure 3 for location (from Shipboard Scientific Party, 1993b). VE = vertical exaggeration at the seafloor.

top of the platform limestone to a level about 260 m below the top, they assign the strata to the late Albian, and from 260 to 657 mbsf, to the middle(?)–late(?) Albian. From 657 to 706 mbsf, the benthic foraminifers were assigned to the upper Aptian(?)–lower Albian(?).

Age Constraint from Rudists

The only rudists recovered in cores from Hole 865A are identified by Swinburne and Masse (this volume) as *Requienia* cf. *R. migliorinii*, a species known elsewhere from inner-platform facies of Barremian to late Albian age.

Age Estimates from Strontium Isotopes

Correlation of $^{87}Sr/^{86}Sr$ values for limestones from Hole 865A limestone determined by Jenkyns et al. (this volume) with values from well-dated outcrops in England (Jones, 1992; Jones et al., 1994) indicates that the entire succession in Hole 865A is Albian in age. Values from near the top of the section correspond to values in the English successions from near the Albian/Cenomanian boundary, whereas values from the lowest beds sampled at Hole 865A, at a depth of 846 mbsf, suggest a level close to the Albian/Aptian boundary. Jenkyns et al. (this volume) express uncertainty, however, in the age estimated from the Sr-isotope gradient near the bottom of the hole, noting that a bias caused by the underlying basalt sills is possible.

Age Estimate from Seismic Data

As shown by seismic profiles (Figs. 16 and 17), as much as 600 m of limestone probably underlies the sills. Given an average subsidence rate of about 60 m/m.y., calculated from strontium-isotopic age estimates (Jenkyns et al., this volume), the additional 600 m of limestone implies an age of basement at least several million years older than that of the sills (Fig. 18).

Lithofacies

Facies Succession at Site 865

The major feature of the lithologic succession at Hole 865A is a gradual upward diminution of land-derived clay and plant debris through the lower 250 m of limestone. Clay is almost entirely absent above this level. As suggested by the geometry of reflectors on the seismic profile (Fig. 16), gradual onlap and burial of original relief on

the volcanic basement reduced the supply of volcanic detritus to the surrounding parts of the platform until the volcanic terrain was completely covered by limestone. Accompanying this trend is a gradual change from facies representing alternations of somewhat restricted anoxic environments and somewhat more open-water conditions to facies representing platform-interior environments, at first partly restricted and finally in more open connection with the surrounding sea.

As documented by Winterer et al. (this volume), the original subaerial relief consisted of two volcanic ridges, one along the western side of the guyot, trending north-northwest, and the other along the southeastern side of the guyot, trending east-northeast. The ridges connect about 5 to 10 km north of Site 865. The general form of the now-buried volcanic relief is revealed on a map showing the post-Albian, pre-Turonian unconformity that separates platform limestone from pelagic sediments. Limestone strata are draped over the volcanic relief, owing to differential compaction effects (Fig. 19).

As at Site 866 on Resolution Guyot, the construction of a complete stratigraphic column for the drilled limestone strata at Hole 865A is greatly hampered by poor core recovery, but is partly offset by the suite of downhole logs. The main divisions of the lithologic succession are shown in Figure 4.

Hole 865A bottomed within a series of basalt sills, and an estimated 600-m thickness of basalt and limestone lies between the deepest level reached by the drill and the volcanic basement below. Winterer et al. (this volume) present evidence that deposition of sediments began while about 1300 m of topographic relief was still on the volcanic island (Figs. 17 and 19). As the island subsided and erosion continued on the highland, the original relief was gradually buried under sediment. By the time the sills at Hole 865A were intruded, probably only a few hundred meters of volcanic relief remained.

The lower 33 m of the succession (871–838 mbsf; Subunit IVD) consists of clayey limestone intruded by three alkali basalt sills, one of which is about 15 m thick (Shipboard Scientific Party, 1993b). Contact relationships indicate that the sills intruded the limestones while the latter were still unconsolidated. The limestone within the sill complex comprises interbedded clayey limestone and slightly dolomitic limestone, strongly burrowed and with abundant shallow-water marine fossils, including oysters, gastropods, sponge spicules, red algae, echinoderm fragments, and benthic foraminifers. Beds of pyritic claystone and lignite are common, and large, carbonized roots and other plant fragments occur at several levels. The clays are smectitic, and these, along with scattered silt- and sand-size grains of volcanic provenance, indicate the presence of a nearby volcanic island. The
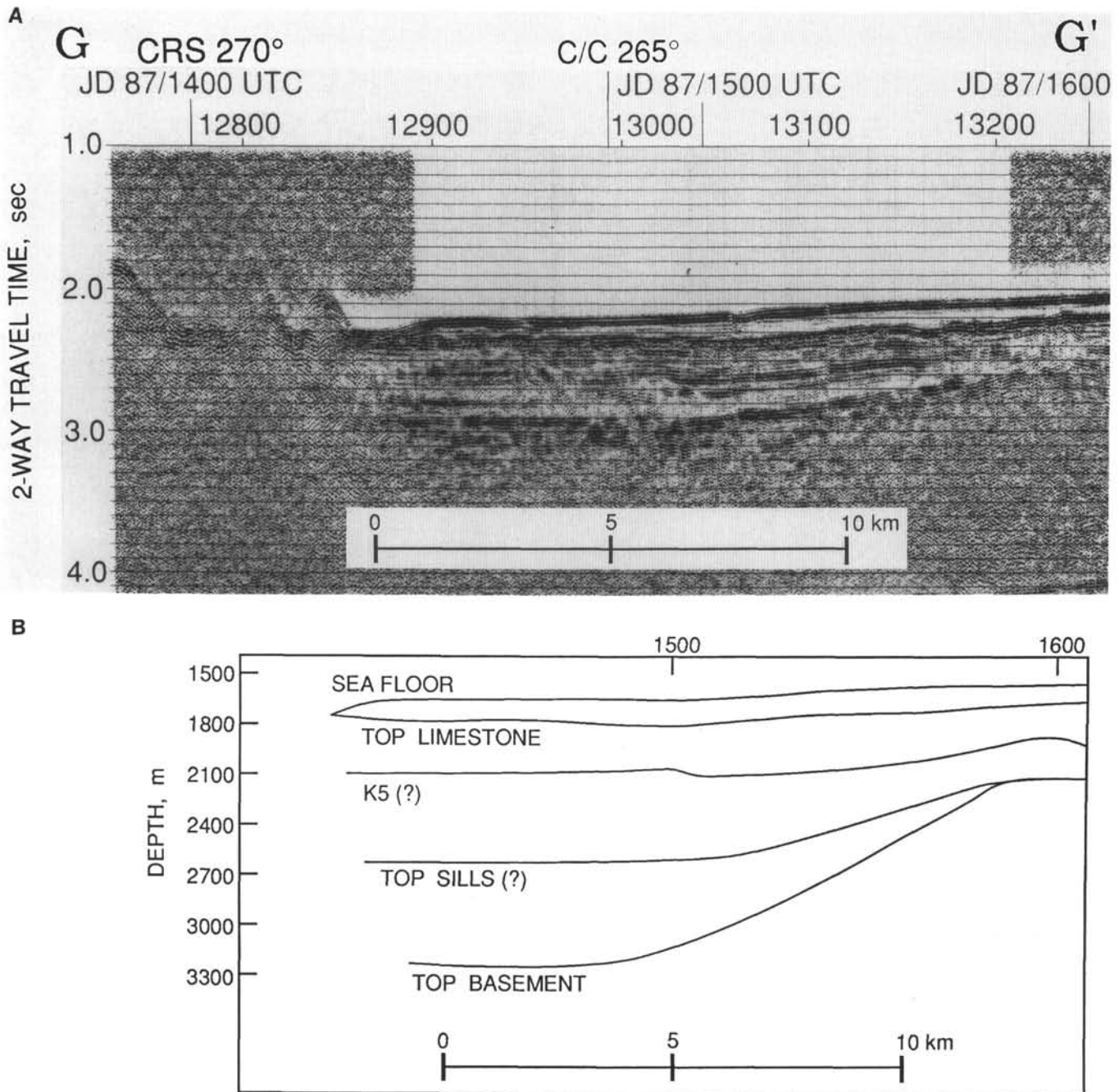
A

B

Figure 17. Profile across southeastern part of Allison Guyot. Location shown by Line G-G′ in Figure 3. **A.** Processed (0.2 s AGC, mixed) seismic line, showing buried volcanic basement topography. Reflector at 2.90 s two-way traveltime is interpreted as corresponding to the sills drilled at Site 865. The limestone strata onlap the basement progressively to the west (right). Vertical exaggeration at the seafloor is about 4×. **B.** Depth section along the line of the seismic profile, using the velocity structure determined from drilling at Site 865, extrapolated to basement using an average velocity of 3.3 km/s in the limestones between the sills and basement (from Winterer et al., this volume).

lithology and biota indicate very shallow water, generally in good connection with the open sea, but intermittently more swamplike, with anoxic or dysoxic conditions and nearby vegetated areas that supplied plant debris to the site. The intrusion of the sills may have created local low relief on the overlying shallow seafloor, thus creating the local restricted-circulation environments.

A thickness of about 216 m (838–622 mbsf; Subunits IVC to IVA) of limestone and clayey limestone succeeds the basalt sills. Core recovery was poor in the upper part of the interval, but the recovered limestone beds are mainly bioturbated wackestone and packstone,

with claystone laminae and reworked claystone pebbles. Stylolites are common. Volcanic detritus, as smectite and volcanic mineral grains, decreases in abundance toward the top of the interval and is virtually absent above 660 mbsf. Plant debris (including a stump and root in growth position) and finely dispersed carbonaceous matter likewise diminish in abundance upward to about 738 mbsf, where they disappear. Pyrite occurs in burrowed limestone, which is commonly dolomitized.

The biota in this interval is composed of benthic foraminifers, including orbitolinids and cuneolinids, gastropods, and, in the upper
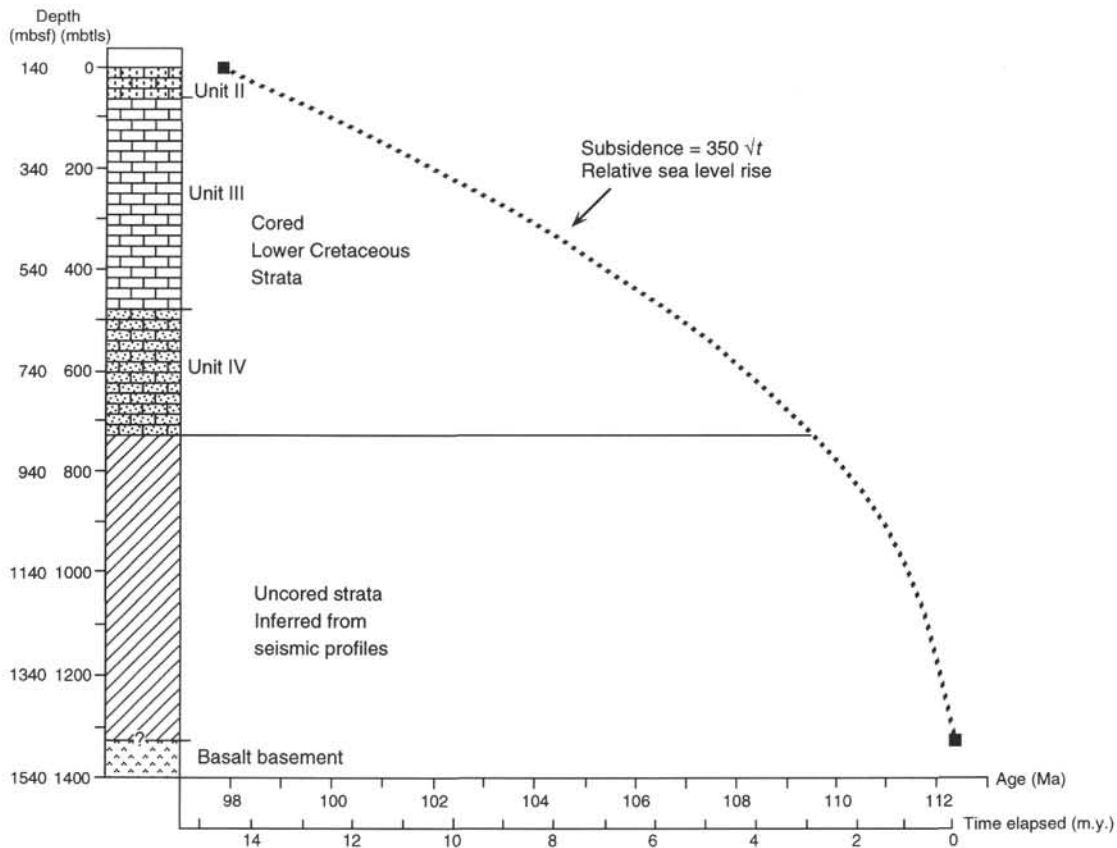
Figure 18. Inferred subsidence curve for Site 865 on Allison Guyot. The curve was constructed using an age of 98 Ma for the top of the limestone section, and a total thickness of 1330 m for the limestone, consisting of the actual drilled thickness at Hole 865A, plus the additional, undrilled thickness estimated from the seismic profile (Fig. 17).

116 m of the interval, a diverse assemblage that also includes ostracodes, bivalves, solitary corals, sponges, and dasycladacean algae. We interpret this succession as indicating a progressive disappearance of the subaerial volcanic terrain as the island subsided, accompanied by a change in the shallow water from muddy to clear conditions.

The clayey limestone is succeeded by a unit consisting of wackestone (207–622 mbsf; Unit III). Recovery was poor in this interval, but we can reconstruct the lithology as mainly bioturbated wackestone, with lesser packstone, and peloidal mudstone plus scattered intervals of grainstone that probably resulted from winnowing of wackestone. The biota is mainly gastropods, small bivalves, sponges, benthic foraminifers, ostracodes, and dasycladacean algae. A few beds of requieniid rudists, with still-articulated valves, are intercalated in the wackestone. Weak indications of exposure (red staining, brecciation) are present in a few places.

The upper 140 m of the limestone succession (207–140 mbsf; Unit II), beneath the unconformity that separates the limestones from overlying Upper Cretaceous and Cenozoic pelagic limestone and ooze, consists of phosphatized limestone. The section is lithologically similar to the underlying strata, but the beds are increasingly phosphatized upward, as shown by testing with ammonium molybdate and by the high gamma-ray values exhibited in the downhole logs (Shipboard Scientific Party, 1993b; Cooper et al., this volume).

Rocks Dredged from Allison Guyot

During the Roundabout Leg 10 cruise, aboard the *Thomas Washington*, limestone samples were dredged from four different sites around the guyot (van Waasbergen, this volume). From a site located in an erosional sinkhole and trough that cuts across the perimeter rim, the dredge recovered samples of packstone containing gastropods,

similar to the common rocks recovered from Unit II and Subunit IIIA in Hole 865A. This facies is probably typical of much of the interior part of the upper Albian platform. The occurrence of this relatively low-energy facies within about 500 m of the break in slope of the platform suggests that the profile across the edge of the platform at Allison Guyot was similar to the one inferred from drilling at Resolution Guyot (Fig. 15).

All the other dredge sites at Allison Guyot were located on the southeastern slope of the guyot, where a Cenozoic slump has exposed virtually the entire limestone section of the platform (Winterer et al., this volume), and therefore the samples in the dredge bag may have come from outcrops almost anywhere up the slope. Recovered rocks include bioturbated peloidal packstone and sponge-algal bafflestone. The depth at which the dredge was placed to begin its traverse up the slope was at 2922 m, which was within the pre-limestone basalt, as shown by basalt fragments in the dredge. The bafflestone may have come from near the bottom of the limestone slope, from a position that had been close to the exterior of the platform, as the sponge bafflestones at Site 868 on the exterior part of the platform on Resolution Guyot, or perhaps from a patch bioherm in the platform interior region.

Clay and Organic Matter

As reflected in measured calcium-carbonate contents, the upper 480 m of shallow-water limestone beds at Allison Guyot are nearly clay-free, with only traces reported in XRD data from shipboard analyses (Shipboard Scientific Party, 1993b). Below this level, the sediments constitute alternations of limestone and clayey limestone, with carbonate contents in some beds as low as about 10%. The downhole gamma-ray logs also record intervals of relatively high values, especially in the intervals from about 790 to 810 mbsf, where the cores are
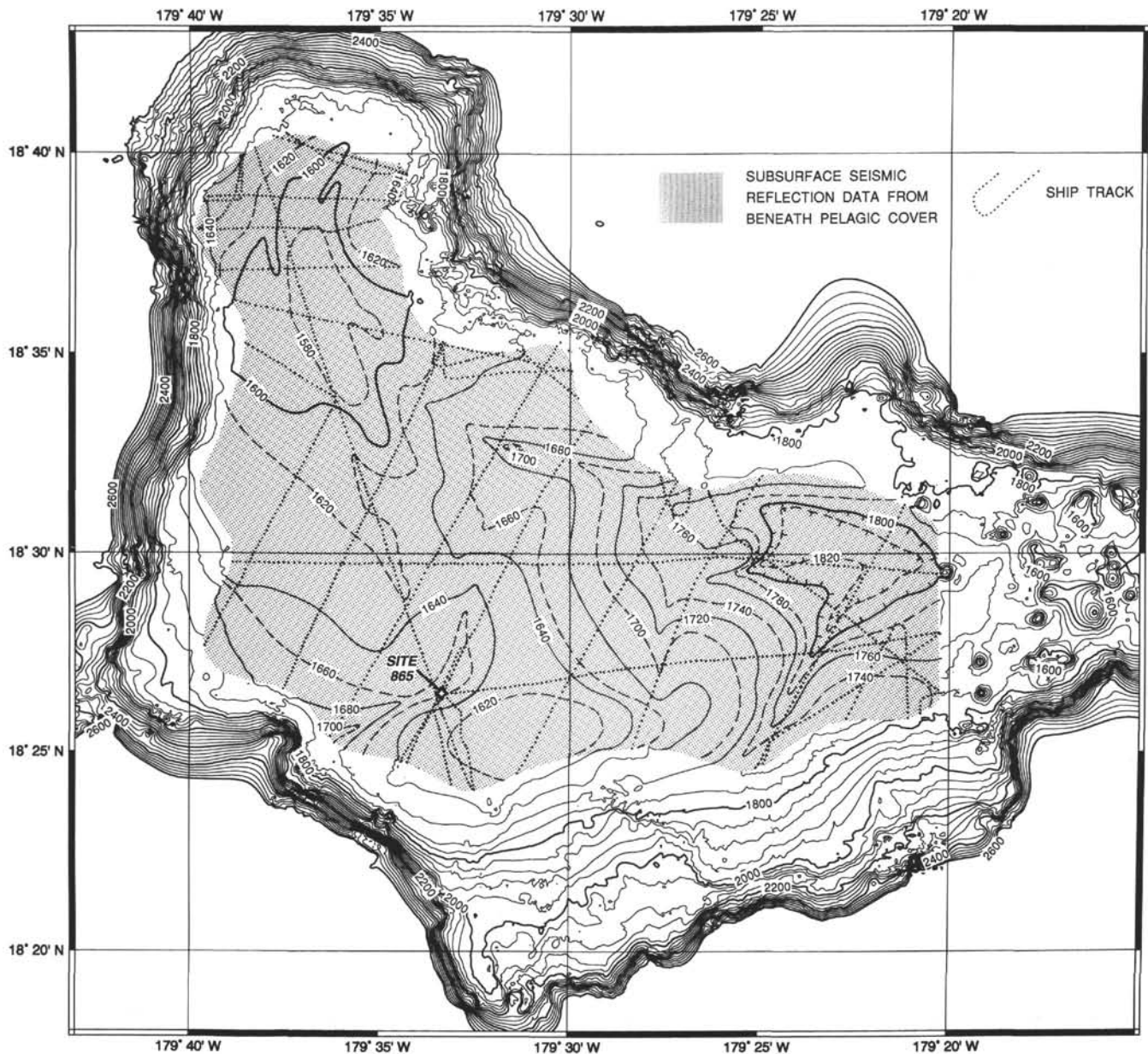
Figure 19. Contour map of the upper surface of the Lower Cretaceous platform limestone on Allison Guyot. Over the central region of the guyot, the surface is covered by pelagic sediments (stippled). Depths were estimated from multibeam bathymetry, 3.5-kHz echo-sounder, and seismic survey data collected by the research vessel *Thomas Washington* during Scripps Institution of Oceanography cruises Roundabout Leg 10 and Aries Leg 5 and from the *JOIDES Resolution* during Leg 143. Contour interval is 40 m, with additional 20-m contours shown beneath pelagic cover. Dotted lines show seismic profiler tracks used for constructing the map (from Winterer et al., this volume).

mainly wackestone with scattered black, clay-rich seams, and from 725 to 780 mbsf, where the cores are clayey limestone.

The XRD and differential-thermal-analysis studies by Baudin et al. (this volume) of clays in the lower 200 m of limestone show mainly illite-smectite, mixed-layer clays in the limestones, intercalated with the basalt sills at the bottom of Hole 865A. The overlying section, from about 827 to 760 mbsf, has about 80% of the clay fraction as kaolinite + berthierine. Above about 760 mbsf, the clays are again illite-smectite. The illite-smectite clays reflect derivation from weathering of volcanic rocks, which were probably still exposed on remnant hills in the interior parts of the guyot (Winterer et al., this volume). Baudin et al. (this volume) interpret the kaolinite as indicating warm, humid conditions for weathering of the volcanic terrain and

diagenetic alteration of kaolinite to berthierine in well-oxygenated waters, where iron was remobilized.

Studies of the organic matter in the lower 220 m of limestone by Baudin et al. (this volume) show that the clayey wackestones and packstones and the gray green pyritic claystone layers have less than about 0.5% organic carbon, whereas brown and black claystone and coaly claystone layers contain from 6% to 50% organic carbon. Petrographically, the carbon-rich layers are seen to consist of black particles of higher-plant debris, as well as brown, yellow, and red particles, some of which are probably algal. Pyrolysis studies show that the organic matter is largely Type III (terrestrial) and immature. Vitrinite studies confirm the immaturity of the organic matter, even close to the basaltic sills. Two samples show Type I or II pyrolysis

patterns, indicative of marine or lacustrine algal materials. The petroleum potential of all but a few samples from near the base of the drilled section is low to very low.

Subsidence Rates

Based on paleontologic, isotopic, and radiometric age data (Jenkyns et al., this volume; Arnaud-Vanneau and Sliter, this volume; Pringle and Duncan, this volume), we estimate the age of the uppermost limestone beds at Hole 865A at about 98 Ma, close to the top of the Albian, and place the bottom of the hole at the radiometric date of the sills, at 110.7 Ma, which is close to the bottom of the Albian (Harland et al., 1990; Obradovich, 1994). From seismic reflection data, we also estimate that a probable 600 m of additional sediments is on the guyot, beneath the level of the sills (Winterer et al., this volume), for a total of about 1330 m of sediment. We use the conventional thermal subsidence parameters (depth = $k \sqrt{T}$) to construct a curve for a total subsidence of 1330 m, and a subsidence of 730 m during the final 12.7 m.y., from 110.7 to 98 Ma (the part of the column actually drilled). The curve, as shown in Figure 18, goes through the point at 871 mbsf at an age of 110.7 Ma, which is the radiometric age of the sills. The sills were intruded into unconsolidated sediments, and we therefore assume that the sediments are the same age as the sills. The curve extrapolates to an age of 113.9 Ma at the base of the estimated total sediment thickness of 1330 m. This date falls just below the Aptian/Albian boundary in the time scales of Harland et al. (1990) and Obradovich (1994). These estimates contain many assumptions, but the results appear plausible and within the bounds of the available data. Rates of subsidence (or sedimentation) estimated for the drilled section at Hole 865A are as follows: Unit IV = from 93 m/m.y. at the base to 66 m/m.y. at the top; Unit III = 66–44 m/m.y.; and Unit II = 44–42 m/m.y.

Cycles and Sea Level

One of the main objectives of Leg 143 was to test whether relative rises and falls of sea level recorded in Lower Cretaceous successions in other parts of the world, and ascribed by some authors to eustatic (global) fluctuations of sea level, could be identified in the shallow-water limestone successions on guyots in the Pacific, half a world away and in a completely different tectonic environment. Before Leg 143, we thought that the continuity of seismic reflectors across most of the width of some of the guyots, including both Resolution and Allison guyots, suggested that sea-level oscillations might be recorded in the seismic stratigraphy, as shown by combined seismic and drilling data from the Neogene lagoonal sediments at modern Anewetak Atoll (Grow et al., 1986; Wardlaw and Quinn, 1991).

Two approaches to the sea-level problem were used by Leg 143 investigators. One focused on the lithologic variations in the cores with better recovery from Hole 866A (Strasser et al., this volume). This study showed, at a scale of about 1 to 10 m, significant systematic changes in facies that could be interpreted as caused by changes in relative sea level (Strasser et al., this volume). The second focused on a comparison of Hole 866A logging data and cores (Arnaud et al., this volume). This study showed longer, decameter-scale cycles attributed to systematic rises and falls of relative sea level. In addition, the downhole-logging data were also treated to Fourier analysis to detect cycles (Cooper, this volume), using estimates of isotopic age as control.

Meter-scale Cycles

Hole 866A (Resolution Guyot)

As seen in cores, a large proportion of the total limestone column at Site 866 is organized into shallowing-upward successions on a meter scale. Although the reconstructed core successions commonly are only about 1 m long (Strasser et al., this volume), the most common thicknesses, as seen in the logs (Cooper, this volume; Cooper et

al., this volume), is from about 10 m in the lower part of the succession to about 3 m in the upper part. We think that this discrepancy is almost entirely the result of low recovery and that the log thicknesses are probably representative of the true thicknesses of the lithologic variations and, hence, of the cyclic-appearing successions.

The next question is whether these cyclic-appearing units are the result of periodic fluctuations of relative sea level. As pointed out by Strasser et al. (this volume), with only a single drill hole and coarse seismic control, the lateral facies relations of most of the succession at Site 866 cannot be determined; therefore, we cannot easily discriminate between autocyclic (e.g., migration of shoals and passes to the open sea) and eustatic control. Evidence of prolonged emergence, in the form of calcrete horizons, implies some external process because marine carbonates cannot be deposited above sea level.

The persistence and strength of the 95- to 123-ka peaks in the Fourier analyses of the downhole resistivity and gamma-ray logs (Cooper, this volume) point toward control by periodic fluctuations in Milankovitch-frequency bands (in this case, in the ellipticity of Earth's orbit) of whatever environmental variables affect changes in sediment porosity. These include primary depositional changes, such as changes in texture (e.g., grainstone vs. packstone) or in clay content, and secondary, diagenetic changes, such as changes in degree of cementation or in development of secondary porosity. These changes may reflect periodic fluctuations in sea level and/or climate. Where accumulation rates were faster, as for the sediments in the lower part of Hole 866A, both eccentricity and obliquity (41 ka) frequencies are observed, but the precession frequency (19–23 ka) is likely below the level of resolution of the logging data.

Given our data, neither the duration nor magnitude of emergence can be estimated, but the carbon-isotope data reported by Jenkyns (this volume) track closely the values measured in contemporaneous pelagic carbonates on the Mediterranean Tethys and show no effects of precipitation of calcite in meteoric-water conditions. This suggests some combination of short exposure times and small drops of sea level. Over the range of guyot-subsidence rates of about 25 to 200 m/m.y. (Fig. 14), and with sea-level fluctuations of 95- to 123-ka frequency, we can assume an amplitude and calculate the proportion of time the sediment surface was below sea level. For example, for a subsidence rate of 50 m/m.y., about the average for Site 866, and with sea-level fluctuations of 5 m at a 100-ka frequency, the sediment surface was below sea level for only about 25% of the time and emergent for the other 75%. Considering that probably a delay occurred between the beginning of submergence during rising sea level and the deposition of the first sediments, the actual proportion of time recorded in the sediment sequences bounded by emersion surfaces may be on the order of only about 15% to 20%. Most of this sediment was deposited during the last part of the rise in sea level, when rates of rise are diminishing. For greater amplitudes of fluctuation, the proportion of emergent time increases.

The rate of accumulation of low-latitude carbonate sediments in water less than about 10 m deep, from comparisons to modern carbonate environments, is about 3 m/k.y. (Bosence and Waltham, 1990). At this rate, it would take but a few thousand years to raise the sediment surface to intertidal depths, and thus, the accommodation space can easily be filled in the small fraction of the total cycle interval when sea level is above the sediment surface.

Given that the lithologic evidence at Site 866 argues unequivocally for deposition of almost the entire succession at very shallow subtidal and peritidal depths, over a time span of about 30 m.y., and accepting the evidence from the Fourier analyses of the downhole logs that the main control on changes in lithology corresponds to Milankovitch frequencies, we can then ask if there is any way to estimate the amplitude of fluctuations in eustatic sea level. In this, we assume that subsidence rates were smoothly following an exponential curve, without short-term erratic increases or decreases (Fig. 14). At subsidence rates that ranged from about 25 to 200 m/m.y. during accumulation of the 1620 m of limestone, subsidence during a 100-ka

interval generally ranged from about 3 to 10 m. If sea level returned each time after a fall to about the same level, this would be the accommodation space to fill, and cycle thickness would mainly fall in this thickness range. As shown by the peritidal facies at the tops of most cycles (Strasser et al., this volume), carbonate-accumulation rates at Site 866 were sufficiently rapid so that whatever accommodation space was created during a rise in sea level was filled back up essentially to intertidal depths (estimated tidal range < 2 m, by comparison to Pacific mid-ocean stations today) during one 100-ka cycle. At least for one part of the column, from about 950 to 1040 mbsf, Cooper (this volume) shows a remarkably constant cycle thickness of about 8 m, a thickness that corresponds closely to the estimated subsidence rate for this part of the section (Fig. 15). This implies that the amplitude of fluctuation in sea level for the 100-ka cycle was at least 8 m.

The actual amplitude may have been greater than this amount, but this is difficult to estimate. The height and duration of emersion during lowstands of sea level is controlled by the combined rate of tectonic subsidence and the particular shape of the sea-level curve. Were the amplitude much larger than the cycle thicknesses, then evidence of exposure of the former sediment surface during lowstands might possibly include substantial evidence of supratidal environments, such as tepees, terra rossa, erosional channels, and evaporites. Such evidence is absent in most of the recovered material, but in some intervals, evidence of substantial emersion is common. In Hole 866A, pseudomorphs of gypsum crystals occur in upper Barremian–lower Aptian sediments (between about 830 and 1030 mbsf) in association with algal laminites, and a few intervals were recovered that had tepee structures in the algal laminites. Limonitic crusts (hardgrounds) occur at a few levels, but not genuine terra rossa. Good evidence for exposure is provided by thin calcrete intervals, which are particularly notable in the hard limestone in the interval from 271 to 435 mbsf. Some of the dolomite may have formed during lowstands in a mixed-water zone or in an evaporitic environment, where seawater sulfate concentrations were diminished by meteoric waters or by removal as $CaSO_4$. At stratigraphic levels above 1200 mbsf, dolomite decreases and is essentially absent shallower than about 1000 mbsf. We suggest that amplitudes of sea-level fluctuation of from 3 to 10 m appear plausible for most of the succession at Hole 866A.

We tentatively infer from this line of evidence that global changes in sea level in the Milankovitch frequency band during the time from late Hauterivian to late Albian were mainly of amplitudes in the range of meters, rather than tens or hundreds of meters. For longer time intervals, other researchers, using the patterns of seismic reflectors to infer former positions of sea level, have estimated eustatic fluctuations of from 20 to 50 m for Early Cretaceous "third-order" cycles, with durations on the order of 2 m.y. (Haq et al., 1987), and the possible occurrence of these longer-term oscillations is discussed below.

Hole 867B (Resolution Guyot)

Within the beach and storm-rubble facies in Hole 867B (Fig. 15), Strasser et al. (this volume) recognize meter-scale successions of subtidal-foreshore overlain by storm-washover deposits that built beach berms and spread into the lagoon behind. They interpret the base of a washover deposit as a transgressive surface.

Hole 868A (Resolution Guyot)

At the most seaward site on Resolution Guyot (Fig. 15), sponge and rudist bioherms about 10 to 20 cm thick are bounded below by erosional attachment surfaces and truncated above by erosional surfaces with borings and a hardground. Strasser et al. (this volume) interpret these as products of fluctuating sea level in water depths of a few tens of meters, where storms might have eroded the sea bed. Hardgrounds may represent deposits during rapid rises of sea level, and truncations may represent lower sea-level stands, when storm waves were most destructive to sponge bioherms on the seafloor.
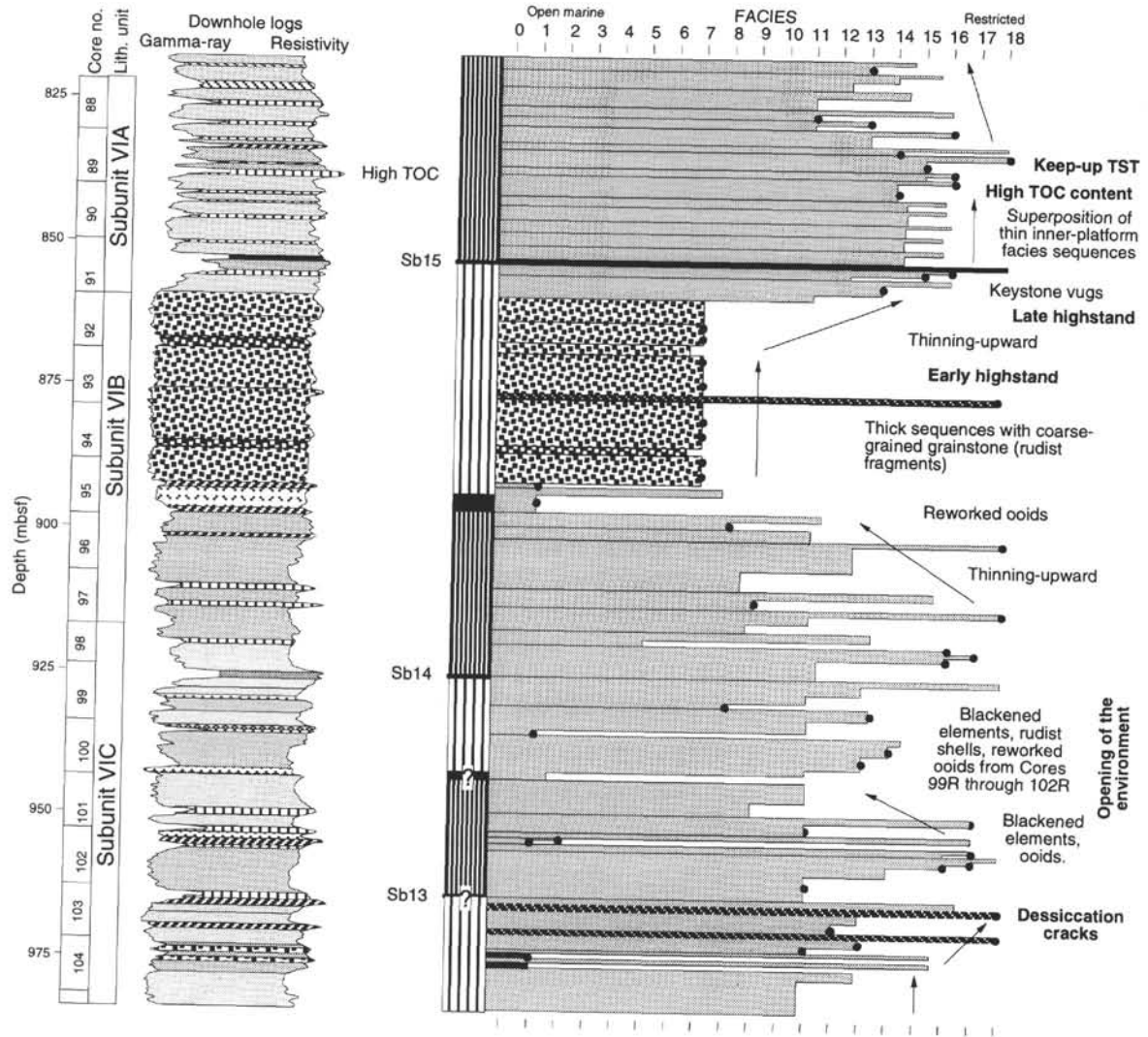
Hole 865 (Allison Guyot)

Core-recovery rates in the Lower Cretaceous limestone beds at Hole 865A, except in the lower 120 m, averaged only a few percent, and detection of any cyclicity in the lithology depends on analysis of downhole logs. Fourier analysis of these logs (Cooper, this volume), in the interval from 250 to 330 mbsf, gave power spectra dominated by a frequency of about 3.5 cycles/80 m, which at the estimated accumulation rate of about 55 to 60 m/m.y, indicates a cycle duration of about 400 ka, near the orbital eccentricity frequency of 413 ka. For the interval from 330 to 490 mbsf, the dominant frequency is close to the 123-ka ellipticity cycle. Deeper in the column, at about 600 to 650 mbsf, with accumulation rates of about 75 to 80 m/m.y, inspection of the gamma and resistivity logs suggests cycles at about 10-m intervals, which would also fall very close to the 123-ka cycle.

Decameter-scale Cycles

In addition to the small-scale sequences (which some authors would term "parasequences"), Arnaud et al. (this volume) have attempted to use core and logging data from the lower part of Hole 866A to discern larger-scale sequences corresponding to the third-order cycles of Haq et al. (1987), which are generally attributed to the eustatic rise and fall of sea level (Van Wagoner et al., 1988; Sarg, 1988). Using a detailed study of the core lithology and more than 600 thin sections, Arnaud et al. (this volume) classify the sediments into different facies, each reflecting environmental conditions that mainly depend on "openness" to normal-salinity marine waters (e.g., open, somewhat restricted, restricted), water depth (e.g., subtidal, peritidal, supratidal), and turbulence or "energy" in the water (e.g., quiet, above fairweather wave base, beach or foreshore, storm deposits). In the cores, a total of 18 facies were recognized, mainly by their textures and sedimentary structures, particle compositions, and biota. Each facies was plotted vs. depth, in comparison with logging variations, to create a continuous column showing facies shifts with time (Fig. 20).

Sequence boundaries were interpreted at significant shifts in facies types, following the general practices of sequence stratigraphy in the recognition of transgressive systems tracts, maximum-flooding surfaces, and highstand system tracts. In spite of often poor recovery, the facies-succession graph shows striking long-term (0.5–3 m.y.) shifts, keeping in mind that nearly all the facies represent water depths probably shallower than about 10 m. The sequence model for Site 866 is compared by Arnaud et al.(this volume) to similar schemes worked out from outcrop data from Lower Cretaceous strata in platform-margin and basinal settings in Venezuela and France; however, correlations, given the lack of precision in the dating of strata at Site 866, remain speculative. A strong case cannot be made from these data for eustatism, except possibly for the occurrence of organic-rich (14%) beds in Subunit VIA in Hole 866A (Fig. 7) that correlate with the black shales known as the Selli Beds in Europe (Jenkyns, this volume) (Fig. 14). At Hole 866A, as elsewhere, this stratigraphic level is within a sequence marked by a significant relative rise of sea level.

Much of the variation in facies at Hole 866A may be the result of environmental changes from more open to more restricted, or more turbulent to more sheltered, as sand bars, islands, and passes near the perimeter of the platform shifted position from time to time, thus opening up or shutting in parts of the platform interior, and changing the patterns of tidal channels and interchannel flats. Short-term, Milankovitch-frequency oscillations of sea level are essentially independent of these local environmental shifts, but the two signals, the eustatic and the autocyclic, are convolved almost inextricably in the sedimentary record. Although Fourier analysis yields a plausible case for strong sea-level control for the thin (<10 m) sequences; for the thicker sequences, the case for orbital control is weak. The typical thicknesses for the six sequences postulated by Arnaud et al. (this volume) in the interval from 1200 to 1450 mbsf are about 40 m. Age controls imply this corresponds to time intervals of about 0.5 m.y., suggesting possible control through the 413-ka orbital cycle.

Figure 20. A sequence-stratigraphy interpretation (Arnaud et al., this volume) for a part of the limestone succession cored in Hole 866A. Depths and core numbers are shown at the left. Gamma-ray and resisitivity logs are shown with their lithologic interpretation done by Cooper et al. (this volume) using the FMS log for comparison. Next to these is a detailed facies column constructed by Arnaud et al. (this volume) from comparisons among lithologies observed in the cores, thin sections (marked by a black dot at the right side of the diagram), and the Cooper et al. figure (this volume). Horizontal bars on facies chart represent environment, from more open on the right to more restricted on the left. Arrows give the sense of facies trends. Sequence boundaries are labeled Sb13, Sb14, and Sb15. TOC = total organic carbon, TST = transgressive systems tract.

Diagenesis

As succinctly documented by Röhl and Strasser (this volume), the shallow-water limestone succession on Resolution Guyot has been extensively and progressively altered by diagenesis, from the time of deposition until almost the present day. The wide range of original depositional environments, expressed in the range of facies described by Strasser and Arnaud (this volume) and by Arnaud et al. (this volume), allowed for a wide range of diagenetic processes and pathways. The essentials of the distribution of diagenetic features affecting sediments from the various original sedimentary environments is shown diagrammatically in Figure 21, which also shows the inferred diagenetic environments and the timing of the processes.

Dissolution, Cementation, and Replacement

As shown from petrographic studies (Röhl and Strasser, this volume), during early diagenesis, the dominant process was dissolution, especially of aragonitic shells and skeletal particles. Molds of shells, especially of gastropods, are common. Early cementation was generally spotty, with the result that much of the section, especially in the upper parts lacking in clay, remained friable and unrecoverable by present drilling technology. Low bulk densities given by the logs of about 2.15 to 2.25 g/cm^3 in the upper 1200 m of Hole 866A, and porosities of 20% to 30% measured from discrete samples over this interval (Shipboard Scientific Party, 1993c) are consistent with weak cementation.

The observed styles of cementation suggest both marine and meteoric phreatic environments (Röhl and Strasser, this volume). Beneath repeatedly exposed surfaces, such as storm beaches and oolite sand bars, both marine and meteoric waters could precipitate cements, whereas in more consistently submerged environments, only marine cements formed. In none of the cements from Resolution or Allison guyots do the available carbon- and oxygen-isotopic data give unequivocal indications of meteoric waters, in spite of the evidence for meteoric-water environments from textures and structures. Evidently, if any crystals formed in meteoric waters, they were replaced in whole or in part by calcite formed in marine or burial environments. We infer that much of the original aragonite that escaped dissolution was replaced by high-magnesium calcite. Röhl and Strasser (this volume) report high concentrations (200–400 mg/kg) of strontium in many of the algal laminite layers, suggesting the former presence of aragonite. Because high porosities probably allowed easy access by seawater to the deeply buried interior of the platform, just as is the case today (Paull et al., this volume), during later diagenesis, blocky, low-magnesium calcite precipitated in earlier-formed secondary porosity, and as burial proceeded, early-formed meteoric-water calcite may have been replaced by calcites in isotopic equilibrium with the burial environment.

Dolomite

As suggested by Strasser et al. (this volume), the dolomite in the lower 400 m of Hole 866A may have formed partly during early diagenesis, by evaporative pumping in sequences bounded by clayey, organic-rich algal laminites. The formation of dolomite in normal marine waters is inhibited by the presence of sulfate ions (Baker and Kastner, 1981), and generally some mechanism must be found to reduce sulfate concentration to form dolomite. These mechanisms include dilution of seawater by fresh meteoric waters during emergence and removal of sulfate ions by precipitation of sulfate or sulfide minerals. At Site 866, the algal laminites may have played a role in removing sulfate, by reaction with organic matter to form pyrite, which is present in many of the clayey and organic laminites. Many levels in the limestone succession, especially in parts of the column having algal laminites, display pseudomorphs of gypsum crystals. On the other hand, in the most dolomitic part of the succession, below about 1200 mbsf, gypsum and pyrite were not detected; if they were formerly present, they were destroyed during diagenesis.

Flood and Chivas (this volume) report Sr-isotopic data from a dozen samples of dolomite, taken from the lower part of the succession at Hole 866A, that suggest much of it formed long after deposition. The samples have $^{87}Sr/^{86}Sr$ ratios appropriate to about 90 Ma, implying that Late Cretaceous seawater bathed the permeable interior of the carbonate pile, with inward and upward circulation possibly driven by "endo-upwelling," that is, by the thermal gradient imposed by a still-warm volcanic basement beneath the pile of carbonate strata. Given that the Sr-isotope ratio of late Aptian and early Albian seawater was not much different (Jones et al., 1994), another plausible possibility is that this dolomite formed during late Aptian time, only about 15 to 20 m.y. after deposition, as suggested by Röhl and Strasser (this volume). However, two samples of unusually pale white dolomite from near the top of the dolomitized succession, analyzed by Flood and Chivas (this volume), yielded Sr-isotope ratios that suggest formation in interstitial seawater at about 30 Ma.

Compaction

Compaction began early, in some strata, even preceding cementation. Röhl and Strasser (this volume) note interpenetration of grains and spalling of fringing cements and shells, and their photomicrographs also show an abundance of line contacts between grains. As documented by Winterer et al. (this volume), compaction continued during burial, as evidenced by the progressive warping (supratenuous folding) of originally horizontal seismic reflectors over buried volcanic hills (Fig. 17). Compaction continued even after cessation of shallow-water limestone accumulation during late Albian time. This is shown by the continued development of supratenuous folds over buried hills, reflected in the present-day undulating topography of the uppermost limestone beds, which were deposited as horizontal strata at sea level (Winterer et al., this volume).

THE MID-CRETACEOUS EMERGENCE

Evidence of Emersion

At both Resolution and Allison guyots, Albian shallow-water platform carbonate sedimentation appears to have ended at the same time as an episode of emergence and subaerial erosion. We see this emergence hypothesis as the cleanest explanation of several different lines of evidence. Throughout the MPM and northwestern Pacific, seismic reflection and multibeam bathymetric data show that the carbonate caps of many guyots have a karstic topography (Winterer and Metzler, 1984; van Waasbergen and Winterer, 1993). Apparently, during the emergence, subaerial erosion removed some of the limestone and created local sinkholes. On Resolution Guyot, subaerial erosion created a drainage divide close to the perimeter of the guyot, which is expressed in the morphology as a raised rim, behind which there is commonly a moatlike depression (Fig. 11). Where it is locally preserved, the sea-level lowstand is expressed by a wavecut bench seaward of the rim. On Resolution Guyot, this morphology is typical; the three-site transect drilled during Leg 143 sampled the moat (Site 866), the rim (Site 867), and the wavecut bench (Site 868). On Allison Guyot, the raised rim is developed only locally.

From geophysical evidence, a minimum estimate of about 100 m for the magnitude of the relative fall in sea level at Resolution Guyot comes from the relative depths of features thought to have been produced during the emergence. The wavecut bench is about 25 m deeper than the crest of the perimeter rim, and the moat is at about the same depth as the bench. Layers of limestone younger and as much as 75 m shallower than those drilled at the rim are present in the central part of the guyot, and a surface of erosion truncates the upper parts of the limestone succession (Figs. 11 and 12). Sinkholes and remnant limestone pinnacles on the guyot, partly buried by pelagic sediments, show a local relief of about 100 m. At Allison Guyot, the morphology
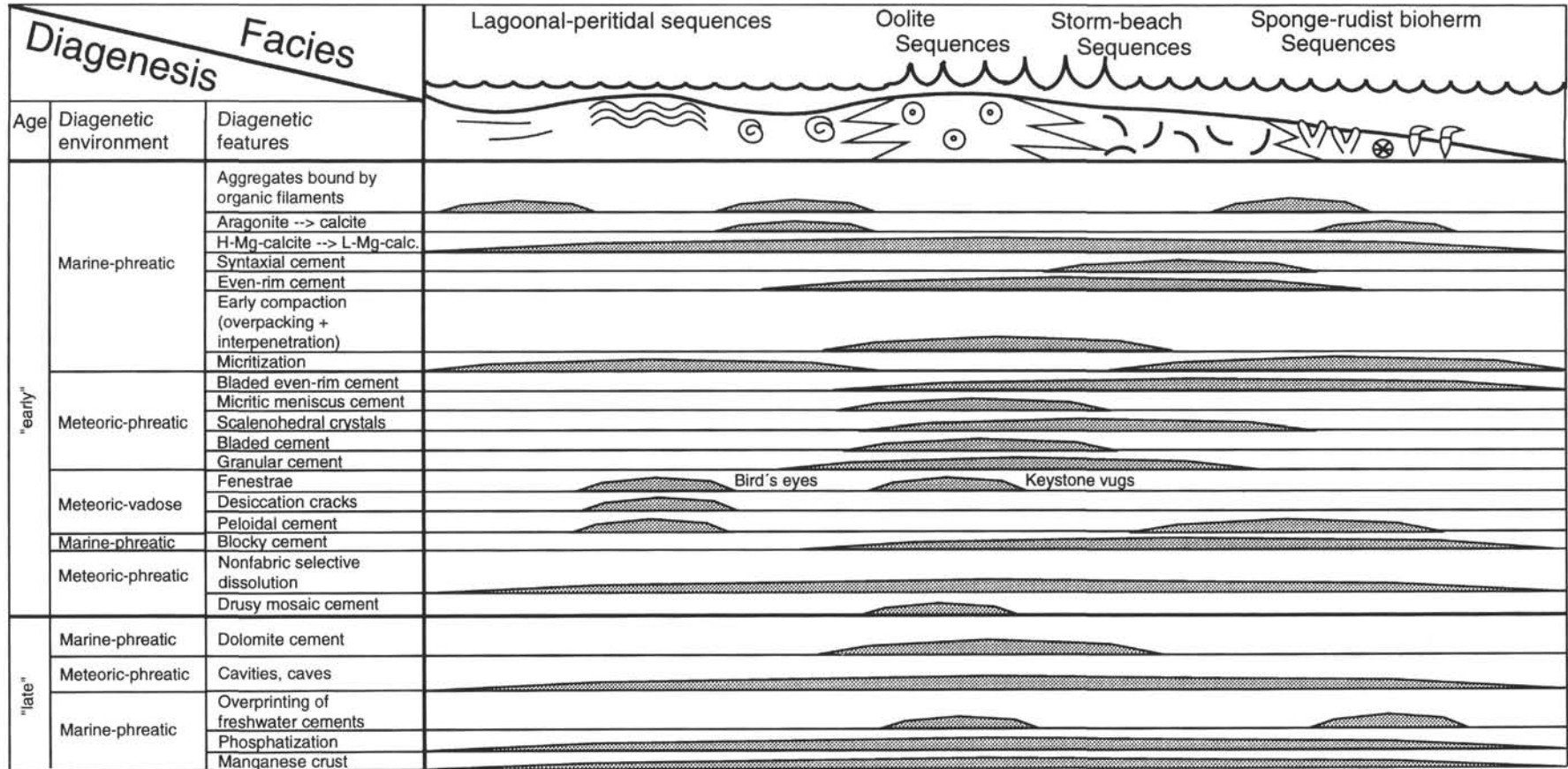
Figure 21. Diagenetic model for the Lower Cretaceous limestone strata of Hole 866A. The principal lithologic-environmental facies are arranged from the more interior to the more exterior parts of the guyot, and the diagenetic features associated with the facies are indicated by stippled patterns. Diagenetic environments, in terms of marine and meteoric and phreatic and vadose, are indicated, as well as the time at which the diagenetic features were developed (from Röhl and Strasser, this volume).

suggests as much as 200 m of emergence. A set of sinkholes is aligned along the moat behind the low perimeter ridge in one area, and the deepest of these is about 200 m below its surroundings (van Waasbergen and Winterer, 1993; Winterer et al., this volume). No lowstand terrace is unequivocally identified at Allison Guyot.

Drilling produced several clues that support the emergence hypothesis. Cores from near the top of the limestone in Hole 865B on Allison Guyot and Holes 866A and 867B on Resolution Guyot displayed dissolution cavities, whose interconnectedness and connection to the surface were shown by mineralized pelagic sediments within (Shipboard Scientific Party, 1993b, 1993c). Moreover, in Hole 867B, the drill appeared to intersect a large (approximately 9 m) cavity and cores displayed speleothems (Shipboard Scientific Party, 1993d). This observation implies that the surface of the guyot contains caverns, such as those well known from meteoric-water dissolution of limestones. Logging data showed that the upper part of the limestones at Allison Guyot gave unusually high gamma-ray values, possibly the result of phosphates contained within the portion of the limestone that is riddled with interconnected cavities.

Timing of Emergence

The exact timing of the emergence episode at Resolution and Allison guyots is uncertain, being constrained by the late Albian age of benthic foraminifers in the upper part of the limestone successions, and by planktonic foraminifers of early to middle Turonian age found within internal sediments inside a cavity in the uppermost part of the shallow-water limestone succession at Allison Guyot (Shipboard Scientific Party, 1993b). Regionally, the evidence for an episode of late Albian emergence is widespread on guyots of the northwest Pacific (van Waasbergen and Winterer, 1993) and in the MPM (Winterer and et al., this volume) and timing constraints, wherever they are tight, are within the interval from late Albian to early–middle Turonian. The narrowest limits are provided by drilling results from MIT Guyot, where planktonic foraminifers of latest Albian age (top of *Biticinella breggiensis*/base of *Rotalipora appenninica* zones) were found inside a manganese nodule within Pleistocene pelagic ooze about 3 m above the top of the upper Albian platform limestone (Shipboard Scientific Party, 1993f). A similar estimate comes from Grötsch and co-workers (Grötsch and Flügel, 1992; Grötsch et al., 1993), who studied dredge samples from the Roundabout Leg 10 site survey and postulated a "drowning facies" based on the occurrence of late Albian benthic foraminifer assemblages, including *Cuneolina pavonia*, *Vercorsella* sp., *Arenobulimina* sp., and *Pseudotriloculina* sp., which they considered an indication of a hemipelagic environment below the wavebase. At Resolution and Allison guyots, however, this fauna occurs at least 100 m downsection from the top of the limestones; thus, it cannot truly represent a "drowning facies," especially as the carbonate platforms drowned long after these foraminifers were deposited.

It is possible that the timing of exposure was different on different guyots, given the variable gap on various guyots between the end of shallow-water carbonate deposition and the subsequent preservation of the first pelagic sediments. On the other hand, atop at least three guyots (Allison, Resolution, and MIT), the cessation of carbonate platform sedimentation appears to have been simultaneous, in the latest Albian, approximately 1 or 2 m.y. before the close of this stage. On a fourth, Takuyo-Daisan Guyot, also drilled during Leg 144, the cessation is at the same time (latest Aptian to Albian), within the accuracy of the uncertain biostratigraphic dating (Shipboard Scientific Party, 1993g). Thus, it appears that Albian carbonate platforms died out nearly simultaneously on a wide scale in the Pacific.

Interestingly, this same emergence and drowning event may have occurred in Europe and South America. After studying dredge samples collected during the Scripps Roundabout Leg 10 site-survey cruise, Grötsch and co-workers (Grötsch and Flügel, 1992; Grötsch et al., 1993) postulated a short-term cooling event, during the *R. appenninica* Zone (latest Albian), that caused a fall in sea level in the

Pacific Ocean. As evidence of the extent of the event, they also documented several other examples of carbonate platform drowning during the same zone in Slovenia, Spain, and Venezuela. For the Slovenian and Spanish localities, evidence also exists of an episode of emergence just before drowning. Bosellini et al. (1993) described a regional unconformity in southern Italy eroded subaerially across platform limestones and correlative slope and basinal sediments of the late Albian *Biticinella breggiensis* Zone. Emergence is indicated by bauxite on the unconformity. The age of the overlying submarine-slide megabreccias is known only as pre-middle Turonian. Whether the emergence in southern Europe and in the central Pacific are from the same cause is an open question.

Cause of Emergence

The cause of this large (100–200 m) terminal-Albian relative fall in sea level, over a region that extends from the eastern parts of the MPM to the westernmost of the Japanese guyots, covering an area of about 5000 × 1500 km, is unknown. The two main hypotheses are (1) a eustatic drop of sea level or (2) a regional tectonic uplift. A eustatic cause is attractive because it might help to explain why no additional shallow-water sediments were deposited on the guyots when the sea returned to its former level. Continued normal tectonic subsidence during a eustatic fall, at rates of about 50 to 70 m/m.y., would place the former summit beneath the sea if the period of emersion lasted for about 3 m.y. If combined with a fairly rapid rise in sea level following the lowstand, no further shallow-water accumulation might take place.

Grötsch and Flügel (1992) favored the eustatic-fall hypothesis and concluded that the evidence of emersion supported a hypothesis of "short-term cooling" during the time of the *R. appenninica* Zone and pointed out a large basinward shift in the coastal-onlap curve of Haq et al. (1987) at about this level. For a eustatic fall in sea level of about 200 m, only two mechanisms are plausible: (1) rapid filling of a previously empty, isolated ocean basin or (2) glaciation, with ice volumes equal to or exceeding those of the Pleistocene. To produce a fall in sea level of the magnitude suggested by Pacific guyots, an isolated basin must have a volume of about 4.5×10^6 km^3, or about the dimensions of the entire present-day Angola Basin. Although a substantial salt basin was indeed present in the nascent South Atlantic, its age is Aptian (Hsü and Winterer, 1980), and by late Albian time, normal sedimentation would have resumed in the basin at global sea level. No isolated and desiccated basin of the required dimension and late Albian age has as yet been reported. Moreover, even though some evidence of a cool, humid climate may be found in uppermost Albian strata, no evidence is known to us for continental glaciation at that time on the scale of the times of maximum accumulation of ice during the Pleistocene. With no evidence of a hydrologic shift of the required amount, we put aside the eustatic hypothesis as the main cause of emergence of the guyots.

The alternative hypothesis, regional tectonism, requires a near-synchronous uplift of the seafloor over a vast region of the western Pacific, in a pulse beginning around 2 m.y., before the close of the Albian (i.e., about 100.5 Ma in the Obradovich [1994] and 99 Ma in the Harland et al. [1990] time scales). At some places, the amount of uplift would have been about 200 m; however, magnitude must be estimated for a large population of guyots to see if the uplift is uneven and has any systematic pattern. The available regional data are reviewed in van Waasbergen and Winterer (1993). A corollary of this hypothesis is that a corresponding rise of sea level of about 4 m would appear elsewhere in the world; this amount is probably too small to be recognized against the background of sea-level fluctuations from other causes.

The only regional tectonic event at about 100 Ma was the inception of volcanism from about 96 to 100 Ma on the Musician Seamount chain (Pringle, 1993). As noted in the section on paleolatitudes (this chapter), it was also at about this time that the latitudinal motion of the Pacific Plate stalled. New northward motion recorded by the Line

Islands and the northern Marshall chains may have started somewhat later, at about 85 Ma (Schlanger et al., 1984; Pringle and Dalrymple, 1993; Winterer et al., 1993b). These events may have been associated with a significant change in the direction of motion of the Pacific Plate with respect to hotspots (Duncan and Clague, 1985). Widespread new volcanism and perhaps regional accumulation of heat in the plate during the stall, in turn, could be associated with thermal uplift over a large region of the Pacific Plate, such as the Darwin Rise (Menard, 1964) and its modern descendant, the South Pacific Superswell (McNutt and Fischer, 1987; McNutt et al., 1990), which has been a continual locus of volcanic activity from Early Cretaceous time until the present.

The initiation of volcanism along new sets of seamount chains, beginning about 100 Ma, may be associated with a reorientation of stresses in the Pacific Plate, associated with a shift in the dominant locus of subduction. Assuming that trench-pull is an important determinant in plate dynamics, this new set of chains may record vigorous activity along the system of trenches at the north margins of the Bering Sea. The new orientation of plate motion may have reoriented stresses in the plate, leading to tension and mid-plate volcanism, similar to that suggested for the Line Islands during the Eocene (Sager and Keating, 1984) and now documented as the source of long sets of volcanic ridges in the troughs of gravity "rolls" seen on satellite altimetry maps of the Pacific (Winterer and Sandwell, 1987; Sandwell et al., 1993; Winterer et al., 1993a; Sandwell et al., 1994).

RE-SUBMERGENCE AND POST-ALBIAN PELAGIC SEDIMENTATION

Late Cretaceous

Stratigraphic Record

Following emergence and subaerial erosion of the Early Cretaceous carbonate platforms in the northwest Pacific, they re-submerged. In spite of their being in relatively low latitudes, within about 15° of the equator (Sager and Tarduno, this volume; Tarduno et al., this volume), no additional shallow-water carbonates accumulated on their summits. Only at MIT Guyot, about 2000 km northwest of the MPM, is there clear paleontological evidence for the timing of re-submergence of the guyot and the beginning of pelagic sedimentation, during latest Albian time. In the MPM, the oldest pelagic sediments recovered so far are of early to middle Turonian age, and these occur as phosphatized internal sediments in cavities in the Albian limestone in Hole 865A, on Allison Guyot (Shipboard Scientific Party, 1993b).

On Allison Guyot, in addition to the Turonian fossils in one of the cavities, pebbles of pelagic limestone at the contact between the shallow-water Albian limestone and the overlying pelagic sediments contain pelagic fossils of Maastrichtian age, but these are the only other records of sedimentation on the guyot during the Late Cretaceous (Sliter, this volume). No record at all of sedimentation during this time is preserved at Resolution Guyot, although barren, laminated, phosphatized micrite occurs as internal sediment in cavities at Site 867. During the Late Cretaceous, net accumulation rates on these two guyots were certainly low, and sedimentation was accompanied by the accumulation of phosphate, as crusts and as impregnations and replacements of older sediments.

We interpret this skimpy Upper Cretaceous record as indicating that the guyots (for that is what the former shallow-water carbonate banks had now become) were in an environment where the summit areas were swept by currents that tended to inhibit the permanent accumulation of pelagic sediments. Only in protected places, such as in solution cavities, were sediments preserved from this time. The transient rates of sedimentation (i.e., the fall-out rate of pelagic sediments from the shallow, lighted waters above) may have been fairly rapid, given that the guyots were located in near-equatorial latitudes. At Site 463, in the basin adjacent to Resolution Guyot, pelagic sedimentation during the Late Cretaceous was at rates of about 100 to 200 m/m.y., at paleodepths

of about 1 to 2 km (Shipboard Scientific Party, 1981). Calcareous microfossils in the Upper Cretaceous at Site 463 are well preserved, and we therefore conclude that at the even shallower depths over the summit of Resolution Guyot, little or no dissolution of microfossils would have taken place. Therefore, their absence is ascribed to their having been removed by currents, most likely before they had long resided on the seafloor. The presence at Site 463 of redeposited shallow-water benthic foraminifers in Cenomanian and Maastrichtian pelagic sediments gives direct evidence of material transfer from the guyot to the adjacent basin floor during the Late Cretaceous.

Subsidence Rate as a Possible Cause for Nondeposition

Estimates of paleodepths (i.e., subsidence curves, Figs. 14 and 18) for Resolution and Allison guyots during the Late Cretaceous are not well constrained. We know the present-day depths of the erosional surface at the top of the drowned Albian platform. This surface has deepened slightly since Albian time, owing to compaction of the limestones, but most of the deepening has occurred by thermal subsidence. At Allison Guyot, the subsidence may have been perturbed by the emplacement of a field of small, conical volcanoes at the eastern end of the guyot during the Late Cretaceous. A dredge sample from one of these cones yielded a radiometric date of 85.6 ± 1.3 Ma (Pringle and Duncan, this volume). The fact that no shallow-water biota became attached to the summit of either Allison or Resolution guyots during the part of the subsidence immediately following the episode of emergence suggests rapid subsidence during the early part of the Late Cretaceous. Normally, upward growth rates of platform carbonate biotas are of the order of 100 to 1000 m/m.y. (Schlager, 1981; Bosence and Waltham, 1990), and subsidence rates of that same order would be needed to assure drowning. Because subsidence rates at Allison and Resolution guyots during the later history of platform-limestone accumulation were about 50 to 70 m/m.y., a figure much less than the upward growth potential of the organisms, a large increase in rate would be needed. Thermal rejuvenation of the lithosphere at about 98 Ma (the emergence episode) would lead to an increase in subsequent subsidence rates, perhaps to values comparable to those of near-ridgecrest lithosphere. Thus, it is possible that rates of more than 100 m/m.y. were achieved early in the post-emergence history of subsidence and that combined with a time lag after flooding and before the beginning of sediment accumulation, the emergent and eroded platforms subsided into water too deep for carbonate accumulation to catch up with rising sea level. This line of reasoning pushes sediment accumulation rates close to their lower limits and subsidence rates close to their upper limits, and strains credibility.

Paleoceanography as a Possible Cause for Nondeposition

Two paleoceanographic hypotheses have been advanced to explain the mid-Cretaceous drowning of Pacific carbonate platforms. Grigg and Hey (1992) suggested the interruption of larval migration routes from the Caribbean into the Pacific by the growth of tectonic barriers in Central America. Alternatively, Vogt (1989) invoked upwelling of anoxic waters near the equator to inhibit shallow-water biotas on seamounts. Grigg and Hey's hypothesis does not explain the equally puzzling dearth of Cenomanian–Campanian shallow-water carbonates in the Caribbean and Gulf of Mexico. Vogt's hypothesis must rely on the Cenomanian/Turonian episode of anoxia, because previous anoxic episodes took place during the growth of the MPM platforms in the Early Cretaceous (Bralower et al., 1993). Given our uncertainties about the timing of the drowning of the MPM guyots (pre-lower to middle Turonian), this Cenomanian/Turonian event is suspect.

There is an absence of post-Albian shallow-water carbonates not only on Resolution and Allison guyots, but on every guyot in the Northwest Pacific with a cover of Albian shallow-water limestone that has been explored with dredge or drill. Shallow-water carbonate accumulation began anew in the Campanian and extended through the Maastrichtian in the Line Islands (Schlanger et al., 1984) and in Mar-

shall Islands (Lincoln et al., 1993). At Site 869, drilled during Leg 143 in the basin immediately west of Wodejebato Guyot in the Marshall Islands, the thick pile of redeposited upper Cenomanian volcanic breccias and sandstones, probably derived from the nearby guyot, has no redeposited shallow-water carbonates, whereas these materials do make an appearance in sediments of Turonian to Maastrichtian age (Shipboard Scientific Party, 1993e). Thus, there is a general paucity in the Pacific of shallow-water carbonates of Cenomanian age.

Cenozoic

Stratigraphic Record

Atop Allison Guyot, a mound of Cenozoic pelagic sediments about 160 m thick covers most of the guyot summit area, and the Lower Cretaceous limestone strata crop out only around the edges (Fig. 16). Site 865 was located on the flank of the mound and penetrated 140 m of the Cenozoic sediments, mainly of Paleocene and Eocene age.

The Eocene and Paleocene sediments are of special interest because they provide biostratigraphers with a well-preserved and nearly complete record of Paleogene successions of foraminifers and nannofossils deposited at modest paleodepths (<1500 m) in low paleolatitudes (approximately 5° to 10°N). The average rate of sedimentation for the Eocene and Paleocene sediments at Site 865 was about 5 m/m.y., but it may have been as high as 15 m/m.y. during the Paleocene (Shipboard Scientific Party, 1993b). The detailed biostratigraphic results for nannofossils are reported in Bralower and Mütterlose (this volume) and for ostracodes in Boomer and Whatley (this volume). The main features of the foraminiferal biostratigraphy are given in the "Site 865" chapter (Shipboard Scientific Party, 1993b) and in a chapter by Premoli Silva and Sliter (in press) for publication in the *Scientific Results* volume for Leg 144.

According to Bralower and Mütterlose (this volume), the nannofossil succession begins in nannofossil Zone CP3 in the lower Paleocene and extends to Zone CP15 in the upper Eocene. These authors were able to determine the precise stratigraphic position of about 142 zonal and nonzonal events (i.e., first and last appearances of species). The succession at this site, in their opinion, makes it an ideal low-latitude reference section.

To exploit the high-resolution biostratigraphy of the Paleocene and Eocene pelagic sediments at Site 865, Bralower et al. (this volume) analyzed the $\delta^{18}O$ and $\delta^{13}C$ compositions of three different species of planktonic foraminifers, with especially close sampling (~1/m) near the Eocene/Paleocene boundary. Interpretation of these isotopic data is being prepared by Bralower et al. for publication elsewhere.

Post-Eocene sediments at Site 865 are thin (about 18 m) and punctuated by hiatuses. The upper 1 m consists of foraminiferal sands of Pleistocene age that rest unconformably on about 20 m of lower Oligocene to lower Miocene foraminiferal nannofossil ooze (Shipboard Scientific Party, 1993b). Seismic sections (Fig. 16) indicate an additional 0.06 s (two-way traveltime) of sediments above the level at which the holes at Site 865 were spudded. Assuming a sound velocity of 1.7 km/s, we estimate the thickness of this additional, post-early Miocene section at about 50 m.

Effects of Bottom Currents

Seismic profiles (Fig. 16) crossing the mound of pelagic sediments atop Allison Guyot typically shows that the entire series of reflectors within the mound of Cenozoic sediments is truncated on the sides by erosion. Much of the mound's shape results from shaping of the pile of Cenozoic ooze by currents during the late Neogene, such as those documented at Horizon Guyot, in the eastern end of the MPM (Lonsdale et al., 1972). Ripple and dune forms and erosional truncation of Eocene pelagic sediments were observed in bottom photographs at Horizon Guyot, and currents capable of transporting foraminiferal sand were measured near the seafloor there with current meters (Lonsdale et al., 1972).

Close inspection of the seismic layering within the mound on this and other seismic profiles (see Figs. 5 and 6 in Winterer et al., this volume) shows that earlier layers also tend to mound over the central part of the guyot and to downlap onto the unconformity surface that truncates the Lower Cretaceous shallow-water limestone strata. We suggest that bottom currents, perhaps not so strong as those that acted during the late Neogene, have been intermittently active on Allison Guyot since the re-submergence of the guyot during mid-Cretaceous time.

Phosphorite and Ferromanganese Crusts

Currents were most effective in sweeping away pelagic sediment from the marginal parts of the summit plateau, and in those areas, the accumulation of phosphorite and ferromanganese crusts was favored. On Resolution Guyot, at Site 867, the topmost 29 cm of sediment, of early Eocene age, is phosphatized foraminiferal nannofossil limestone, covered with manganese dendrites. In addition, the underlying Cretaceous limestone is somewhat phosphatized to a depth of about 18 mbsf. A spectacular pavement of phosphorite and manganese was photographed on the transit between Sites 867 and 868, when a television camera on the drill pipe was towed across the wide terrace between the sites. The seafloor consisted of a dark pavement of nearly horizontal slabs, estimated to be about 30 cm thick, separated by fissures and cracks, generally not wider than a few tens of centimeters. Some of the slabs are slightly tilted. A discontinuous cover of white sediment partly fills the cracks and fissures, and forms ponds on the irregular upper surface of the slabs.

Dredges from Resolution and Allison guyots, as at virtually all the guyots in the MPM and elsewhere in the Northwest Pacific, generally recover manganese and phosphorite crusts and phosphatized limestone. Because of the pelagic cover on many of the guyots, and because the dredge generally operates most efficiently in breaking off and capturing rocks when pulled up a slope, the great majority of dredge samples from the guyots have been taken from the upper slopes and outermost parts of the summit plateau, in just the places where currents inhibit permanent accumulation of pelagic sediment, and thus where growth of phosphorite and manganese crusts can most easily take place. The dredged samples commonly show crusts from a few centimeters to as much as 15 cm thick, generally including phosphatized Lower Cretaceous limestone at the base, overlain in some samples by heavily phosphatized Upper Cretaceous or Paleogene pelagic sediments and capped by manganese. In some samples, an alternation between thin layers of phosphorite and manganese is seen.

GEOPHYSICAL SIGNATURES

Leg 143 drilling and associated research gave enlightening insights to the geophysical characteristics of MPM guyots and other similar edifices by implication. Deep drilling into two guyots provided the rare opportunity of having geologic ground truth, in the form of core and logging data, so that with these constraints, it was feasible to create more realistic models than previously possible.

Seismic Stratigraphy

Much of our knowledge of the carbonate caps of Pacific guyots comes from single-channel seismic reflection lines run over their summits (e.g., Heezen et al., 1973; Winterer and Metzler, 1984; van Waasbergen and Winterer, 1993). Profiles from Allison and Resolution guyots are typical of many similar edifices that display parallel, continuous reflectors within the carbonate cap and a deep reflector, below which no acoustic energy seems to penetrate. The interior zones of parallel reflectors are thought to represent lagoonal sediments (van Waasbergen and Winterer, 1993). What is more, the reflectors themselves are thought to have been caused by emersion surfaces, created by fluctuations in sea level analogous to similar features imaged and drilled in the Tertiary lagoonal sediments of
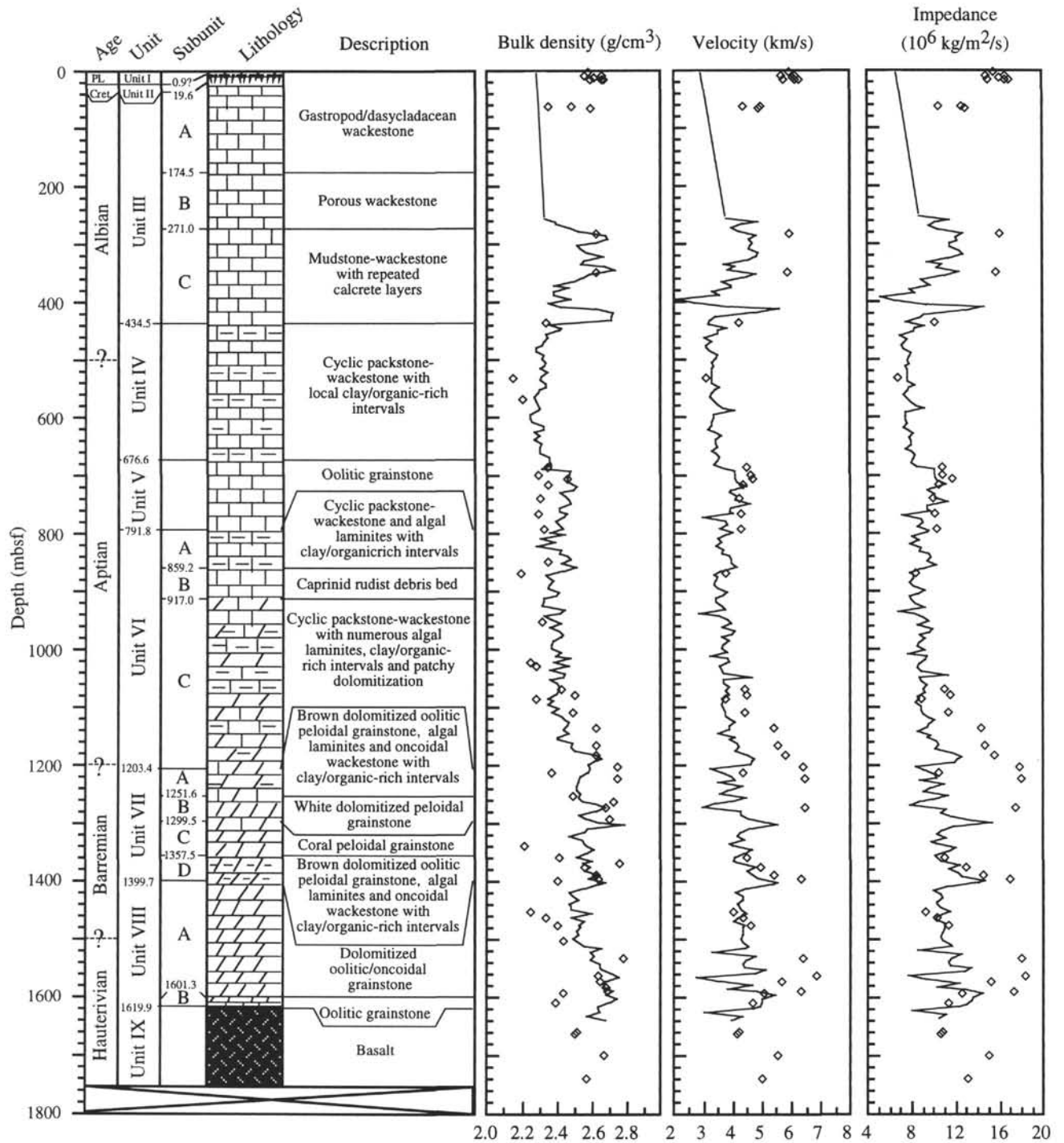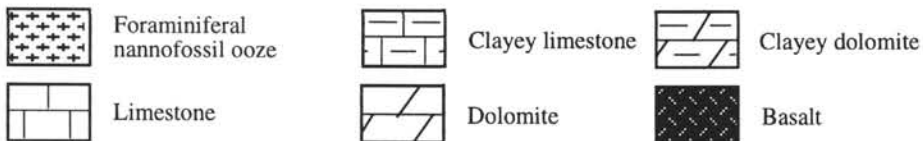
Figure 22. Bulk density, *P*-wave velocity, and acoustic impedance compared with lithology, Hole 866A. Individual symbols indicate discrete measurements, corrected to in-situ confining pressure. Curves are smoothed neutron density, sonic, and calculated impedance from downhole logs (from Kenter and Ivanov, this volume).
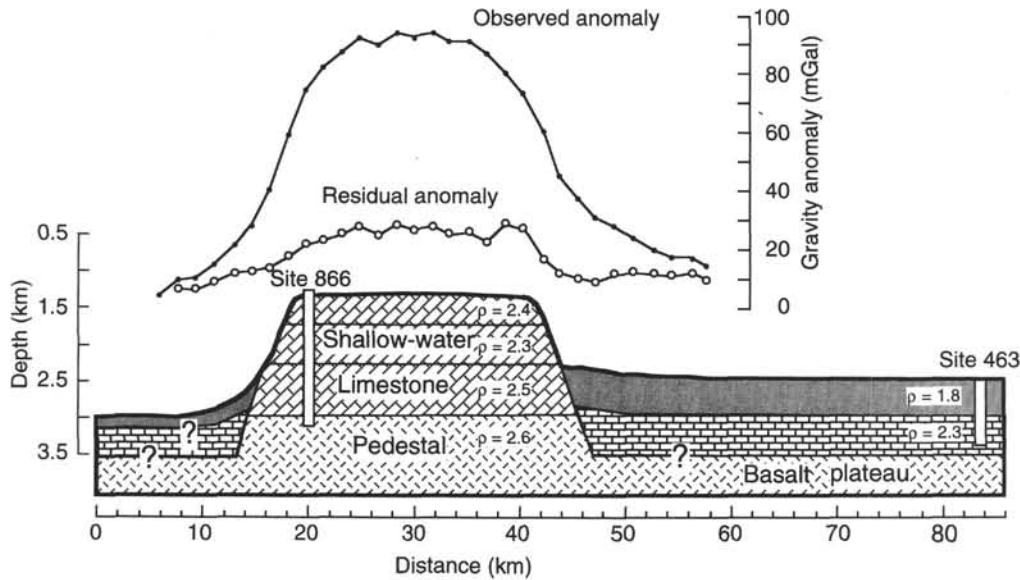
Figure 23. Gravity anomaly and density model for Resolution Guyot. At top are observed free-air anomaly and residual anomaly calculated by subtracting the calculated topographic effect of the guyot. Density values from measurements on cores recovered from Sites 463 (Shipboard Scientific Party, 1981) and 866 (Shipboard Scientific Party, 1993c) (from Sager, this volume).

present-day Pacific atolls (Quinn and Matthews, 1990; Wardlaw and Quinn, 1991). One of the main goals of Leg 143 was to ascertain the cause of these reflectors, and if they resulted from sea-level effects, to attempt to correlate one edifice with another. The terminal reflector at the bottom of the section is typically interpreted as igneous "basement" and is thought to be the top of the basaltic pedestal beneath the carbonate cap (e.g., Heezen et al., 1973). Identification of this surface is critical, for example, when modeling tectonic subsidence (e.g., Winterer and Metzler, 1984).

At both Allison and Resolution guyots, the depth to "basement" predicted from seismic reflection data was incorrect. This was in part owing to the absence of acoustic velocity data from similar settings that could be used to estimate a velocity/depth relationship. Even more fundamental was the fact that on both guyots the reflector thought to show the top of the basaltic pile was not this interface. Although basalt was cored in Hole 865A, true igneous basement was not reached. Instead, the basalts are sills, and subsequent examination of the reflection record suggests faint layering that may represent perhaps 600 m of sediments and igneous intrusives below the bottom of the hole (Shipboard Scientific Party, 1993b; Winterer et al., this volume). In contrast, the "basement" reflector beneath Hole 866A was the top of a zone of pervasive dolomitization that created an abrupt increase in seismic impedance (Shipboard Scientific Party, 1993c; Kenter and Ivanov, this volume).

Two chapters in this volume examine logging and sample physical properties measurements of the Hole 866A section and the implications for acoustic reflections within a guyot carbonate cap (Kenter and Ivanov, this volume; Kenter and Stafleu, this volume). These authors describe a complex distribution of seismic-wave velocities vs. depth (Fig. 6). Although the general trend is an increase in velocity with depth of burial, as expected, the section is riddled with low-porosity, high-velocity layers caused by diagenetic alteration (Kenter and Ivanov, this volume). The two most notable of these are from approximately 435 to 271 mbsf, corresponding to lithologic Subunit IIIC, and from about 1203 mbsf to the limestone/basalt contact at 1620 mbsf, which encompasses lithologic Units VII and VIII (Fig. 22). The shallower zone makes a high-velocity "lid" on the limestone sequence and consists of a mudstone-wackestone section with abundant calcrete layers that indicate exposure. In contrast, the deeper zone is the result of pervasive dolomitization of the bottom of the limestone carapace. From a comparison of the velocity distribution

with various logging measurements, Kenter and Ivanov (this volume) conclude that the primary cause of seismic reflection is variations in porosity owing to diagenetic replacement and cementation. These variations in porosity change both bulk density and seismic-wave velocity, causing a change in acoustic impedance.

These findings have important implications for the "dip-stick" hypothesis, which suggests that atolls should record variations in relative sea level (Wheeler and Aaron, 1991). As shown by other Leg 143 research, the limestone section does indeed record relative fluctuations in sea level; however, the amplitudes are mostly smaller than those expected before Leg 143 (see "Cycles and Sea Level" section, this chapter). Thus, the sea-level effects are probably not the cause of the layered, continuous-parallel reflections seen in guyot caps; indeed, in most places, the meter- to decameter-scale, sea-level cycles are too small to be imaged with low-frequency (~100 Hz), single-channel, seismic reflection equipment.

Although the cored basalt section in Hole 866A was short, and the logged basalt section even shorter owing to hole collapse, the recovered cores and logging data were sufficient to show that seismic velocities and densities within the basalts are highly variable, not evidently greater than the dolomitized limestone above (Fig. 22; Shipboard Scientific Party, 1993c). Given the numerous layers in the limestone sequence that could cause reflections, it seems that the basalt/limestone interface in a section such as that at Site 866 would be hard to recognize (Kenter and Stafleu, this volume). It should not cause a strong reflection and the energy from a small acoustic source may be mostly lost before it can penetrate to this depth. These results suggest that caution is required when interpreting the depth to "basement" in reflection profiles over some guyots.

Gravity Anomalies

Resolution Guyot presents a unique opportunity for studying the gravity anomaly of a guyot because its entire limestone carapace and much of the thickness of the sedimentary section surrounding it was cored at Sites 866 and 463. This guyot was also peculiar because its entire topography consists of limestone; whatever basaltic pedestal lies beneath it has been completely buried. Thus, Sager (this volume) undertook a three-dimensional model study of the gravity anomaly, using densities from core samples from Sites 866 and 463 as model constraints (Fig. 23).
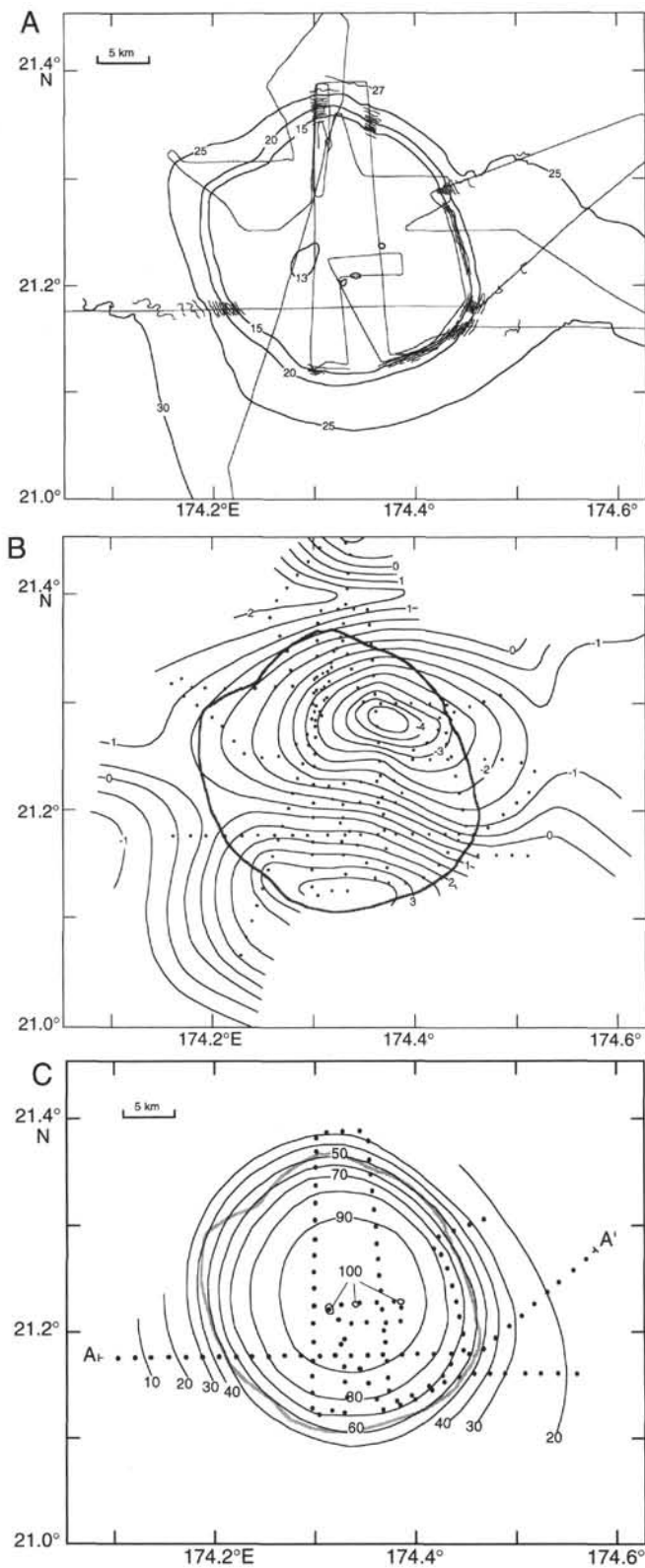
Figure 24. Bathymetry (**A**), magnetic anomaly (**B**), and gravity anomaly (**C**) over Resolution Guyot. Bathymetric contours at 100-m intervals where multibeam echo-sounder data are available. Heavy contours are at 500-m intervals, labeled in hundreds of meters. Magnetic anomaly contours are at 50-nT intervals, labeled in hundreds of nannoteslas. Dots show tracks with magnetic measurements. Gravity contours are at 10-mGal intervals, labeled in mGal. Dots show tracks with gravity measurements; Line A-A' corresponds to cross section in Figure 23.

The free-air anomaly over Resolution Guyot reaches a little more than 100 mGal (Fig. 24), similar in amplitude to that over nearby "Heezen" Guyot, Allison Guyot, and other MPM edifices. The procedure followed in this study was to subtract from the free-air anomaly the effect of the topographic expression and then to fit the residual with a series of models having different geometries. Model geometries were defined by various assumptions about the deep structure.

Sager (this volume) found that the topography accounts for about 65% of the observed free-air anomaly, leaving a 35 mGal residual. Much of the residual can be explained by the large density contrast between the dolomite section and surrounding sediments (Fig. 23), but probably a small contribution comes from the buried basalt. Moreover, the residual displays a concentration beneath the center of the guyot edifice that can be modeled either by relief on the basalt pedestal, perhaps a buried, conical erosional remanent, or more likely, by a denser, more or less cylindrical magma conduit.

Sager (this volume) also shows that nearby "Heezen" Guyot gives a residual anomaly much like that of Resolution Guyot, implying a similar deep structure. In contrast to the residual anomaly at Resolution Guyot, which is centered beneath that edifice, the "Heezen" residual is offset to one side of that elongated guyot. This suggests that unlike the Resolution limestone cap, which appears to have a horizontally homogeneous density structure, the "Heezen" density structure is laterally heterogeneous.

Magnetic Anomalies and Paleomagnetic Poles

Much of our knowledge about the tectonic drift of the Pacific Plate has come from paleomagnetic poles derived from inversions of magnetic anomalies over seamounts (e.g., Sager and Pringle, 1988). This is because the Pacific Plate is almost entirely covered with water, so oriented paleomagnetic samples are extremely difficult to obtain, whereas magnetic-anomaly data are usually acquired as a matter of course in geophysical surveys over seamounts. Such paleomagnetic poles have also been pressed into service to examine the history of volcanism in certain seamount chains (Sager and Keating, 1984; Sager and Pringle, 1987; Sager et al., 1993) as well as across the Pacific Plate as a whole (Sager, 1992).

Several assumptions are critical to magnetic modeling, among them that the seamount magnetization is generally uniform and the contribution of induced magnetization is small, but these assumptions may be violated in nature (Parker et al., 1987; Gee et al., 1989). Leg 143 provided samples of basalt from the interiors of Allison and Resolution guyots, so that a comparison can be made between magnetic-anomaly and sample-magnetic observations. Moreover, the magnetic anomalies of these guyots give important clues about the gross volcanic development of these two guyots.

Nogi et al. (this volume) analyze downhole magnetic logs from Sites 865 and 866 and compare estimates of remanent magnetization inclination to measurements made on core samples. Their work confirms shipboard paleomagnetic interpretations (Shipboard Scientific Party, 1993b, 1993c) that the basalts on Allison Guyot acquired a normal polarity in the Southern Hemisphere, whereas the basalts on Resolution Guyot were reversely polarized in the same hemisphere. Although the logged section at Site 866 was abbreviated because the bottom of the hole caved in before the magnetometer log was run (Shipboard Scientific Party, 1993c), the available data indicate that the magnetization of the basalts at this site shows large variations, owing to vertical lithologic changes. Comparison of magnetization inclinations estimated from the logs, by Nogi et al. (this volume), with measured inclinations from samples (Shipboard Scientific Party, 1993b, 1993c) implies that the induced component of the magnetization, relative to the geologically significant remanent component, ranges from negligible to overwhelming.

This implication may explain a discrepancy between core measurements and interpretations of the magnetic anomaly of Resolution Guyot. The anomaly has an amplitude of more than 500 nT (Fig. 24)
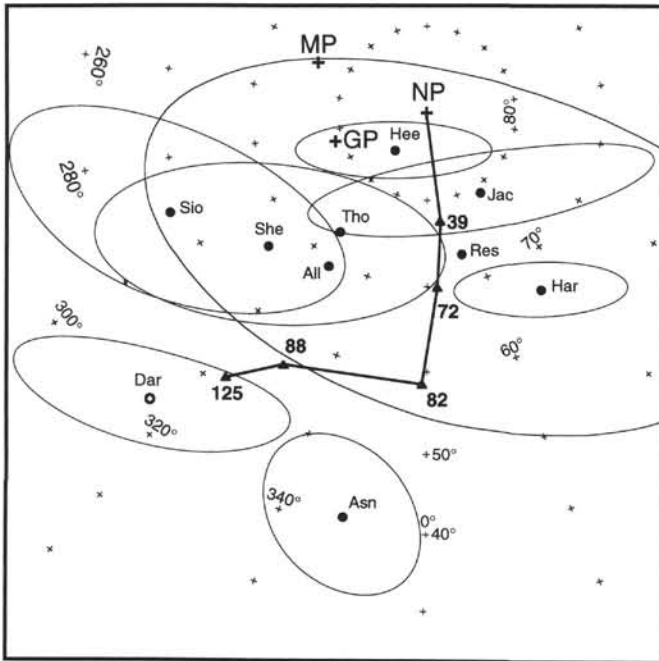
Figure 25. Polar equal-area plot showing paleomagnetic poles for guyots of the Mid-Pacific Mountains, calculated from the inversions of magnetic anomalies (see Table 1). Heavy line connecting triangles shows Pacific Plate apparent polar wander path; triangles show mean pole locations, labeled by age in Ma. Seamount paleomagnetic poles are shown by filled circles, labeled by the first three letters of the seamount name (i.e., All = "Allen" Guyot; Asn = Allison Guyot, Dar = Darwin Guyot, Har = "Harvey" Guyot, Hee = "Heezen" Guyot, Jac = "Jacqueline" Guyot, Res = Resolution Guyot, She = Shepard Guyot, Sio = Sio Guyot, Tho = "Thomas" Guyot). Ellipses show 95% confidence regions for the paleomagnetic poles, where available. NP, MP, and GP denote the north geographic pole, magnetic pole, and geomagnetic pole, respectively.

and is developed over the guyot, suggesting that indeed a basaltic pedestal forms a magnetization contrast with the surrounding limestones and sediments. A negative lobe is seen to the north of the center of the guyot and a positive lobe to the south, but this implies a normal magnetic polarity, not the reversed polarity suggested by core samples. Indeed, a seminorm inversion of the anomaly (Parker et al., 1987) gives a mean magnetization having an inclination and declination of 10.9° and 354.6°, respectively, indicating normal polarity. What is more, the paleomagnetic pole implied by these parameters is at 73.4°N, 13.5°E (Table 1). This is in the vicinity of the north geomagnetic pole, rather than in the Cretaceous part of the Pacific apparent polar wander path (Fig. 25), which also suggests an induced magnetization. One possible explanation of these observations is that most of the basalt pedestal is normally magnetized, whereas the part that was drilled has been reversed. On the other hand, given that the pedestal cannot stand very tall above the plateau below, it seems more likely that the magnetization of the basalts has been mainly induced.

Although most seamounts seem to give paleomagnetic results that suggest dominance of remanent magnetization over induced (Sager, 1987), magnetic modeling of other MPM seamounts gives results whose similarities imply that Resolution Guyot is not unusual for MPM volcanoes. Of nine MPM guyots, five have paleomagnetic poles in northern latitudes near the geomagnetic pole or the Tertiary part of the apparent polar wander path (Fig. 25). Although some of these poles might indicate Tertiary volcanism in the MPM, a more likely explanation is that induced magnetization is dominant, with a variable amount of remanent magnetization.

Magnetic-inversion results from the MPM are unusual in the high amount of paleomagnetic-pole scatter (see Winterer et al., 1993b).
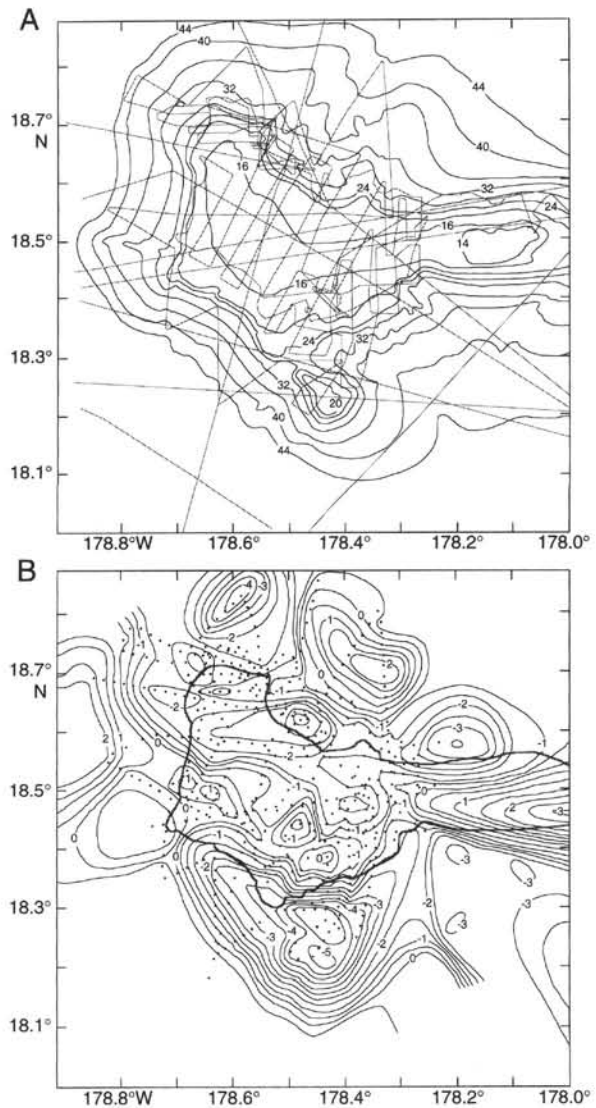

Figure 26. Bathymetry (**A**) and magnetic anomaly (**B**) maps of Allison Guyot. Bathymetry contours shown at 400-m intervals, labeled in hundreds of meters. Straight and zig-zag lines denote ships' tracks. Magnetic contours are shown at 50-nT intervals, labeled in hundreds of nannoteslas. Dots show tracks with magnetic data.

Most seamount groups on Cretaceous or older seafloor give paleomagnetic poles that cluster along the Pacific Plate apparent polar wander path (Sager, 1992; Sager et al., 1993); however, all those of the MPM are located all over the North Atlantic, seemingly anywhere but along the polar path (Fig. 25). One explanation is induced magnetization, as above, but this cannot explain all of the poles. Some of the scatter may indicate a violation of the other paleomagnetic assumption, that the magnetization is grossly homogeneous. Some of the guyots are located at or near the edge of the plateau that underlies the MPM; thus, an edge-effect anomaly from the plateau might mix with the guyot anomaly. In addition, some of the guyots seem to contain lavas of more than one polarity.

Allison Guyot is a possible example of the latter situation. Although an inversion gave a normal magnetic polarity (Table 1), the anomaly is complex, with many positive and negative lobes (Fig. 26). Radiometric dates (see "Radiometric Dates" section, this chapter) indicate that a second episode of volcanism occurred on this guyot, at about 86 Ma, well after its initial formation. This is close enough to the end of the Cretaceous Quiet Period (83 Ma; Harland et al., 1990)

Table 1. Paleomagnetic data from magnetic anomaly inversions of MPM guyots.

Seamount	Location		Paleopole		Incl. (deg.)	Decl. (deg.)	95% confidence ellipse			Ref.
	Lat. (°N)	Long. (°E)	Lat. (°N)	Long. (°E)			Maj.	Min.	Az.	
Sio (south peak)	18.0	171.2	58.2	291.7	1.1	27.0	20.5	10.0	41	1
Darwin	22.1	171.6	43.4	316.6	31.5	205.9	15.5	5.9	55	2
"Harvey"	17.8	172.7	65.6	32.3	−2.7	344.7	9.8	3.1	122	1
"Heezen"	21.2	173.8	84.4	321.5	30.6	3.1	11.1	3.3	52	3
"Thomas"	17.3	173.9	73.3	324.2	5.3	8.2				3
"Allen"	18.3	174.1	69.2	328.6	−1.2	8.8				3
Resolution	21.2	174.3	73.4	13.5	10.9	354.4	37.8	19.9	121	1
"Jacqueline"	19.4	176.7	79.0	35.4	20.7	355.4	20.0	4.4	116	4
Allison	18.5	180.3	40.9	348.7	−48.7	10.1	10.5	7.4	147	4
Shepard	19.3	180.3	66.1	310.5	−6.3	198.1	20.0	9.4	43	1

Notes: Incl., Decl. = inclination and declination of mean magnetization. 95% confidence ellipse: Maj. = major semiaxis length; Min. = minor semiaxis length; Az. = azimuth of major semiaxis relative to north. Ref. = paleomagnetic reference: (1) Sager, unpubl. data, 1994; (2) Hildebrand and Parker (1987); (3) Sager (1992); (4) Winterer et al. (1993b).

that the secondary eruptive phase may have added reversed-polarity lavas or re-magnetized portions of the basalt pile. Results from "Jacqueline" Guyot have similar implications. It was best modeled as an edifice that was mainly normal magnetic polarity, but with a southern flank that is of reversed polarity. Notably, "Jacqueline" is a volcano whose date seems to depart from the eastward-younging trend that seems to fit most MPM seamounts (see "Radiometric Dates" section, this chapter).

SUMMARY: A TALE OF TWO GUYOTS

Toward the end of the Jurassic, the MPM began to form near the Pacific-Farallon ridge crest as a plateau, approximately 1 to 2 km in height. The simplest explanation for the plateau, and one that also explains the general eastward younging of dates from the chain, is that it formed as the Pacific Plate drifted generally westward over a mantle plume. It is unclear whether a time lag existed between the eruption of the plateau and the formation of the first seamounts atop it, but the simplest idea is that they both formed simultaneously. The basaltic pedestals that were later to become the locus of carbonate-platform sedimentation were probably small, at Resolution Guyot only about 500 m high. Nevertheless, they protruded above the sea's surface and were capped with subaerial flows and exposed to weathering.

The initial volcanism formed Resolution Guyot at about 128 Ma and Allison Guyot slightly before 111 Ma. By about 85 to 90 Ma, the volcanism had reached the junction with the Line Islands, completing the underpinnings of the MPM. Both guyots formed at near 14°S, within the equatorial zone where shallow-water carbonate banks flourish. As the volcanic foundations subsided, they were covered with shallow-water limestones. Paleolatitude data indicate that the guyots drifted slightly northward through the mid-Cretaceous, to about 8° to 10°S, but they did not change latitude significantly again until well after their carbonate platforms had drowned.

Both volcanoes subsided rapidly following their formation, but not so fast that carbonate accumulation could not keep up. Resolution Bank acquired a thick succession of Hauterivian to Aptian limestones, initially at rates of about 175 to 200 m/m.y., but slowing to 40 to 50 m/m.y. By this time, Allison Guyot was forming, and it, too, sank rapidly at first, at rates of about 90 m/m.y., slowing gradually to 40 m/m.y. In all, the limestones accumulated to a thickness of 1620 m on Resolution Bank at Site 866. On Allison Guyot, only 732 m of limestone was drilled, but perhaps another 600 m lies below the bottom of the hole, for a total thickness of about 1330 m. On both banks, the water depth appears to have remained shallow (<10 m).

The facies successions showed that environmental conditions in the platform interior were generally restricted, with episodes when the platform was more open to the sea. Clays were significant components of the sediments, while volcanic erosional remnants existed above sea level; however, the clays disappeared when sediments eventually covered the remnant summits of the basaltic volcano. Although rudists and sponges, among others, congregated at the edges of the carbonate

platforms, it seems that no highstanding framework reefs were available to protect the interior. Instead, shifting perimeter sand shoals and storm-built islands damped the waves and shallow subtidal to peritidal environments prevailed over most of the platform.

Sea level fluctuated during the evolution of the carbonate platforms, mostly driven by orbital frequency (Milankovitch) fluctuations of a few meters amplitude. A few larger, decameter-scale oscillations may have taken place. These fluctuations left a record of meter-scale, fining-upward deposits, progressing from shallow subtidal to peritidal sediments, and finally to exposure. Each time, the carbonate factory quickly piled up lime sediments as sea level rose, commonly leaving the sediment surface emergent during the succeeding fall. The emergence periods left behind a record of desiccation cracks, calcretes, tepee structures, and "birds-eye" vugs. Estimates place the exposure at 75% or more of the total time; thus, the stratigraphic record is probably punctuated by short hiatuses and diastems.

During the buildup, extensive diagenesis occurred within the carbonate pile. The dominant process was dissolution of aragonitic grains and skeletal particles that left a moldic porosity within wackestone layers. Compaction, both during and after deposition, caused warping of the once horizontal layers over the buried volcanic topography. Dolomitization was pervasive within the lowest 400 m of strata on Resolution Guyot. The timing and cause of this dolomitization is unclear, but an attractive hypothesis is that higher heat flow within the edifice drove endo-upwelling that pumped seawater through the limestone pile, leaving behind dolomites that formed within a few tens of millions of years after deposition. On the other hand, some data imply that some of the dolomitization may have occurred much later.

Near the end of the Albian, at about 98 Ma, relative sea level fell by 100 to 200 m over a region at least 5000 km wide, from the MPM to the guyots just east of Japan. High above the water, the carbonate platforms were subaerially eroded, forming a summit morphology—a so-called Makatea—that superficially resembles a modern atoll that has a perimeter mound ringing the summit and a moat just behind it. Below the rim of the platforms, the sea carved lowstand terraces. Furthermore, meteoric waters partly dissolved the summit strata, leaving karstic sinkholes, caverns, and cavities, in some of which speleothems formed.

The cause of the relative fall in sea level remains unclear. Although a eustatic mechanism is attractive, scant evidence exists of a glacial episode or desiccated basin of the right age and volume to explain the magnitude of the fall. Furthermore, widely published sea-level curves, developed mainly from Atlantic Ocean stratigraphy, show no such single, extraordinary event. Thus, the cause may have been a regional uplift of the Pacific, which had a large effect in the source region, but a small effect elsewhere. Significantly, overprinting volcanism appeared within the MPM at numerous localities, apparently at about the same time (99–86 Ma).

Apparently, the emergence event was too much for the carbonate factories, for they were never reestablished atop these guyots, despite being at favorable latitudes of about 8° to 11°S. A rapid relative rise

in sea level, combined with subsidence, may have taken the guyot summit to depths too great for the carbonate factories to flourish. Alternatively, some oceanographic cause, such as the blocking of faunal migration or the upwelling of anoxic waters, may have caused the drowning. Whatever the cause, it was some time before sediments again accumulated on most guyots. On Allison Guyot, the oldest pelagic sediments to accumulate are mid- to late Turonian in age, whereas Resolution Guyot never accumulated a significant pelagic sediment cover.

Finally, during the Late Cretaceous, the Pacific Plate began to drift rapidly northward, perhaps after the commencement of subduction in a trench along the north side of the Bering Sea. This northward drift carried the guyots across the equator, probably during Paleocene/Eocene time. Allison Guyot accumulated a thick pile of sediments of this age, winnowed by currents, but the same currents kept the summit of Resolution Guyot nearly free of sediments. Owing to long exposure to the sea, the summits were coated with a hardground consisting of phosphorite and ferromanganese crusts, some of which penetrated tens of meters into the porous summit limestones.

ACKNOWLEDGMENTS

REFERENCES[*]

Baker, P.A., and Kastner, M., 1981. Constraints on the formation of sedimentary dolomite. *Science,* 213:215–216.

Batiza, R., 1977. Age, volume, compositional and spatial relations of small isolated oceanic central volcanoes. *Mar. Geol.,* 24:169–183.

Bosellini, A., Neri, C., and Luciani, V., 1993. Guida Cretaceo-Eocenico di scarpata e bacino del Gargano (Italia Meridionale). *Ann. Univ. Ferrara Sez 9: Sci. Geol. Paleontol.,* 4 (Suppl.):1–77.

Bosence, D., and Waltham, D., 1990. Computer modeling the internal architecture of carbonate platforms. *Geology,* 18:26–30.

Bralower, T.J., Sliter, W.V., Arthur, M.A., Leckie, R.M., Allard, D.J., and Schlanger, S.O., 1993. Dysoxic/anoxic episodes in the Aptian-Albian (Early Cretaceous). *In* Pringle, M.S., Sager, W.W., Sliter, M.V., and Stein, S. (Eds.), *The Mesozoic Pacific: Geology, Tectonics, and Volcanism.* Geophys. Monogr., Am. Geophys. Union, 77:5–37.

Clague, D.A., and Dalrymple, G.B., 1987. The Hawaiian-Emperor volcanic chain: Part I, Geologic evolution. *In* Decker, R.W., Wright, T.L., and Stauffer, P.H. (Eds.), *Volcanism in Hawaii.* Geol. Surv. Prof. Pap. U.S., 1350:5–73.

Cox, A., and Gordon, R.G., 1984. Paleolatitudes determined from paleomagnetic data from vertical cores. *Rev. Geophys. Space Phys.,* 22:47–72.

Darwin, C., 1842. *The Structure and Distribution of Coral Reefs:* London (John Murray).

Duncan, R.A., and Clague, D.A., 1985. Pacific plate motion recorded by linear volcanic chains. *In* Nairn, A.E.M., Stehli, F.G., and Uyeda, S. (Eds.), *The Ocean Basins and Margins* (Vol. 7A): *The Pacific Ocean:* New York (Plenum), 89–121.

Epp, D., 1984. Possible perturbations to hotspot traces and implications for the origin and structure of the Line Islands. *J. Geophys. Res.,* 89:11273–11286.

Erba, E., Bergersen, D.D., Larson, R.L., Lincoln, J.M., Nakanishi, M., and ODP Leg 144 Scientific Party, 1993. Paleolatitude and vertical subsidence histories of ODP Leg 144 guyots. *Eos,* 74:353.

Fischer, A.G., Heezen, B.C., et al., 1971. *Init. Repts. DSDP,* 6: Washington (U.S. Govt. Printing Office).

Gee, J., Staudigel, H., and Tauxe, L., 1989. Contribution of induced magnetization to magnetization of seamounts. *Nature,* 342:170–173.

Gordon, R.G., 1990. Test for bias in paleomagnetically determined paleolatitudes from Pacific Plate Deep Sea Drilling Project sediments. *J. Geophys. Res.,* 95:8397–8404.

Gradstein, F.M., Agterberg, F.P., Ogg, J.G., Hardenbol, J., Van Veen, P., and Huang, Z., in press. A Mesozoic time scale. *J. Geophys. Res.*

Grigg, R.W., and Hey, R., 1992. Paleoceanography of the tropical eastern Pacific Ocean. *Nature,* 255:172–178.

Grötsch, J., and Flügel, E., 1992. Facies of sunken Early Cretaceous atoll reefs and their capping late Albian drowning succession (northwestern Pacific). *Facies,* 27:153–174.

Grötsch, J., Schroeder, R., Noé, S., and Flügel, F., 1993. Carbonate platforms as recorders of high-amplitude eustatic sea level fluctuations: the late Albian *appenninica* event. *Basin Res.,* 5:197–212.

Grow, J.A., Lee, M.W., Miller, J.J., Agena, W.F., Hampson, J.C., Foster, D.S., and Woellner, R.A., 1986. Multichannel seismic-reflection survey of KOA and OAK craters. *In* Folger, D.W. (Ed.), *Sea-floor Observations and Subbottom Seismic Characteristics of OAK and KOA Craters, Enewetak Atoll, Marshall Islands.* U.S. Geol. Surv. Bull., 1678-D:D1–D46.

Hamilton, E.L., 1956. Sunken islands of the Mid-Pacific Mountains. *Mem.—Geol. Soc. Am.,* 64.

Haq, B.U., Hardenbol, J., and Vail, P.R., 1987. Chronology of fluctuating sea levels since the Triassic. *Science,* 235:1156–1167.

Harland, W.B., Armstrong, R.L., Cox, A.V., Craig, L.E., Smith, A.G., and Smith, D.G., 1990. *A Geologic Time Scale 1989:* Cambridge (Cambridge Univ. Press).

Hart, S.R., 1984. A large-scale isotope anomaly in the Southern Hemisphere mantle. *Nature,* 309:753–757.

Heezen, B.C., Matthews, J.L., Catalano, R., Natland, J., Coogan, A., Tharp, M., and Rawson, M., 1973. Western Pacific guyots. *In* Heezen, B.C., MacGregor, I.D., et al., *Init. Repts. DSDP,* 20: Washington (U.S. Govt. Printing Office), 653–723.

Henderson, L.J., 1985. Motion of the Pacific Plate relative to the hotspots since the Jurassic and model of oceanic plateaus of the Farallon plate [Ph.D. dissert.]. Northwestern Univ., Evanston, IL.

Hess, H.H., 1946. Drowned ancient islands of the Pacific Basin. *Am. J. Sci.,* 244:772–791.

Hildebrand, J.A., and Parker, R.L., 1987. Paleomagnetism of Cretaceous Pacific seamounts revisited. *J. Geophys. Res.,* 92:12695–12712.

Hsü, K.J., and Winterer, E.L., 1980. Discussion of paper by Donovan, D.T., and Jones, E.J.W., 1979. Causes of world-wide changes in sea level (*Quat. J. Geol. Soc. London,* 136:187–192). *Quat. J. Geol. Soc. London,* 137:509–510.

Jackson, E.D., Koizumi, I., et al., 1980. *Init. Repts. DSDP,* 55: Washington (U.S. Govt. Printing Office).

Jarrard, R.D., and Clague, D.A., 1977. Implications of Pacific island and seamount ages for the origin of volcanic chains. *Rev. Geophys. Space Phys.,* 15:57–76.

Jones, C.E., 1992. The strontium isotopic composition of Jurassic and Early Cretaceous seawater [Ph.D. dissert.]. Oxford Univ.

Jones, C.E., Jenkyns, H.C., Coe, A.L., and Hesselbo, S.P., in press. Sr-isotopic variations in Jurassic and Cretaceous seawater. *Geochim. Cosmochim. Acta.*

Kennett, J.P., and Stott, L.D., 1991. Abrupt deep-sea warming, paleoceanographic changes and benthic extinctions at the end of the Palaeocene. *Nature,* 353:225–229.

Kroenke, L.W., Kellogg, J.N., and Nemoto, K., 1985. Mid-Pacific Mountains revisited. *Geo-Mar. Lett.,* 5:77–81.

Ladd, H.S., Newman, W.A., and Sohl, N.F., 1974. Darwin guyot, the Pacific's oldest atoll. *Proc. 2nd. Int. Coral Reef Symp.,* 2:513–522.

Lancelot, Y., Larson, R.L., et al., 1990. *Proc. ODP, Init. Repts.,* 129: College Station, TX (Ocean Drilling Program).

Larson, R.L., and Lowrie, W., 1975. Paleomagnetic evidence for motion of the Pacific plate from Leg 32 basalts and magnetic anomalies. *In* Larson, R.L., and Moberly, R., et al., *Init. Repts. DSDP,* 32: Washington (U.S. Govt. Printing Office), 571–577.

Larson, R.L., Moberly, R., et al., 1975. *Init. Repts. DSDP,* 32: Washington (U.S. Govt. Printing Office).

Larson, R.L., and Sager, W.W., 1992. Skewness of magnetic anomalies M0 to M29 in the northwestern Pacific. *In* Larson, R.L., Lancelot, Y., et al., *Proc. ODP, Sci. Results,* 129: College Station, TX (Ocean Drilling Program), 471–481.

Larson, R.L., and Schlanger, S.O., 1981. Geological evolution of the Nauru Basin, and regional implications. *In* Larson, R.L., Schlanger, S.O., et al., *Init. Repts. DSDP,* 61: Washington (U.S. Govt. Printing Office), 841–862.

---

[*]Abbreviations for names of organizations and publications in ODP reference lists follow the style given in *Chemical Abstracts Service Source Index* (published by American Chemical Society).

Larson, R.L., Steiner, M.B., Erba, E., and Lancelot, Y., 1992. Paleolatitudes and tectonic reconstructions of the oldest portion of the Pacific Plate: a comparative study. *In* Larson, R.L., Lancelot, Y., et al., *Proc. ODP, Sci. Results,* 129: College Station, TX (Ocean Drilling Program), 615–631.

Lincoln, J.M., Pringle, M.S., and Premoli-Silva, I., 1993. Early and Late Cretaceous volcanism and reef-building in the Marshall Islands. *In* Pringle, M.S., Sager, W.W., Sliter, W.V., and Stein, S. (Eds.), *The Mesozoic Pacific: Geology, Tectonics, and Volcanism.* Geophys. Monogr., Am. Geophys. Union, 77:279–305.

Lonsdale, P., 1988. Geography and history of the Louisville hotspot chain in the Southwest Pacific. *J. Geophys. Res.,* 93:3078–3104.

Lonsdale, P., Normark, W.R., and Newman, W.A., 1972. Sedimentation and erosion on Horizon Guyot. *Geol. Soc. Am. Bull.,* 83:289–315.

Mammerickx, J., and Smith, S.M., 1985. *Bathymetry of the North Central Pacific.* Geol. Soc. Am., Map and Chart Ser., MC-52.

Matthews, J.L., Heezen, B.C., Catalano, R., Coogan, A., Tharp, M., Natland, J., and Rawson, M., 1974. Cretaceous drowning of reefs on Mid-Pacific and Japanese guyots. *Science,* 184:462–464.

McNutt, M.K., and Fischer, K.M., 1987. The South Pacific superswell. *In* Keating, B.H., Fryer, P., Batiza, R., and Boehlert, G.W. (Eds.), *Seamounts, Islands, and Atolls.* Geophys. Monogr., Am. Geophys. Union, 43:25–34.

McNutt, M.K., Winterer, E.L., Sager, W.W., Natland, J.H., and Ito, G., 1990. The Darwin Rise: a Cretaceous superswell? *Geophys. Res. Lett.,* 17:1101–1104.

Menard, H.W., 1964. *Marine Geology of the Pacific:* New York (McGraw-Hill).

Moberly, R., Schlanger, S.O., et al., 1986. *Init. Repts. DSDP,* 89: Washington (U.S. Govt. Printing Office).

Morgan, W.J., 1972a. Deep mantle convection plumes and plate motions. *AAPG Bull.,* 56:203–213.

————, 1972b. Plate motions and deep mantle convection. *Mem.—Geol. Soc. Am.,* 132:7–22.

Nakanishi, M., Tamaki, K., and Kobayashi, K., 1992. Magnetic anomaly lineations from Late Jurassic to Early Cretaceous in the west-central Pacific Ocean. *Geophys. J. Int.,* 109:701–719.

Nemoto, K., and Kroenke, L.W., 1985. Sio Guyot: a complex volcanic edifice in the western Mid-Pacific Mountains. *Geo-Mar. Lett.,* 5:83–89.

Obradovich, J.D., in press. A Cretaceous time scale. *In* Caldwell, W.G.E., and Kauffman, E.G. (Eds.), *Cretaceous Evolution of the Western Interior Basin of North America.* Spec. Pap. Geol. Assoc. Can.

Ozima, M., Kaneoka, I., Saito, K., Honda, M., Yanagisawa, M., and Takigami, Y., 1983. Summary of geochronological studies of submarine rocks from the western Pacific Ocean. *In* Hilde, T.W.C., and Uyeda, S. (Eds.), *Geodynamics of the Western Pacific-Indonesian Region.* Am. Geophys. Union Geodyn. Ser., 11:137–142.

Parker, R.L., Shure, L., and Hildebrand, J.A., 1987. The application of inverse theory to seamount magnetism. *Rev. Geophys.,* 25:17–40.

Pringle, M.S., 1993. Age progressive volcanism in the Musicians Seamounts: a test of the hot-spot hypothesis for the Late Cretaceous Pacific. *In* Pringle, M.S., Sager, W.W., Sliter, W.V., and Stein, S. (Eds.), *The Mesozoic Pacific: Geology, Tectonics, and Volcanism.* Geophys. Monogr., Am. Geophys. Union, 77:187–215.

Pringle, M.S., and Dalrymple, G.B., 1993. Geochronological constraints on a possible hot spot origin for Hess Rise and the Wentworth Seamount chain. *In* Pringle, M.S., Sager, W.W., Sliter, W.V., and Stein, S. (Eds.), *The Mesozoic Pacific: Geology, Tectonics, and Volcanism.* Geophys. Monogr., Amer. Geophys. Union, 77:263–277.

Quinn, T.M., and Matthews, R.K., 1990. Post-Miocene diagenetic and eustatic history of Enewetak Atoll: model and data comparison. *Geology,* 18:942–945.

Sager, W.W., 1987. Late Eocene and Maastrichtian paleomagnetic poles for the Pacific Plate: implications for the validity of seamount paleomagnetic data. *Tectonophysics,* 144:301–314.

————, 1992. Seamount age estimates from paleomagnetism and their implications for the history of volcanism on the Pacific Plate. *In* Keating, B.H., and Bolton, B.R. (Eds.), *Geology and Offshore Mineral Resources of the Central Pacific Basin.* Circum-Pac. Counc. Energy Miner. Resour., Earth Sci. Ser., 14:21–37.

Sager, W.W., Duncan, R.A., and Handschumacher, D.W., 1993. Paleomagnetism of the Japanese and Marcus-Wake seamounts, Western Pacific Ocean. *In* Pringle, M.S., Sager, W.W., Sliter, W.V., and Stein, S. (Eds.), *The Mesozoic Pacific: Geology, Tectonics, and Volcanism.* Geophys. Monogr., Am. Geophys. Union, 77:401–435.

Sager, W.W., and Keating, B.H., 1984. Paleomagnetism of Line Islands seamounts: evidence for Late Cretaceous and early Tertiary volcanism. *J. Geophys. Res.,* 89:11135–1115.

Sager, W.W., and Pringle, M.S., 1987. Paleomagnetic constraints on the origin and evolution of the Musicians and South Hawaiian seamounts, central Pacific Ocean. *In* Keating, B.H., Fryer, P., Batiza, R., and Boehlert, G.W. (Eds.), *Seamounts, Islands and Atolls.* Geophys. Monogr., Am. Geophys. Union, 43:133–162.

————, 1988. Mid-Cretaceous to Early Tertiary apparent polar wander path of the Pacific Plate. *J. Geophys. Res.,* 93:11753–11771.

Saito, K., and Ozima, M., 1976. ^{40}Ar/^{39}Ar ages of submarine rocks from the Line Islands: implications on the origin of the Line Islands. *In* Sutton, G.H., Manghnani, M., and Moberly, R. (Eds.), *The Geophysics of the Pacific Ocean Basin and its Margins.* Geophys. Monogr., Am. Geophys. Union, 19:369–374.

Sandwell, D.T., Johnson, C., Levitt, D., Lynch, M.A., Mammerickx, J., Small, C., Winterer, E.L., and Simons, M.S., 1993. Survey of Pukapuka volcanic ridge system in the trough of a gravity roll. *Eos,* 74:285.

Sandwell, D.T., Winterer, E.L., Mammerickx, J., Duncan, R.A., Lynch, M.A., Levitt, D.A., and Johnson, C.L., in press. Evidence from the Pukapuka ridges for diffuse extension of the Pacific plate: no mini hot spots, no convection. *J. Geophys. Res.*

Sarg, J.F., 1988. Carbonate sequence stratigraphy. *In* Wilgus, C.K., Hastings, B.S., Kendall, C.G.St.C., Posamentier, H., Ross, C.A., and Van Wagoner, J. (Eds.), *Sea-Level Changes: An Integrated Approach.* Spec. Publ.—Soc. Econ. Paleontol. Mineral., 42:155–181.

Sayre, W.O., 1981. Preliminary report on the paleomagnetism of Aptian and Albian limestones and trachytes from the Mid-Pacific Mountains and Hess Rise, Deep Sea Drilling Project Leg 62. *In* Thiede, J., Vallier, T.L., et al., *Init. Repts. DSDP,* 62: Washington (U.S. Govt. Printing Office), 983–994.

Schlager, W., 1981. The paradox of drowned reefs and carbonate platforms. *Geol. Soc. Am. Bull.,* 92:197–211.

Schlanger, S.O., Garcia, M.O., Keating, B.H., Naughton, J.J., Sager, W.W., Haggerty, J.A., Philpotts, J.A., and Duncan, R.A., 1984. Geology and geochronology of the Line Islands. *J. Geophys. Res.,* 89:11261–11272.

Schlanger, S.O., Jackson, E.D., et al., 1976. *Init. Repts. DSDP,* 33: Washington (U.S. Govt. Printing Office).

Shipboard Scientific Party, 1973. Site 171. *In* Winterer, E.L., Ewing, J.I., et al., *Init. Repts. DSDP,* 17: Washington (U.S. Govt. Printing Office), 283–334.

————, 1975. Site 313: Mid-Pacific Mountains. *In* Larson, R.L., Moberly, R., et al., *Init. Repts. DSDP,* 32: Washington (U.S. Govt. Printing Office), 313–390.

————, 1981. Site 463: western Mid-Pacific Mountains. *In* Thiede, J., Vallier, T.L., et al., *Init. Repts. DSDP,* 62: Washington (U.S. Govt. Printing Office), 33–156.

————, 1993a. Introduction and scientific objectives. *In* Sager, W.W., Winterer, E.L., Firth, J.V., et al., *Proc. ODP, Init. Repts.,* 143: College Station, TX (Ocean Drilling Program), 7–12.

————, 1993b. Site 865. *In* Sager, W.W., Winterer, E.L., Firth, J.V., et al., *Proc. ODP, Init. Repts.,* 143: College Station, TX (Ocean Drilling Program), 111–180.

————, 1993c. Site 866. *In* Sager, W.W., Winterer, E.L., Firth, J.V., et al., *Proc. ODP, Init. Repts.,* 143: College Station, TX (Ocean Drilling Program), 181–271.

————, 1993d. Sites 867/868. *In* Sager, W.W., Winterer, E.L., Firth, J.V., et al., *Proc. ODP, Init. Repts.,* 143: College Station, TX (Ocean Drilling Program), 273–296.

————, 1993e. Site 869. *In* Sager, W.W., Winterer, E.L., Firth, J.V., et al., *Proc. ODP, Init. Repts.,* 143: College Station, TX (Ocean Drilling Program), 297–374.

————, 1993f. Site 878. *In* Premoli Silva, I., Haggerty, J., Rack, F., et al., *Proc. ODP, Init. Repts.,* 144: College Station, TX (Ocean Drilling Program), 331–412.

————, 1993g. Site 879. *In* Premoli Silva, I., Haggerty, J., Rack, F., et al., *Proc. ODP, Init. Repts.,* 144: College Station, TX (Ocean Drilling Program), 413–441.

————, 1993h. Synthesis of results, Leg 143. *In* Sager, W.W., Winterer, E.L., Firth, J.V., et al., *Proc. ODP, Init. Repts.,* 143: College Station, TX (Ocean Drilling Program), 13–29.

Sliter, W.V., 1989. Aptian anoxia in the Pacific Basin. *Geology,* 17:909–912.

Smith, W.H.F., Staudigel, H., Watts, A.B., and Pringle, M.S., 1989. The Magellan Seamounts: Early Cretaceous record of the south Pacific isotopic and thermal anomaly. *J. Geophys. Res.,* 94:10501–10523.

Staudigel, H., Park, K.-H., Pringle, M.S., Rubenstone, J.L., Smith, W.H.F., and Zindler, A., 1991. The longevity of the South Pacific isotopic and thermal anomaly. *Earth Planet. Sci. Lett.,* 102:24–44.

Steiner, M.B., and Wallick, B.P., 1992. Jurassic to Paleocene Paleolatitudes of the Pacific Plate derived from the paleomagnetism of the sedimentary sequences at Sites 800, 801, and 802. *In* Larson, R.L., Lancelot, Y., et al., *Proc. ODP, Sci. Results,* 129: College Station, TX (Ocean Drilling Program), 431–446.

Tarduno, J.A., 1990. Absolute inclination values from deep sea sediments: a reexamination of the Cretaceous Pacific record. *Geophys. Res. Lett.,* 17:101–104.

Thiede, J., Dean, W.E., Rea, D.K., Vallier, T.L., and Adelseck, C.G., 1981. The geologic history of the Mid-Pacific Mountains in the central North Pacific Ocean—a synthesis of deep-sea drilling studies. *In* Thiede, J., Vallier, T.L., et al., *Init. Repts. DSDP,* 62: Washington (U.S. Govt. Printing Office), 1073–1120.

van Waasbergen, R.J., and Winterer, E.L., 1993. Summit geomorphology of Western Pacific guyots. *In* Pringle, M.S., Sager, W.W., Sliter, W.V., and Stein, S. (Eds.), *The Mesozoic Pacific: Geology, Tectonics, and Volcanism.* Geophys. Monogr., Am. Geophys. Union, 77:335–366.

Van Wagoner, J.C., Posamentier, H.W., Mitchum, R.M., Jr., Vail, P.R., Sarg, J.F., Loutit, T.S., and Hardenbol, J., 1988. An overview of the fundamentals of the sequence stratigraphy and key definitions. *In* Wilgus, C.K., Hastings, B.S., Ross, C.A., Posamentier, H.W., Van Wagoner, J.C., and Kendall, C.G.St.C. (Eds.), *Sea-Level Changes: An Integrated Approach.* Spec. Publ.—Soc. Econ. Paleontol. Mineral., 42:39–45.

Vogt, P.R., 1989. Volcanogenic upwelling of anoxic, nutrient-rich water: a possible factor in carbonate-bank/reef demise and benthic faunal extinctions? *Geol. Soc. Am. Bull.,* 101:1225–1245.

Wardlaw, B.R., and Quinn, T.M., 1991. The record of Pliocene sea-level change at Enewetak atoll. *Quat. Sci. Rev.,* 10:247–258.

Weissert, H., 1989. C-isotope stratigraphy, a monitor of paleoenvironmental change: a case study from the Early Cretaceous. *Surv. Geophys.,* 10:1–61.

Weissert, H., and Lini, A., 1991. Ice age interludes during the time of Cretaceous greenhouse climate? *In* Müller, D.W., McKenzie, J.A., and Weissert, H. (Eds.), *Controversies in Modern Geology: Evolution of Geological Theories in Sedimentology, Earth History and Tectonics:* New York (Academic Press), 173–191.

Wheeler, C.W., and Aharon, P., 1991. Mid-oceanic carbonate platforms as oceanic dipsticks: examples from the Pacific. *Coral Reefs,* 10:101–114.

Wilson, J.T., 1963. A possible origin of the Hawaiian Islands. *Can. J. Phys.,* 41:863–870.

Winterer, E.L., Ewing, J.I., et al., 1973. *Init. Repts. DSDP,* 17: Washington (U.S. Govt. Printing Office).

Winterer, E.L., Johnson, C., Levitt, D., Lynch, M.A., Mammerickx, J., Sandwell, D., and Small, C., 1993a. Morphology of Pukapuka volcanic ridge system, southeast Pacific. *Eos,* 74:285.

Winterer, E.L., and Metzler, C.V., 1984. Origin and subsidence of guyots in Mid-Pacific Mountains. *J. Geophys. Res.,* 89:9969–9979.

Winterer, E.L., Natland, J.H., van Waasbergen, R.J., Duncan, R.A., McNutt, M.K., Wolfe, C.J., Premoli Silva, I., Sager, W.W., and Sliter, W.V., 1993b. Cretaceous guyots in the Northwest Pacific: an overview of their geology and geophysics. *In* Pringle, M.S., Sager, W.W., Sliter, W.V., and Stein, S. (Eds.), *The Mesozoic Pacific: Geology, Tectonics, and Volcanism.* Geophys. Monogr., Am. Geophys. Union, 77:307–334.

Winterer, E.L., and Sandwell, D.T., 1987. Evidence from en-echelon cross-grain ridges for tensional cracks in the Pacific plate. *Nature,* 329:534–537.